L

Laboratory Simulations of Organic Geochemical Processes at Elevated Temperatures

Jeffrey S. Seewald
Marine Chemistry and Geochemistry Department, Woods Hole Oceanographic Institution, Woods Hole, MA, USA

Definition

Organic matter undergoes a series of chemical transformations when heated in natural environments. The chemical and physical evolution of this material as a function of time and temperature, commonly referred to as thermal maturation, involves numerous organic and inorganic reactions that can be simulated in the laboratory using artificial maturation experiments. A variety of techniques have been developed to provide information regarding the rates of reactions as a function of time and temperature, the amounts of products generated, reaction pathways and mechanisms, and the role of water and other inorganic species.

Introduction

Organic compounds are pervasive in a broad range of geologic environments where they are involved in numerous geochemical processes at elevated temperatures and pressures. The generation and accumulation of petroleum (oil and natural gas) in sedimentary basins is an obvious and economically important example. Others include the transport and deposition of ore-forming metals in hydrothermal systems, sediment diagenesis, and the formation of methane gas-hydrates. Organic compounds formed in many of these environments also represent a source of nutrients and energy that can support microbial communities. Therefore, a major goal for the organic geochemist is to understand geochemical processes that regulate the production and degradation of organic matter. Owing to the complexity and, in many cases, difficulties associated with accessing geologic environments, factors that regulate organic transformations are difficult to determine from field studies alone. Consequently, a variety of approaches involving laboratory experiments have been developed to provide information regarding geochemical processes that regulate the abundance of naturally occurring organic compounds. Many of these efforts are focused on understanding the origin of oil and natural gas in relation to the thermal maturation of organic-rich sediments, while others have examined the generation and stability of organic compounds dissolved in water.

Oil and Natural Gas Formation

The thermal degradation of kerogen to produce liquid oil and natural gas is generally believed to occur at temperatures from 50 °C to 120 °C (Hunt 1996; Tissot and Welte 1984). Continued heating of oil at higher temperatures may result in its subsequent degradation and conversion to natural gas. Because natural maturation processes typically occur on million year time scales, it is common practice to conduct laboratory simulations at temperatures higher than in natural systems to enhance reaction rates and allow observation of organic transformations on laboratory time scales. Results of experiments generating petroleum as a function of time and/or temperature can be used to determine the rate of oil and natural gas formation in sedimentary basins (Behar et al. 1992; Burnham et al. 1987; Espitalié et al. 1977; Lewan 1985; Schenk and Dieckmann 2004). Indeed, such experiments have played an important role in guiding much of the petroleum exploration that has occurred to date in conventional sedimentary systems. A key premise underpinning this practice is the assumption that petroleum generation is primarily a kinetically controlled process in which the effects of time and temperature are interchangeable.

W. M. White (ed.), *Encyclopedia of Geochemistry*,
https://doi.org/10.1007/978-3-319-39312-4

Extrapolation of reaction rates observed at high temperatures in the laboratory to lower temperatures that characterize petroleum producing sedimentary basins is achieved through use of the Arrhenius equation:

$$k = A_0 e^{-(Ea/RT)}$$

where k is the rate constant, A_0 is the pre-exponential constant, E_a is the activation energy, R is the ideal gas constant, and T is temperature. There are important limitations associated with this approach. In particular, because the thermal maturation of sedimentary organic matter to produce oil and natural gas is an inherently complex process involving millions of sequential and parallel reactions, often in complex reaction networks, even the most complex kinetic models based on the Arrhenius equation represent gross simplifications of the natural process (Dominé et al. 1998). Moreover, the substitution of time for temperature during laboratory experiments may introduce significant uncertainty in extrapolated reaction rates since at lower temperatures substantial changes may occur in the relative rates of the reactions involved, the relationship between the rates of molecular diffusion and reaction, thermodynamic drives, and reaction mechanisms. Despite these limitations, laboratory experiments provide one of the few means by which processes associated with natural thermal alteration of sedimentary organic matter can be studied and represent effective tools for predicting the geochemical evolution of sedimentary basins.

Laboratory experiments designed to simulate the maturation of sedimentary organic matter vary widely with respect to complexity, the type of information they provide, and the extent to which they replicate natural systems. Collectively, they involve pyrolysis reactions induced by heating sedimentary organic matter in the absence of molecular oxygen. Major differences are related to whether the experimental system is open or closed, the temperature of the simulation, and the presence or absence of added water. In closed-system experiments, bulk sediments, petroleum source rocks, or isolated kerogen (the fraction of sedimentary organic matter insoluble in common organic solvents) are heated in a confined reaction chamber. A variety of reaction chamber designs and materials have been employed for this purpose, including relatively large volume (~500 ml) stainless steel pressure vessels (Lewan 1997) and smaller volume gold (Behar et al. 1992; Gao et al. 2014; Landais et al. 1989) or quartz tubes (Horsfield and Duppenbecker 1991) that are sealed at both ends. Artificial maturation within sealed gold tubes is typically referred to as confined pyrolysis since confining pressure is applied to the flexible tubes by water within an external pressure vessel to eliminate a vapor headspace above the reactants. During closed-system experiments, reaction products remain in the reaction chamber in intimate contact with the starting materials for prolonged periods of time, thereby promoting secondary reactions. In contrast, during open-system experiments (e.g., see programmed temperature pyrolysis), sediment or kerogen is maintained at or near ambient pressure conditions and is continuously swept by an inert carrier gas (usually helium) to remove volatile products to a detection device for quantitation (Burnham et al. 1987; Espitalié et al. 1977). Rapid removal of reaction products from the reaction chamber minimizes secondary reactions. As a result, there are significant compositional differences between organic products generated during open- and closed-system pyrolysis. In particular, alkenes are a major product during open-system pyrolysis, but are only produced during early heating stages in closed-systems and subsequently disappear during prolonged heating (Tannenbaum and Kaplan 1985). Since alkenes are present at relatively low concentrations in naturally occurring crude petroleum, these observations suggest that closed-system experiments more accurately replicate organic transformations responsible for the generation of oil and natural gas under quasi-closed conditions that prevail in natural sedimentary environments. Temperature conditions and the duration of heating also vary widely during laboratory simulations. Closed-system experiments are typically conducted isothermally at temperatures as high as high 550 °C for periods of time ranging from a few hours to several years (Saxby and Riley 1984). In contrast, open-system pyrolysis experiments typically involve relatively rapid non-isothermal heating (several degrees/min) of samples from ambient conditions to temperatures as high as 1000 °C (Burnham et al. 1987; Espitalié et al. 1977).

Role of Water and Other Inorganic Species

Laboratory experiments have been used extensively to examine the role of water and other inorganic materials such as minerals and sulfur species during organic geochemical processes. During the generation of oil and natural gas, water has been identified as an important variable that influences the composition and amounts of individual organic constituents (Lewan 1997; Price and Wenger 1992). Closed-system laboratory experiments reacting sedimentary organic matter or kerogen with added water (referred to as hydrous or aqueous pyrolysis) can also provide information regarding physical expulsion processes since this approach may produce a free-flowing liquid oil that floats on liquid water within the reaction chamber, allowing expelled products to be distinguished from those retained within the rock matrix (Lewan 1997). Hydrous pyrolysis experiments have demonstrated that in addition to acting as a confining medium, liquid water also participates in many organic reactions and acts as a source of hydrogen and oxygen for the generation of hydrocarbons and oxygen-bearing alteration products such as organic acids and

carbon dioxide (Hoering 1984; Lewan 1997; Seewald 2001; Stalker et al. 1994).

Several experimental studies have focused on investigating chemical reactions involving organic compounds dissolved in water at elevated temperatures and pressures (Reeves et al. 2012; Seewald 2001; Shipp et al. 2014; Siskin and Katritzky 2001). Although relevant to organic-rich petroleum producing sedimentary basins, results of these experiments have widespread application to hydrothermal systems located on land and in the marine environment, where, in most instances, the absence of organic-bearing sediments results in substantially lower organic matter abundance. Hydrothermal systems are characterized by higher temperatures than environments responsible for the generation of petroleum in sedimentary basins, allowing experiments focused on hydrothermal organic geochemistry to be conducted at temperatures comparable to natural systems. Recognizing that organic reactions are influenced by both the organic and inorganic chemical environment in which they occur, and that a significant fraction of organic reactions are redox dependent, many of these experiments have utilized approaches that allow key chemical variables such as the activities of H_2, various sulfur species, and H^+ to be carefully regulated or monitored during an experiment. Experiments containing naturally occurring Fe-bearing mineral assemblages that buffer the activity of aqueous H_2 and H_2S have been used to study the stability of individual aqueous hydrocarbons (McCollom et al. 2001; Seewald 2001). Unlike experiments examining the maturation of sedimentary organic matter or kerogen, these experiments typically contain a single or limited number of model compounds, thereby reducing the number of possible reactions and facilitating the identification of specific reaction pathways that may result in the production or degradation of an individual compound or class of compounds. A major finding of these experiments is that kinetic barriers to the attainment of total thermodynamic equilibrium allow the metastable persistence of many organic compounds such as hydrocarbons, alcohols, and ketones that may react reversibly to attain a partial thermodynamic equilibrium state with respect to other organic compounds, water, and redox-dependent minerals (Seewald 2001; Shipp et al. 2013; Yang et al. 2012). Moreover, these experiments have demonstrated that the presence of liquid water promotes aqueous reactions that utilize reaction pathways and mechanisms not available in dry systems.

Other experiments have been instrumental in demonstrating that minerals and aqueous species may be catalytically active during organic reactions. A variety of sulfur species have been shown to play a catalytic role in both the formation and degradation of diverse reduced carbon compounds. For example, organic sulfur radicals released by the decomposition of sulfur-bearing organic compounds accelerate the cleavage of C–C bonds in kerogen, resulting in the generation of oil at lower temperatures from sulfur-rich source rocks (Lewan 1998), while aqueous organic sulfur compounds such as thiols may play a catalytic role in the high temperature decomposition of oils by a process known as thermochemical sulfate reduction (Amrani et al. 2008). Aqueous inorganic sulfur species have also been implicated as being catalytically active during redox reactions that result in the oxidation of aqueous hydrocarbons (Goldhaber and Orr 1995; Seewald 2001; Toland 1960). The sulfide mineral sphalerite (ZnS) has been shown to act as a heterogeneous catalyst for the making and breaking of C–C bonds during isomerization of dimethylcyclohexanes (Shipp et al. 2014). Other heterogeneous catalysts include clay minerals and transition metals that have been shown to accelerate the degradation of petroleum to natural gas (Mango and Hightower 1997; Tannenbaum and Kaplan 1985).

Summary and Conclusions

Laboratory experiments represent a powerful means to identify and quantify geochemical processes associated with the thermal maturation of organic matter in natural environments. The ability to control physical and chemical conditions and remove many of the complexities associated with natural systems allows an assessment of key variables that regulate organic transformations under geologically relevant conditions. Experiments have demonstrated that organic reactions are strongly influenced by the presence or absence of inorganic chemical species. Liquid water is particularly important in facilitating reaction pathways not available in dry systems, and may facilitate the attainment of metastable thermodynamic equilibrium involving organic compounds, water, and minerals. Water also represents an abundant source of hydrogen and oxygen that can be incorporated into organic alteration products in addition to the limited amounts available in organic matter. Many inorganic and organic species have been shown to catalyze organic reactions in both aqueous and dry systems and participate in redox-dependent organic reactions. Information of this type represents an important foundation for the development of predictive models used to constrain geochemical process that regulate the composition and abundance of organic matter in natural systems.

Cross-References

- ▶ Activation Parameters: Energy, Enthalpy, Entropy, and Volume
- ▶ Carbon
- ▶ Fluid–Rock Interaction
- ▶ Geochemical Thermodynamics
- ▶ Hydrogen

- Kerogen
- Kinetics of Geochemical Processes
- Natural Gas
- Organic Geochemistry
- Oxygen
- Petroleum
- Programmed Temperature Pyrolysis
- Sulfide Minerals
- Sulfur

References

Amrani A, Zhang T, Maa Q, Ellis GS, Tang Y (2008) The role of labile sulfur compounds in thermochemical sulfate reduction. Geochim Cosmochim Acta 72:2960–2972

Behar F, Kressmann S, Rudkiewicz JL, Vandenbroucke M (1992) Experimental simulation in a confined system and kinetic modelling of kerogen and oil cracking. Org Geochem 19:173–189. https://doi.org/10.1016/0146-6380(92)90035-V

Burnham AK, Braun RL, Gregg HR, Samoun AM (1987) Comparison of measuring kerogen pyrolysis rates and fitting kinetic parameters. Energy Fuel 1:452–458

Dominé F, Dessort D, Brévart O (1998) Towards a new method of geochemical kinetic modelling: implications for the stability of crude oils. Org Geochem 12:597–612

Espitalié J, Jl L, Madec M, Marquis F, Leplat P, Paulet J, Boutefeu A (1977) Rapid method for source rocks characterization and for determination of petroleum potential and degree of evolution. Inst Fr Pétr Rev 32:23–42

Gao L, Schimmelmann A, Tang Y, Mastalerz M (2014) Isotope rollover in shale gas observed in laboratory pyrolysis experiments: insight to the role of water in thermogenesis of mature gas. Org Geochem 68:95–106. https://doi.org/10.1016/j.orggeochem.2014.01.010

Goldhaber MB, Orr WL (1995) Kinetic controls on thermochemical sulfate reduction as a source of sedimentary H_2S. In: Vairavamurthy MA, Schoonen MAA (eds) Geochemical transformations of sedimentary sulfur. American Chemical Society, Washington, DC, pp 412–425

Hoering TC (1984) Thermal reaction of kerogen with added water, heavy water, and pure organic substances. Org Geochem 5:267–278

Horsfield B, Dueppenbecker SJ (1991) The decomposition of Posidonia Shale and Green River Shale kerogens using microscale sealed vessel (mssv) pyrolysis. J Anal Appl Pyrolysis 20:107–123

Hunt JM (1996) Petroleum geochemistry and geology, 2nd edn. W.H. Freeman and Co., New York

Landais P, Michels R, Poty B, Monthioux M (1989) Pyrolysis of organic-matter in cold-seal pressure autoclaves – experimental approach and applications. J Anal Appl Pyrolysis 16:103–115

Lewan MD (1985) Evaluation of petroleum generation by hydrous pyrolysis experimentation. Phil Trans R Soc Lond A 315:123–134

Lewan MD (1997) Experiments on the role of water in petroleum formation. Geochim Cosmochim Acta 61:3691–3723

Lewan MD (1998) Sulfur-radical control on rates of natural petroleum formation. Nature 391:164–166

Mango FD, Hightower JW (1997) The catalytic decomposition of petroleum into natural gas. Geochim Cosmochim Acta 61:5347–5350

McCollom TM, Seewald JS, Simoneit BRT (2001) Reactivity of monocyclic aromatic compounds under hydrothermal conditions. Geochim Cosmochim Acta 65:455–468

Price LC, Wenger LM (1992) The influence of pressure on petroleum generation and maturation as suggested by aqueous pyrolysis. Org Geochem 19:141–159. https://doi.org/10.1016/0146-6380(92)90033-T

Reeves EP, Seewald JS, Sylva S (2012) Hydrogen isotope exchange between n-alkanes and water under hydrothermal conditions. Geochim Cosmochim Acta 77:582–599

Saxby JO, Riley KW (1984) Petroleum generation by laboratory-scale pyrolysis over six years simulating conditions in a subsiding basin. Nature 308:177–179

Schenk HJ, Dieckmann V (2004) Prediction of petroleum formation: the influence of laboratory heating rates on kinetic parameters and geological extrapolations. Mar Petrol Geol 21:79–95. https://doi.org/10.1016/j.marpetgeo.2003.11.004

Seewald JS (2001) Aqueous geochemistry of low molecular weight hydrocarbons at elevated temperatures and pressures: constraints from mineral buffered laboratory experiments. Geochim Cosmochim Acta 65:1641–1644

Shipp JA, Gould IR, Herckes P, Shock EL, Williams LB, Hartnett HE (2013) Organic functional group transformations in water at elevated temperature and pressure: reversibility, reactivity, and mechanisms. Geochim Cosmochim Acta 104:194–209

Shipp JA, Gould IR, Shock EL, Williams LB, Hartnett HE (2014) Sphalerite is a geochemical catalyst for carbon−hydrogen bond activation. Proc Nat Acad Sci 111:11642–11645

Siskin M, Katritzky AR (2001) Reactivity of organic compounds in superheated water: general background. Chem Rev 101:825–835

Stalker L, Farrimond P, Larter SR (1994) Water as an oxygen source for the production of oxygenated compounds (including CO_2 precursors) during kerogen maturation. Advances in Organic Geochemistry 1993. Org Geochem 22:477–486

Tannenbaum E, Kaplan IR (1985) Low-M_r hydrocarbons generated during hydrous and dry pyrolysis of kerogen. Nature 317:708–709

Tissot BP, Welte DH (1984) Petroleum formation and occurrence. Springer, New York

Toland WG (1960) Oxidation of organic compounds with aqueous sulfate. J Am Chem Soc 82:1911–1916

Yang Z, Gould IR, Williams L, Hartnett H, Shock EL (2012) The central role of ketones in reversible and irreversible hydrothermal organic functional group transformations. Geochim Cosmochim Acta 98:48–65

Lanthanide Rare Earths

Scott M. McLennan
Department of Geosciences, Stony Brook University, Stony Brook, NY, USA

Definition

Rare earth elements (REE) consist of Group 3 (or Group IIIB) transition elements $_{21}$Sc, $_{39}$Y, $_{57}$La, and f-block (inner transition) elements $_{58}$Ce, $_{59}$Pr, $_{60}$Nd, $_{61}$Pm, $_{62}$Sm, $_{63}$Eu, $_{64}$Gd, $_{65}$Tb, $_{66}$Dy, $_{67}$Ho, $_{68}$Er, $_{69}$Tm, $_{70}$Yb, and $_{71}$Lu. In geochemical usage, the term *rare earth elements* refers only to the lanthanides (La–Lu), and commonly Y due to geochemical behavior similar to Ho. However, Sc typically is excluded in discussions of REE because it is a smaller cation with geochemical behavior closer to the first row (ferromagnesian) transition elements Fe, V, Cr, Co, and Ni, with which it is typically grouped. This well-entrenched geochemical

nomenclature differs from formal chemical nomenclature, thus providing a source of confusion. Geochemists also subdivide REE into light rare earths (LREE: La–Sm) and heavy rare earths (HREE: Gd–Lu) with some further recognizing a group of middle rare earths (MREE; Nd (or Sm)–Tb). The REE promethium (Pm) lacks any stable nuclides or long-lived radionuclides and is not normally considered in geochemical discussions. Although only very rarely used in geochemical literature, the International Union of Pure and Applied Chemistry recommends the term "*lanthanoid*" rather than "*lanthanide*," since in chemistry the word-ending "ide" generally refers to anionic species.

General Geochemistry

The mostly trivalent rare earth elements (REE) are arguably the most significant group of trace elements in geochemistry. The lanthanide series develops by filling 4f orbitals, which do not effectively shield each other from increasing nuclear charge, leading to highly coherent geochemical behavior as a group. Among other things, the trivalent state is especially stable in geological settings (Eu^{2+} and Ce^{4+} being the two notable exceptions) and trivalent ionic radii decrease in a particularly systematic fashion: the "*lanthanide contraction*" (e.g., Douglas 1954; Table 1; Fig. 1). The dominant

Lanthanide Rare Earths, Table 1 Selected rare earth element properties

Symbol	Atomic number (Z)	Ground state[a]	Standard atomic weight[b]	Trivalent (except where noted) Ionic radius (pm)[c]		Pauling electro-negativity[a]	50% Oxide condensation (K at 10^{-4} bar)[d]	Seawater mean residence time (year)[e]	Element
				CN6	CN8				
La	57	[Xe] $5d^16s^2$	138.90547	103.2	116.0	1.10	1578	500	Lanthanum
Ce	58	[Xe] $4f^15d^16s^2$	140.116	101.0	114.3	1.12	1478	50	Cerium
Pr	59	[Xe] $5f^36s^2$	140.90766	99.0	112.6	1.13	1582	240	Praseodymium
Nd	60	[Xe] $5f^46s^2$	144.242	98.3	110.9	1.14	1602	400	Neodymium
Pm	61	[Xe] $5f^56s^2$	(~145)	97	110	~1.2	–	–	Promethium
Sm	62	[Xe] $5f^66s^2$	150.36	95.8	107.9	1.17	1590	400	Samarium
Eu	63	[Xe] $5f^76s^2$	151.964	94.7	106.6	~1.2	1356	410	Europium
Gd	64	[Xe] $4f^75d^16s^2$	157.25	93.8	105.3	1.20	1659	520	Gadolinium
Tb	65	[Xe] $5f^96s^2$	158.92535	92.3	104.0	~1.2	1659	570	Terbium
Dy	66	[Xe] $5f^{10}6s^2$	162.500	91.2	102.7	1.22	1659	740	Dysprosium
Ho	67	[Xe] $5f^{11}6s^2$	164.93033	90.1	101.5	1.23	1659	1820	Holmium
Er	68	[Xe] $5f^{12}6s^2$	167.259	89.0	100.4	1.24	1659	2420	Erbium
Tm	69	[Xe] $5f^{13}6s^2$	168.93422	88.0	99.4	1.25	1659	2430	Thulium
Yb	70	[Xe] $5f^{14}6s^2$	173.054	86.8	98.5	~1.3	1487	2440	Ytterbium
Lu	71	[Xe] $4f^{14}5d^16s^2$	174.9668	86.1	97.7	1.27	1659	2890	Lutetium
Sc	21	[Ar] $3d^14s^2$	44.955908	74.5	87.0	1.36	1659	1000	Scandium
Y	39	[Kr] $4d^15s^2$	88.90584	90.0	101.9	1.22	1659	1670	Ytterbium
Eu^{2+}				117	125				
Ce^{4+}				87.0	97.0				

Sources: [a]Emsley (1998); [b]Meija et al. (2016); [c]Shannon (1976); [d]Lodders (2003); [e]Nozaki (2001), Parker et al. (2016)

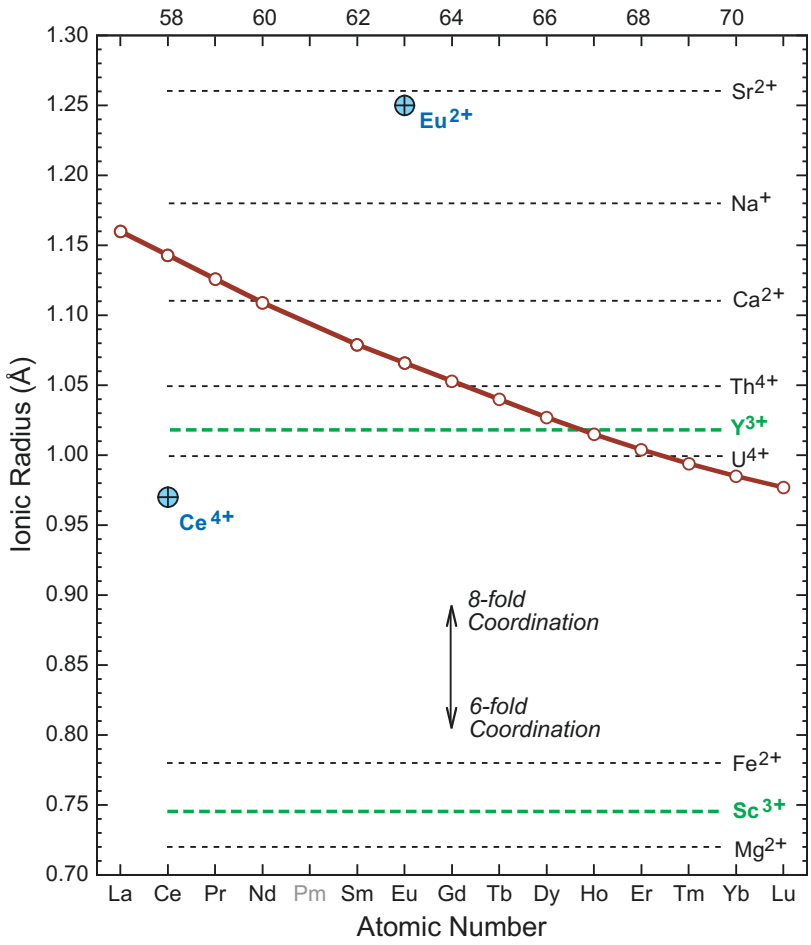

Lanthanide Rare Earths, Fig. 1 Plot of ionic radius versus atomic number for the trivalent lanthanide elements. Also shown for reference are the ionic radii for the other trivalent rare earth elements Y and Sc, for Eu^{2+} and Ce^{4+}, and for other selected cations. The extremely regular decrease in the ionic radii of the trivalent lanthanides is termed the "lanthanide contraction." Note that Sc^{3+} is much smaller than other rare earth elements, more similar in size to Fe^{2+} and Mg^{2+}, which is the reason why it is generally not included with the REE in geochemical literature

controls on the geochemical and cosmochemical behavior of REE are their valence (including redox behavior), size (ionic/crystal radius), volatility (e.g., 50% condensation temperature), and complexing behavior (speciation). Useful reviews of REE geochemistry may be found in Henderson (1984), Taylor and McLennan (1988), Lipin and McKay (1989), Nozaki (2001), Hoatson et al. (2011), Chakhmouradian and Wall (2012), and McLennan and Taylor (2012). Some basic REE properties, of geochemical and cosmochemical interest, are summarized in Table 1.

REE are lithophile and, apart from Sc, in most igneous systems are incompatible (i.e., bulk partition coefficients, $D < 1$) with the degree of incompatibility typically increasing with increasing size (i.e., decreasing atomic number). Accordingly, the trivalent lanthanides (and Y) tend to be concentrated in magmatic liquids and late crystallizing phases. Of the major elements in the crust and mantle, only Na and Ca come close in size (apart from Sc), however substitution for these elements (especially Na) may lead to serious charge imbalances, requiring a coupled substitution (Fig. 1). Traditionally, trivalent lanthanides have also been considered large-ion lithophile elements (LILE) but since their level of incompatibility is more a function of charge than of size, this terminology is now discouraged (Chauvel and Rudnick 2016).

In general, the REE have very low fluid/rock bulk partition coefficients ($D \ll 1$) and thus during most diagenetic, hydrothermal and metamorphic conditions are only significantly redistributed beyond the mineralogical scale at very high fluid/rock ratios. Under aqueous conditions, REE exist mostly as a variety of complexes, with seawater speciation being dominated by metal (REE^{3+}), carbonate ($REECO_3^+$), and bicarbonate ($REE(CO_3)_2^-$), with carbonate complexes being the most abundant. Scandium, on the other hand, is strongly hydrolyzed in seawater (i.e., $Sc(OH)_2^+$, $Sc(OH)_3^0$, $Sc(OH)_4^-$ speciation) (Byrne 2002).

A more controversial influence on REE behavior, notably in aqueous and late-stage magmatic fluids, is the so-called "*tetrad*" or "*double-double*" effect, resulting from 1/4, 1/2, 3/4, and fully filled 4f shells (Masuda et al. 1987). Distinctive M- and W-shaped chondrite-normalized REE patterns have been observed with inflections corresponding to the four tetrads (La-Nd; (Pm)Sm-Gd; Tb-Ho; Er-Lu). McLennan (1994) suggested that many apparent tetrad effects could be artifacts of incomplete analyses, analytical error, inappropriate normalization, or complex mixing processes.

However, claims of tetrad effects continue to appear (e.g., Bau and Koschinsky 2009) and final resolution of the controversy requires systematic interlaboratory comparisons of the same samples by a variety of laboratories and analytical methods.

Eu and Ce Redox Geochemistry

Of great importance to geochemistry is the fact that Eu and Ce commonly exist in other than trivalent states in geological environments ($Eu^{2+/3+}$; $Ce^{3+/4+}$). Reduced Eu^{2+} occurs by reducing, typically magmatic, conditions. The ionic radius of Eu^{2+} is about 17% larger than Eu^{3+} and almost identical to Sr^{2+} (Fig. 1). Accordingly, Eu^{2+} behavior differs considerably, resulting in REE distributions with anomalous Eu abundances (Eu-anomalies; see below). One important example is that Eu becomes highly concentrated in plagioclase feldspar (substituting into the Ca site). Plagioclase is only stable to about 40 km depth on Earth and so anomalous Eu behavior in terrestrial magmatic rocks is commonly taken as a sign of relatively shallow igneous processes (e.g., Taylor and McLennan 1985). Under surficial aqueous conditions, Eu is present in its oxidized form, although under highly reducing and alkaline conditions, Eu reduction could potentially take place (Sverjensky 1984). Evidence for mixed Eu^{2+}/Eu^{3+} under certain hydrothermal conditions has also been documented (e.g., Takahashi et al. 2005).

In contrast, Ce is found in the Ce^{3+} state under magmatic conditions but is readily oxidized under many surficial aqueous conditions, notably in early marine diagenesis to form manganese nodules and under oxidizing weathering conditions. Ce^{4+} is ~15% smaller than Ce^{3+} and tends to form highly insoluble Ce-hydroxide complexes that can thus readily separate from more soluble REE^{3+} complexes, resulting in anomalous REE distribution patterns (Ce-anomalies; see below). The substantial depletion of Ce in seawater (i.e., negative Ce anomalies), resulting ultimately from manganese oxide formation, is a direct manifestation of such redox controls (e.g., Nozaki 2001).

Normalization of Rare Earth Element Abundances

Absolute concentrations of lanthanides are highly variable in rocks, minerals, and natural waters (Table 2), as are relative abundances of adjacent lanthanides in any given sample, due to the Oddo-Harkins (odd-even) effect. Accordingly, it is customary to display lanthanide data as plots of normalized values (on a logarithmic scale) versus atomic number or ionic radius (on a linear scale), termed Coryell-Masuda plots. Yttrium in some cases is also plotted at about the position of the lanthanide Ho, because it typically behaves similarly to this HREE in most geological processes. The two most commonly used datasets for normalization are average chondritic meteorites, reflecting solar and bulk silicate Earth abundances, and average shale, reflecting upper continental crust abundances. Commonly used values are given in Table 2 but for both chondrites and shales, different workers use values that differ by up to ~15% in absolute abundances (but with

Lanthanide Rare Earths, Table 2 Rare earth element abundances in selected geochemical reservoirs (concentrations in ppm except in solar abundances and seawater, as noted)

	Log solar abundance (H = 12.00)[a]	Average volatile-free CI chondrite[b]	Bulk silicate Earth[b]	Oceanic N-MORB basaltic crust[b]	Continental crust[b]			Average Shale[c]	Seawater (ppt)[d]
					Upper	Bulk	Lower		
La	1.10 ± 0.03	0.367	0.546	1.9	30	16	11	38.2	4.17
Ce	1.58 ± 0.04	0.957	1.423	6.0	64	33	23	79.6	0.631
Pr	0.72 ± 0.04	0.137	0.215	0.99	7.1	3.9	2.8	8.83	0.535
Nd	1.42 ± 0.04	0.711	1.057	6.1	26	16	12.7	33.9	2.88
Sm	0.96 ± 0.04	0.231	0.343	2.22	4.5	3.5	3.17	5.55	0.601
Eu	0.52 ± 0.04	0.087	0.129	0.9	0.88	1.1	1.17	1.08	0.152
Gd	1.07 ± 0.04	0.306	0.454	3.5	3.8	3.3	3.13	4.66	0.739
Tb	0.30 ± 0.10	0.058	0.084	0.70	0.64	0.60	0.59	0.774	0.175
Dy	1.10 ± 0.04	0.381	0.566	4.5	3.5	3.7	3.6	4.68	1.06
Ho	0.48 ± 0.11	0.0851	0.126	1.1	0.80	0.78	0.77	0.991	0.330
Er	0.92 ± 0.05	0.249	0.370	2.6	2.3	2.2	2.2	2.85	1.09
Tm	0.10 ± 0.04	0.0356	0.057	0.42	0.33	0.32	0.32	0.405	0.169
Yb	0.84 ± 0.11	0.248	0.368	2.7	2.2	2.2	2.2	2.82	1.12
Lu	0.10 ± 0.09	0.0381	0.057	0.40	0.32	0.30	0.29	0.433	0.227
Sc	3.15 ± 0.04	8.64	13.0	44	13.6	30	35	16	0.98
Y	2.21 ± 0.05	2.25	3.48	25	22	20	19	27	19.6

Sources: [a]Lodders (2003; note that these abundances also equate to assuming $Si=10^{7.51}$); [b]from compilations in Taylor and McLennan (2009); [c]McLennan (1989); [d]Nozaki (2001), Parker et al. (2016)

relative abundances differing by no more than a few percent). In addition to chondrites and shales, other normalization values may be used for specific problems; for example, it is common to normalize data from a related suite of samples to a single sample within the suite to evaluate processes giving rise to variable REE distributions.

Due to variable redox states described above, it is also common that Eu and Ce display anomalous depletion or enrichment on normalized REE plots. These are termed Eu- and Ce-anomalies with negative anomalies denoting relative depletions and positive anomalies denoting relative enrichments. Such anomalies are quantified as follows:

$$Eu/Eu^* = Eu_N/(Sm_N \bullet Gd_N)^{0.5} \text{ and}$$
$$Ce/Ce^* = Ce_N/(La_N \bullet Pr_N)^{0.5}$$

where Eu* and Ce* are the expected values for smooth normalized REE patterns and the subscript "N" denotes the normalized value. Eu/Eu* and Ce/Ce* values of >1 denote positive anomalies whereas values <1 denote negative anomalies and for all but the most precise analyses, anomalies should be greater than ~5% (i.e., $\leq$0.95; $\geq$1.05) to be considered significant.

Isotope Geochemistry Involving Lanthanides

Because the lanthanides have such coherent interelement relationships and are not readily disturbed by later chemical alteration, radiogenic isotope systems involving these elements are especially useful as geochronometers and isotope tracers. The most useful of these is the $^{147}Sm/^{143}Nd$ alpha decay system (^{147}Sm decay constant, $\lambda = 6.54 \bullet 10^{-12}$ year^{-1}) which, for example, is useful for evaluating the timing of extraction of the continental crust from the mantle (DePaolo 1988). The $^{176}Lu/^{176}Hf$ beta decay system ($\lambda = 1.867 \bullet 10^{-11}$ year^{-1}) is well established and useful for examining the fractionation between the least incompatible REE and another refractory element with different geochemical behavior (i.e., high field strength) (Patchett 1983). A final, less used long-lived system involves the branched beta decay of ^{138}La to ^{138}Ce and ^{138}Ba ($T_{1/2} = 3.08 \bullet 10^{11}$ year). In addition to long-lived radiogenic isotope systems, there is one important short-lived system, the alpha decay $^{146}Sm/^{142}Nd$ system. ^{146}Sm has a short half-life ($T_{1/2} = 1.012 \bullet 10^8$ year), considerably less than the age of the Earth, and thus has been "extinct" since early in the history of the solar system. Accordingly, this system can be used to evaluate the fractionation of Sm from Nd very early in planetary histories, prior to the age of the oldest rocks (e.g., early planetary crust formation). A review of isotope geochemistry, including systems involving the lanthanides, can be found in Allègre (2008).

Mineralogy

Most common rock-forming minerals (e.g., olivine, pyroxene, feldspar, micas) do not have cation site conditions (size, charge) that are favorable to substitution of lanthanide REE, which is why they are typically incompatible trace elements for rock-forming minerals under magmatic conditions (i.e., mineral-melt partition coefficients, $K_d < 1$). Nevertheless, both relative and absolute abundances of REE in common rock-forming minerals are highly variable, by orders of magnitude in concentration (Fig. 2). It is this variability, in both abundances and REE pattern shapes (e.g., Eu-anomalies, HREE enrichment), that makes the REE such useful trace elements for evaluating igneous processes because bulk rock REE patterns are sensitive to the mineralogical, and thus the pressure-temperature-compositional, history of the magmatic system (e.g., partial melting, crystal fractionation).

Lanthanides are highly electropositive (i.e., electronegativities in range 1.0–1.3; Table 1) and thus tend to form ionic compounds. REE serve as essential structural constituents in more than 270 different silicate, carbonate, oxide, phosphate, halide, sulfate, arsenate, and vanadate minerals. Among the most abundant REE minerals are bastnäsite [$REE(CO_3)F$], monazite [$(Ce,La,Nd,Th)(PO_4)$], britholite [$(REE,Ca)_5(SiO_4, PO_4)_3(OH,F)$], and xenotime [$YPO_4$]. Some additional REE minerals that are of interest in geochemistry are lanthanite [$(La,Ce,Nd)_2(CO_3)_3 \cdot 8H_2O$], allanite [$(REE,Ca,Y)_2(Al,Fe^{2+}, Fe^{3+})_3(SiO_4)_3(OH)$], the phosphates florencite [$(Ce,La)Al_3(PO_4)_2(OH)_6$], and rhabdophane [$(La,Ce)(PO_4) \cdot H_2O$]. A review of REE mineralogy may be found in Jones et al. (1996).

Sources and Uses of Lanthanides

Based on 2015 United States Geological Survey estimates (Gambogi 2016), China dominates mine production of rare earth elements accounting for 85% of the global production of $1.24 \bullet 10^5$ metric tons of total rare earth oxides, with Australia (8.1%), U.S.A. (3.3%), Russia (2.0%), and Thailand (1.6%) accounting for most of the remaining production. China also possesses the largest fraction (42%) of the global ~$1.3 \bullet 10^8$ metric tons of rare earth oxide reserves. Brazil (17%), Australia (2.5%), India (2.4%), and U.S.A (1.4%) also account for significant reserves, with the remaining ~35% being divided among many countries, including Canada, Greenland, Kyrgyzstan, Malawi, Malaysia, Russia, Sweden, Thailand, Vietnam, Zambia, and others. The past decade has witnessed a considerable increase in REE ore deposit exploration activities due both to a dramatic price increase between 2008 and 2011 (prices subsequently dropped greatly between 2012 and 2016) and growing applications for military and

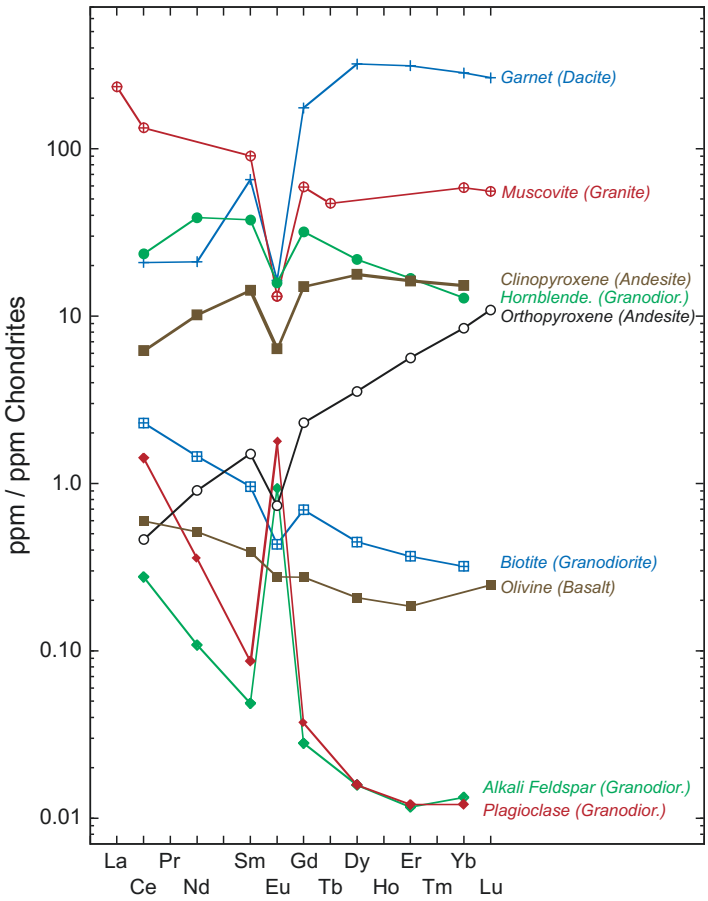

Lanthanide Rare Earths, Fig. 2 Chondrite-normalized REE patterns for selected common igneous rock-forming minerals (with host rocks also shown beside mineral name), illustrating both the overall variation in absolute REE abundances (>10^4) and in the shapes of the REE distributions, including highly variable LREE/HREE ratios and variable Eu-anomalies (Data from the compilation in Taylor and McLennan 1988)

other strategic purposes (e.g., night vision and precision guidance systems, stealth technology).

The major geological settings of REE ore deposits include hydrothermally altered (carbonatite fluid source) Proterozoic dolomitic marbles (Bayan Obo deposit of China, the largest in the world), lateritic ion-adsorption clays (southern China, notable for relative enrichment of scarce HREE), carbonatites (e.g., Mountain Pass, CA, the largest REE deposit in North America), and heavy mineral placer sands. Other REE ores are associated with Precambrian quartz-pebble conglomerate paleoplacers and alkaline magmatism (Castor and Hedrick 2006; Hoatson et al. 2011; Kynicky et al. 2012; Mariano and Mariano 2012).

The industrial applications of rare earth metals and compounds have greatly expanded over the past several decades (Castor and Hedrick 2006; Goonan 2011; Hoatson et al. 2011; Zaimes et al. 2015). Early applications were restricted to polishing agents, incandescent gaslight mantles, and coloring agents in glasses and ceramics. Currently, rare earths have a wide diversity of industrial uses, including (in approximate order of importance by volume) in permanent magnets (e.g., $Nd_2Fe_{14}B$ and $SmCo_5$ magnets); as catalysts in petroleum refining, automobiles, and various other industrial and chemical processes; in various metallurgical applications (e.g., steel and battery alloys); as polishing agents; as coloring agents in glasses and ceramics; and as phosphors in lighting and display screens (e.g., computers, television). Other minor but important uses include as components in lasers (e.g., Nd-YAG and Er-YAG lasers), microwaves (e.g., Y-Fe-garnets or YIG), satellites, chemicals and military systems. In terms of monetary value, applications in magnets, phosphors, and metals account for more than 80% of rare earth oxide markets.

Summary

The lanthanides (La-Lu), along with Y and Sc, comprise the rare earth elements (REE), that are among the most important trace elements for evaluating a wide array of geological processes. In geological settings, they are trivalent (except $Eu^{2+/3+}$ and $Ce^{3+,4+}$), electropositive, and refractory lithophile elements that, apart from Sc, are incompatible in most magmatic settings. In aqueous settings, they have low fluid/rock partition coefficients such that their concentrations in natural waters, along with their oceanic residence times, are very low. Dominant controls on geochemical and cosmochemical distributions are valence (including redox behavior), size and systematic variations in ionic radii (i.e., lanthanide

contraction), volatility, and complexing behavior. Radiogenic isotopes of REE (^{147}Sm-^{143}Nd, ^{176}Lu-^{176}Hf, ^{138}La-^{138}Ce, ^{146}Sm-^{142}Nd) are important geochronometers and isotope tracers. Rare earths are major constituents of >270 (mostly rare) minerals representing most mineral groups (silicates, phosphates, carbonates, etc.) and are mined mainly from hydrothermally altered carbonates, ion-adsorption clays, and carbonatites. Rare earths are strategic metals with wide industrial applications, including many in high technology.

Cross-References

- Cerium
- Complexes
- Cosmic Elemental Abundances
- Dysprosium
- Erbium
- Europium
- Gadolinium
- Geochronology and Radiogenic Isotopes
- Hafnium Isotopes
- Holmium
- Incompatible Elements
- Lanthanum
- Lithophile Elements
- Lutetium
- Neodymium
- Neodymium Isotopes
- Ocean Biochemical Cycling and Trace Elements
- Praseodymium
- Promethium
- Samarium
- Terbium
- Thulium
- Trace Elements
- Transition Elements
- Ytterbium

References

Allègre CJ (2008) Isotope geology. Cambridge University Press, Cambridge, 512pp

Bau M, Koschinsky A (2009) Oxidative scavenging of cerium on hydrous Fe oxide: evidence from the distribution of rare earth elements and yttrium between Fe oxides and Mn oxides in hydrogenetic ferromanganese crusts. Geochem J 43:37–47

Byrne RH (2002) Inorganic speciation of dissolved elements in seawater: the influence of pH on concentration ratios. Geochem Trans 3(2):11–16

Castor SB, Hedrick JB (2006) Rare earth elements. In: Kogel JE et al (eds) Industrial minerals and rocks: commodities, markets, and uses, 7th edn. Society for Mining, Metallurgy, and Exploration, Littleton, CO pp 769–792

Chakhmouradian AR, Wall F (eds) (2012) Rare earth elements. Elements 8:333–376

Chauvel C, Rudnick R (2016) Large-ion lithophile elements. In: White WM (ed) Encyclopedia of geochemistry. Springer, Switzerland. https://doi.org/10.1007/978-3-319-39193-9_232-1

DePaolo DJ (1988) Neodymium isotope geochemistry: an introduction. Springer, Berlin, 187pp

Douglas BE (1954) The lanthanide contraction. J Chem Educ 31:598–599

Emsley J (1998) The elements, 3rd edn. Oxford University Press, Oxford, 292pp

Gambogi J (2016) Rare earths. U S Geol Surv Miner Commod Summ 2016:134–135

Goonan TG (2011) Rare earth elements – end use and recyclability. Scientific investigations report 2011-5094. U. S. Geological Survey, Reston, 15pp

Henderson P (ed) (1984) Rare earth element geochemistry. Elsevier, Amsterdam, 510pp

Hoatson DM, Jaireth S, Miezitis Y (2011) The major rare-earth-element deposits of Australia: geological setting, exploration, and resources. Geoscience Australia, Canberra, 204pp

Jones AP, Wall F, Williams CT (eds) (1996) Rare earth minerals: chemistry, origin and ore deposits.. Chapman & Hall, London, 372pp

Kynicky J, Smith MP, Xu C (2012) Diversity of rare earth deposits: the key example of China. Elements 8:361–367

Lipin BR, McKay GA (eds) (1989) Geochemistry and mineralogy of rare earth elements. Rev Mineral 21:348pp

Lodders K (2003) Solar system abundances and condensation temperatures of the elements. Astrophys J 591:1220–1247

Mariano AN, Mariano A Jr (2012) Rare earth mining and exploration in North America. Elements 8:369–376

Masuda A, Kawakami O, Dohmoto Y, Takenaka T (1987) Lanthanide tetrad effects in nature: two mutually opposite types, W and M. Geochem J 21:119–124

McLennan SM (1989) Rare earth elements in sedimentary rocks: influence of provenance and sedimentary processes. Rev Mineral 21:169–200

McLennan SM (1994) Rare earth element geochemistry and the "tetrad" effect. Geochim Cosmochim Acta 58:2025–2033

McLennan SM, Taylor SR (2012) Geology, geochemistry and natural abundances of the rare earth elements. In: Atwood DA (ed) The rare earth elements: fundamentals and applications. Wiley, Chichester, pp 1–19

Meija J, Coplen TB, Berglund M, Brand WA, De Bièvre P, Gröning M, Holden NE, Irrgeher J, Loss RD, Walczyk T, Prohaska T (2016) Atomic weights of the elements 2013 (IUPAC technical report). Pure Appl Chem 88:265–291

Nozaki Y (2001) Rare earth elements and their isotopes in the ocean. In: Steele JH et al (eds) Encyclopedia of ocean sciences. Academic, London, pp 2354–2366

Parker CE, Brown MT, Bruland KW (2016) Scandium in the open oceans: a comparison with other group 3 trivalent metals. Geophys Res Lett 43:2758–2764

Patchett PJ (1983) Importance of the Lu-Hf isotopic system in studies of planetary chronology and chemical evolution. Geochim Cosmochim Acta 47:81–91

Shannon RD (1976) Revised effective ionic radii and systematic studies of interatomic distances in halides and chalcogenides. Acta Crystallogr A32:751–767

Sverjensky DM (1984) Europium redox equilibrium in aqueous solutions. Earth Planet Sci Lett 67:70–78

Takahashi Y, Kolonin GR, Shironosova GP, Kupriyanova II, Uruga T, Shimizu H (2005) Determination of the Eu(II)/Eu(III) ratios in minerals by X-ray adsorption near-edge structure (XANES) and its application to hydrothermal deposits. Mineral Mag 69:179–190

Taylor SR, McLennan SM (1985) The continental crust: its composition and evolution. Blackwell, Oxford, 312pp
Taylor SR, McLennan SM (1988) Chapter 79, The significance of the rare earths in geochemistry and cosmochemistry. In: Gschneidner KA, Eyring L (eds) Handbook on the physics and chemistry of rare earths, vol 11. North-Holland, Amsterdam, pp 485–578
Taylor SR, McLennan SM (2009) Planetary crusts: their composition, origin and evolution. Cambridge University Press, Cambridge, 378pp
Zaimes GG, Hubler BJ, Wang S, Khanna V (2015) Environmental life cycle perspective on rare earth oxide production. ACS Sustain Chem Eng 3:237–244

Lanthanum

Catherine Chauvel
ISTerre, University Grenoble Alpes, CNRS, Grenoble, France

Element Data
Atomic Symbol: **La**
Atomic Number: **57**
Atomic Weight: 138.9054 g/mol
Isotopes and Abundances: ^{138}La 0.09017%, ^{139}La 99.9098%
1 Atm Melting Point: 920.9 °C
1 Atm Boiling Point: 3456.9 °C
Common Valences: +3
Ionic Radii: 103 pm
Pauling Electronegativity: 1.10
Chondritic (CI) Abundance: 0.2446 microg/g
Silicate Earth Abundance: 0.648 microg/g
Crustal Abundance: 31 microg/g
Seawater Abundance: ≈30 picomole/kg
Core Abundance: unknown

Properties

Lanthanum is a soft and ductile metallic element with a silver-white color that rapidly tarnishes in air. It generally occurs as oxide and hydroxide and in substitution to major elements in minerals.

History and Use

Lanthanum was discovered in Stockholm (Sweden) in 1839 by C.G. Mosander who gave it the name of "latane" [Greek, lanthanein = to lie hidden] because it was "hidden" in cerium carbonate fluoride from the Bastnäs mine (Berzelius 1839). It was isolated only in 1923, almost 100 years later. Lanthanum gave its name to the lanthanide series (also called rare earth elements), a group of 15 similar elements between lanthanum and lutetium in the periodic table.

In the past, lanthanum was not widely used in industry, but the demand increased drastically with the onset of rechargeable batteries for hybrid automobiles.

Geochemical Behavior

Lanthanum, as other rare earth elements, is usually not a constituent of mineral phases on Earth. It is refractory and under most conditions is lithophile and found in the trivalent state. During partial melting and fractional crystallization of magmas, it behaves as an incompatible element and is concentrated in melts. It is therefore enriched in basalts relative to their mantle source and enriched in continental crust relative to Earth mantle. Together with the other rare earth elements, it is widely used in geochemistry to trace geological processes.

Geochronology

Lanthanum has two isotopes, ^{138}La (0.09017%) and ^{139}La (99.9098%). ^{139}La is stable; ^{138}La is radioactive and decays into ^{138}Ce with a half-life of ≈ 292.5 Ga, one of the longest of radioactive decay systems used in isotope geochemistry.

Biological Utilization and Toxicity

Lanthanum has no known biological role and has low to moderate toxicity.

Cross-References

▶ Cerium
▶ Incompatible Elements
▶ Lanthanide Rare Earths
▶ Lithophile Elements
▶ Lanthanide Rare Earths

References

Berzelius (1839) Latanium – a new metal. Philosophical magazine. Ann Phil J Sci XIV:390–391

Large-Ion Lithophile Elements

Catherine Chauvel[1] and Roberta L. Rudnick[2]
[1]ISTerre, University Grenoble Alpes, CNRS, Grenoble, France
[2]Department of Earth Science, University of California, Santa Barbara, CA, USA

Definition

The term large-ion lithophile element (or LILE) is frequently used but poorly defined in the geochemical literature. The word "*lithophile*" comes from the classification of elements suggested by Goldschmidt over a hundred years ago. It describes elements that have an affinity for silicate phases in the Earth. As shown in Fig. 1 from White (2013), the lithophile elements are numerous and generally correspond to elements located at both ends of the periodic table.

The *large-ion* lithophile elements represent only a subset of these lithophile elements and refer to the trace elements characterized by large radius to charge ratio (or low field strength elements; see Fig. 2 below).

Origin of the Term and LILE Geochemistry

The term was first used by Gast (1972) to encompass the cations K, Rb, Sr, Cs, Ba, REE, Th, and U. Gast also included Li as a LILE, since it has a large radius to charge ratio, even though it is small. Because of the confusion in the literature regarding usage of LILE, it is recommended that the term be restricted to lithophile trace elements having large radius to charge ratios and which also have ionic radii greater than those of Ca^{2+} and Na^{1+} (100 and 102 picometers), the largest cations common to rock forming minerals. By this definition, the list of LILE is restricted to K, Rb, Sr, Cs, Ba, and Eu^{2+}.

Because of their large radii, LILE behave incompatibly (see entry ► "Incompatible Elements") during mantle melting and so are highly enriched in mantle melts relative to their source. They are enriched in intraplate basalts (Hofmann 1997) and island arc basalts (Kelemen et al. 2014) relative to more compatible trace elements, but they are depleted in mid-ocean ridge basalts, demonstrating that these lavas derive from a mantle source that experienced prior melt extraction (see entry ► "Mantle Geochemistry"). The LILE are strongly enriched in the upper continental crust (Rudnick and Gao 2014) but occur in lower concentrations in the deep continental crust due to its overall more mafic character and selective loss of some LILE during high-grade metamorphism (see

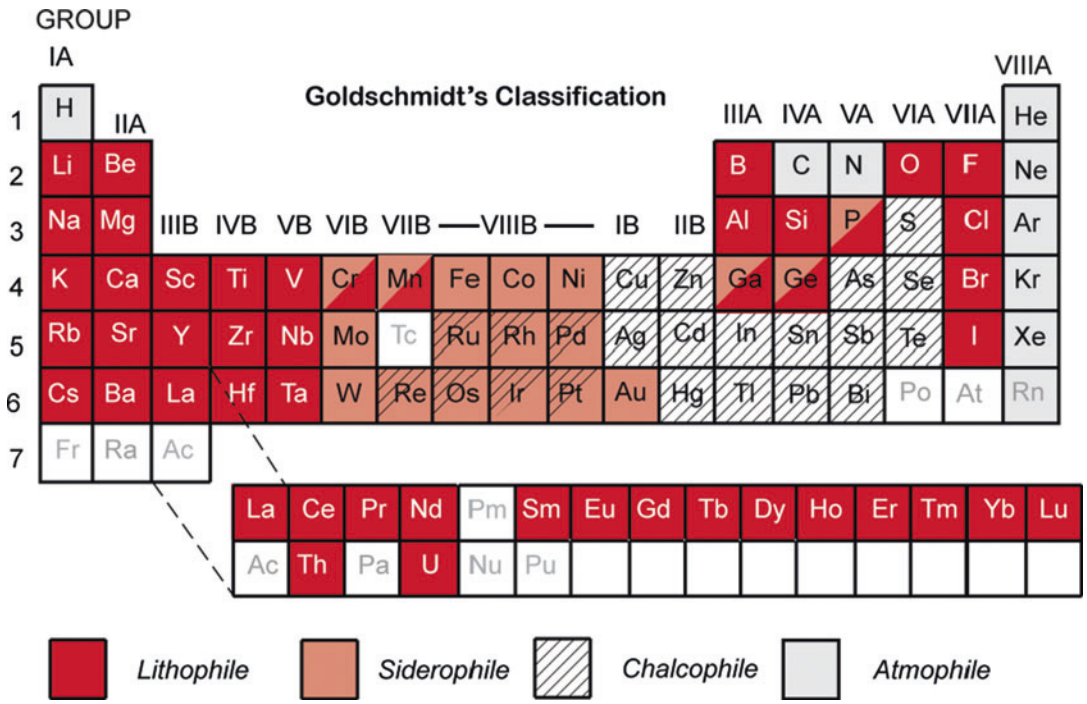

Large-Ion Lithophile Elements, Fig. 1 Goldschmidt's classification of the elements (From White 2013)

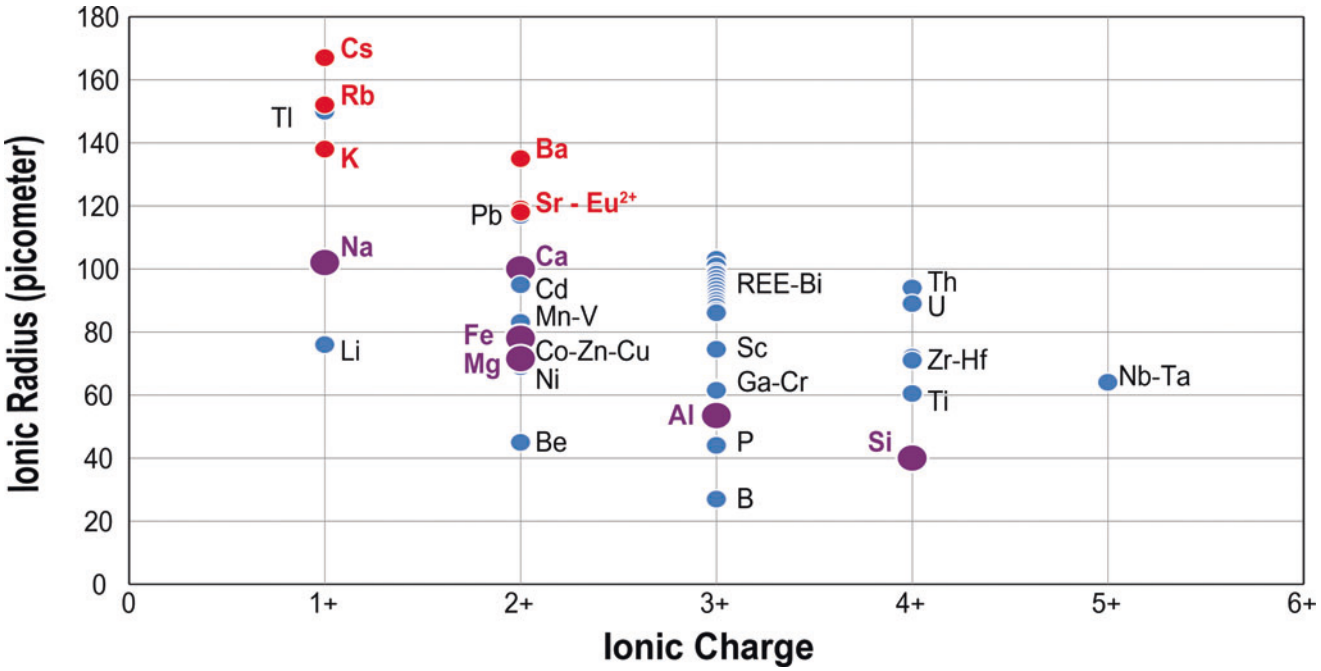

Large-Ion Lithophile Elements, Fig. 2 Ionic radius versus ionic charge diagram showing the LILE in *red*. Major cations are shown in large *purple* symbols and other trace elements are shown as small *blue* symbols

entry ▶ "Earth's Continental Crust"). Between 15–55% of the Earth's LILE budget is found in the continental crust (Rudnick and Fountain 1995).

Summary

The recommended list of large-ion lithophile elements is K, Rb, Sr, Cs, Ba, and Eu^{2+}.

Cross-References

- ▶ Alkali and Alkaline Earth Metals
- ▶ Earth's Continental Crust
- ▶ Incompatible Elements
- ▶ Mantle Geochemistry

References

Gast PW (1972) The chemical composition and structure of the moon. Moon 5:121–148
Hofmann AW (1997) Mantle geochemistry: the message form oceanic volcanism. Nature 385:219–229
Kelemen PB, Hanghøj K, Greene AR (2014) One view of the geochemistry of subduction-related magmatic arcs, with an emphasis on primitive andesite and lower crust. In: Rudnick RL (ed) The crust, Holland HD, Turekian KK (eds) Treatise on geochemistry, 2nd edn. Elsevier, Oxford. pp 749–806
Rudnick RL, Fountain DM (1995) Nature and composition of the continental crust: a lower crustal perspective. Rev Geophys 33:267–309
Rudnick RL, Gao S (2014) Composition of the continental crust. In: Rudnick RL (ed) The crust, Holland HD, Turekian KK (eds) Treatise on geochemistry, 2nd edn. Elsevier, Oxford, pp 1–51
White WM (2013) Geochemistry. Wiley, Chichester. 660p

Laser Ablation – Inductively Coupled Plasma Mass Spectrometry

Takafumi Hirata
Geochemical Research Center, The University of Tokyo, Tokyo, Japan

Definition

Mass spectrometers utilizing atmospheric pressure Ar-ICP as an ion source (ICP-MS) have been widely used for both element and isotopic analyses for geochemical samples such as rocks, minerals, aquatic solutions, as well as gaseous samples. Since the ICP is operating under atmospheric pressure, various sample introduction techniques can be applied for analysis. Among these, the laser ablation sampling technique is likely to become

a method of choice for many geochemists because it is a highly sensitive and versatile method of elemental and isotopic analyses. Laser ablation is the process of removing materials from the surface of solid materials by the irradiation of a laser beam. Laser-induced sample aerosols and vapors will be introduced to the ICP, and the ionized elements are extracted into a high-vacuum and separated by mass. With the LA-ICPMS technique, direct elemental and isotopic analyses can be made without chemical decomposition or dissolution procedures. Moreover, analytical capability for in situ elemental and isotopic analyses can be made in various spatial resolution, ranging from 1 to 1000 μm. The LA-ICPMS technique has opened up new applications for geochemistry, such as in situ stable isotope studies, in situ isotope dating, and simultaneous mappings for major to trace elements (imaging mass spectrometry).

Introduction

The mass spectrometric technique utilizing inductively coupled plasma as an ion source (ICP-MS) has been widely used for both abundance and isotope ratio measurements (e.g., Niu and Houk 1996; Hattendorf et al. 2003; Becker 2007). The basic advantage of the ICP-MS lies in the ion source, which achieves nearly complete ionization efficiency for almost all elements compared to other mass spectrometry techniques, such as thermal ionization mass spectrometry (TIMS) or secondary ion mass spectrometry (SIMS). The ICP high ionization efficiency can be achieved through both the charge-exchange reaction ($Ar^+ + M \rightarrow Ar + M^+$) and electron impact reaction ($M + e^-_{(fast)} \rightarrow M^+ + e^-_{(slow)}$). Moreover, long residence time of the sample in the ICP (i.e., >10 msec) results in smaller contribution of nonmass spectrometric interferences (e.g., matrix effect), providing high quantitative capability for elemental analysis.

The ICP ion source has further analytical advantages as it is possible to analyze dry sample aerosols produced by the laser ablation technique. The laser ablation technique is one of the most versatile solid sampling techniques for the ICP-MS (Durrant 1999; Günther and Hattendolf 2005). The interaction of laser beam with solid materials induce various effects including surface heating and melting to ejection of sample material. The material is released from solid materials as vapor, molten droplets, solid particulates, and its agglomerates. The laser-induced sample particles or vapors are introduced into the ICP, operating at atmospheric pressure, and the produced ions are extracted into the vacuum region through a vacuum interface (Fig. 1). Analytes are separated from major constituents through mass spectrometers, including a magnetic sector (MS), quadrupole (Q), or time-of-flight (TOF)-type mass spectrometers (e.g., Duckworth et al. 1986; Wieser and Schwieters 2005).

Signal intensity for analyses is dependent upon both the concentration and the total amount of sample released. Numerous laser parameters can affect the signal response, and the data quality is influenced by laser types, experimental

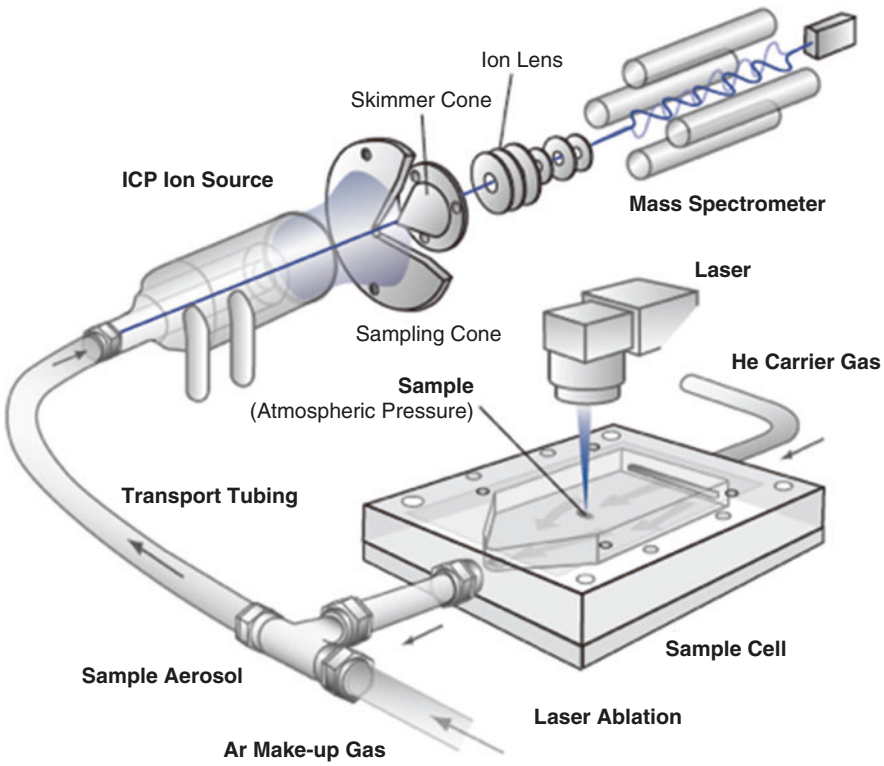

Laser Ablation – Inductively Coupled Plasma Mass Spectrometry,
Fig. 1 Schematic diagram of laser ablation-ICP-mass spectrometer. When focused laser beam with sufficient energy is directed onto the sample, material or constituent elements from surface will be explosively sputtered and evaporated. The laser-induced sample particles or vapors will be transported in mixture of He and Ar gas to the ICP for atomization ionization

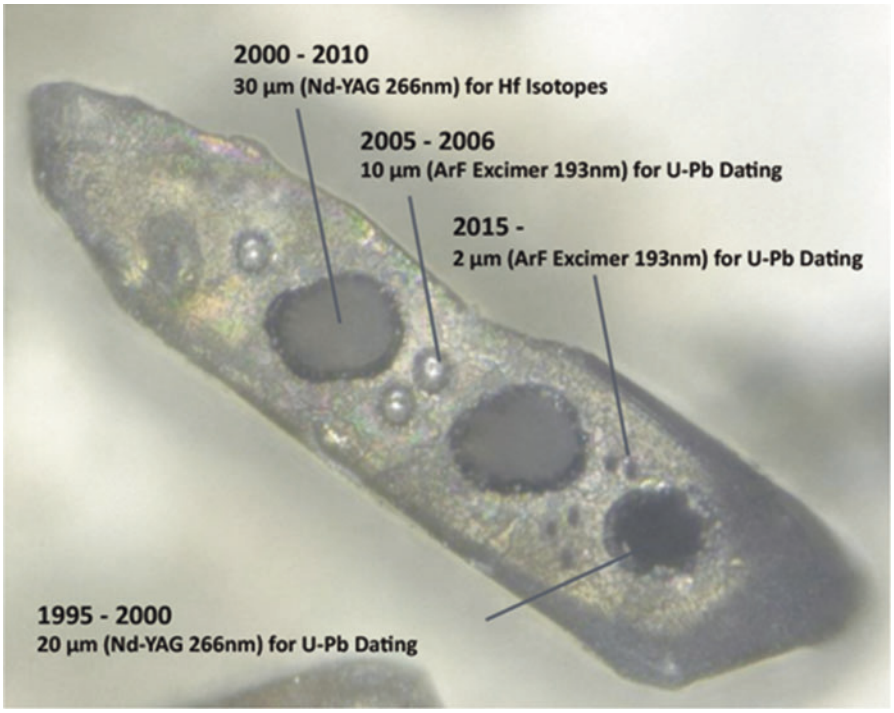

Laser Ablation – Inductively Coupled Plasma Mass Spectrometry,
Fig. 2 Comparison of the ablation pit size for in situ isotope chronology. Progresses in the LA-ICPMS technique can be well demonstrated by the size of ablation pits. With increasing of both the elemental sensitivity of the ICPMS system and better understanding of the mechanism for the laser ablation, smaller ablation pit size can be adopted for in situ elemental and isotopic analyses for geochemical samples (Sample: PMA7, courtesy of Dr. Jean Jacques Peucat, Univ. Rennes, France)

settings, or calibration strategy. Continuous improvements in enhancing the elemental sensitivity of ICP-MS instruments, together with a better understanding of the mechanism of the laser ablation process, have led to successive enhancements in both data quality and spatial resolution for in situ analysis (Fig. 2).

Multi-Element Determinations

The LA-ICPMS technique has been widely used for rapid multielement determinations for major to trace elements in rocks or minerals (e.g., Hattendorf et al. 2003; Jochum et al. 2007; Fricker et al. 2011; YongSheng et al. 2013). Typical size of the laser ablation pit, adopted for the elemental analysis, ranges from approximately 20–60 µm. Despite the slightly poor spatial resolution, the LA-ICPMS technique has major advantages on the elemental sensitivity, compared to the conventional probe techniques, including electron probe microprobe analyzer (EPMA) or micro-X-ray fluorescence (µXRF) techniques (e.g., Weiss et al. 2008).

Limits of detection and the resulting precision of the measurements are significantly influenced by three major parameters: (a) matrix effect, (b) particle size distribution of laser-induced same particles, and (c) mass spectrometric inferences by isobaric ions or polyatomic ions (Longerich et al. 1996; Günther et al. 1997; Kozlov et al. 2003; Koch et al. 2006). Among these, size distribution of the laser-induced sample particles is one of the most important parameters to achieve better precision and accuracy of the measurements (Koch et al. 2004; Kuhn et al. 2004). For geochemical samples, UV wavelength lasers, such as ArF Excimer laser (193 nm) or Nd:YAG 5HG (213 nm), can produce smaller size distribution of the sample particles, which result in higher atomization and ionization efficiency in the ICP. Moreover, with the smaller sample particles, a smoothed signal intensity profile can be obtained, resulting in higher precision in the elemental analysis. With UV laser and with ablation pit of 30–40 µm, typical detection limits of better than 10 ng/g can be achieved by the LA-ICPMS system.

The limits of detection for trace elements in silicates or ceramic materials are generally superior to those for the elements in metallic materials. The lower signal response from metallic materials is mainly due to reduced ablation yield, which is caused by the energy loss through high-thermal conductivity of the metallic materials. Moreover, incomplete heating results in the release of molten particles from solid samples or preferential release of the volatile elements from the samples (i.e., large elemental fractionation during the laser ablation), which can be a major source of analytical error. To minimize the elemental fractionation during the laser ablation, the use of shorter pulse duration could be the best solution as the rate of thermal diffusion for metallic materials (e.g., >10 ps) is significantly longer than the typical pulse duration achieved by femtosecond lasers (10–500 fs) (Koch et al. 2004, 2006; Hirata and Miyazaki 2007). Smaller contribution of the laser-induced heating onto the sample materials can result in minimal size-related elemental fractionation during the laser ablation. With femtosecond lasers, signal responses obtained from metallic Cu improve by a

factor of 20, compared with that obtained with conventional nanosecond lasers (Zeng et al. 2004; Horn and Blanckenburg 2007; Hirata and Kon 2008).

Quantification Protocol

The LA-ICPMS technique has further analytical advantages as it is less sensitive to the matrix effect (non-mass spectrometric interferences) for the analytes. The smaller contribution of the matrix effect is mainly related to two factors. (1) A long-residence time for the ionization process within the ICP with typical time duration for the sample particles exceeding 10 ms, which is significantly longer compared to most other ion sources adopted for the mass spectrometer. (2) Post-ionization system setup in the LA-ICPMS technique as the sampling (laser ablation) and ionization processes are separate steps. This implies that laser operational settings and ionization conditions can be optimized independently. In fact, qualitative or semiquantitative analysis can be made with a nonmatrix matched calibration standard. Nevertheless, it should be noted that the matrix-matched calibration standard is highly desired for elemental and isotopic analysis of solid geochemical materials.

Availability of a calibration standard is a key issue to obtain reliable elemental and isotopic data. For the LA-ICPMS technique, matrix-matched standards have been widely used for the calibration. However, data traceability cannot be maintained based on an inhouse standard, in which the evaluation of heterogeneity would be difficult. To overcome this, calibration using the synthetic glass standards (e.g., USGS BCR-2G, BHVO-2G, BIR-1G etc.), NIST SRM glasses (e.g., NIST SRM610, 612, or 613 etc.) or MPI-DING (MPI-DING glasses KL2-G, ML3B-G, StHs6/80-G, GOR128-G etc.), combined with internal standardization using major-minor elements (e.g., Ca, Si, P, or Sr) is a widely adopted analytical approach (e.g., Myers et al. 1995; Pearce et al. 1997; Jochum et al. 2005; Jochum et al. 2006). Typical precision or accuracy of the abundance measurements ranges from 1% to 20% with a spatial resolution of 30 μm. One of the major sources of the analytical error is the counting statistics, and therefore, great care must be given to control the number of analytes. Although longer ablation can reduce the contribution of counting statistics for the analytes, laser ablation with high aspect-ratio craters (i.e., deep ablation pit) can induce elemental fractionation during analysis (e.g., down-hole fractionation) (Hirata and Nesbitt 1995; Horn et al. 2000). To obtain reliable abundance data, data acquisition must be made with a minimal number of analytes and short-time duration for the laser ablation.

Several additional techniques can be applied for quantitative analysis. Isotope dilution represents an important choice for elemental determinations. For the LA-ICPMS technique, mixing of analytes and enriched-isotopes can be achieved by mixing of laser-induced aerosols released from a sample and standard, which contains the selected enriched isotopes. This can be achieved by applying galvanometric optics (Fig. 3), which is utilizing a pair of two moving mirrors. The position of the laser ablation can be moved by changing the angle of the mirrors. With galvanometric optics, ablation points can be jumped with a time interval of 10 ms or shorter, and therefore, the simultaneous laser ablation for two or more solid materials

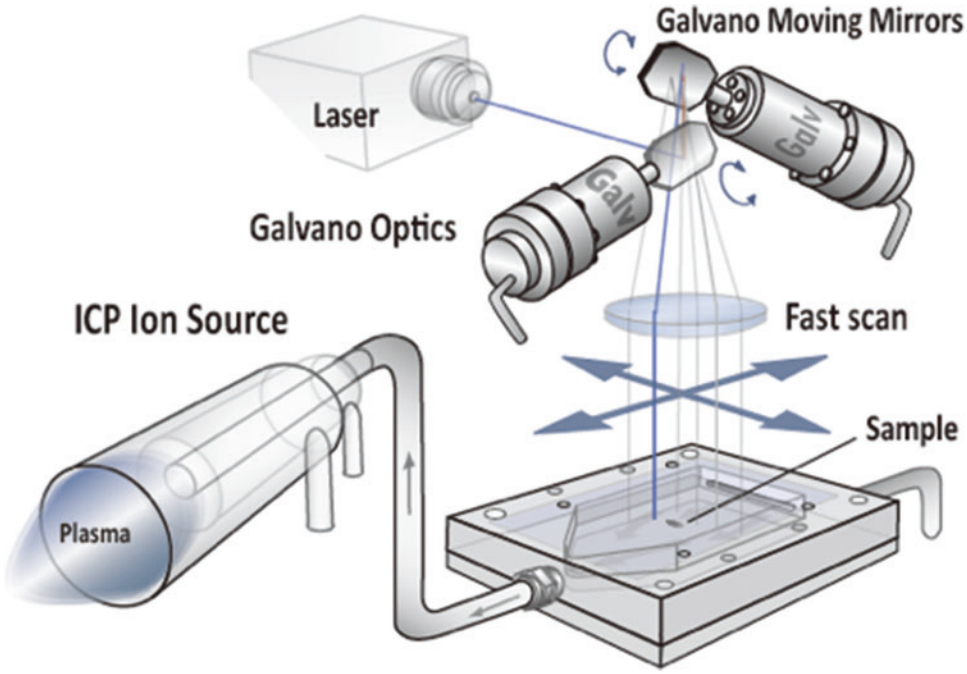

Laser Ablation – Inductively Coupled Plasma Mass Spectrometry,
Fig. 3 Schematic diagram of galvanometric optics for LA-ICPMS. Galvanometric optics consists of two moving mirrors. Ablation points can be moved by adjusting the angle of two mirrors. With the LA system equipped with the galvanometric optics, two or more sample can be ablated nearly at the same time. This suggests that analytes in the different solid materials can be mixed

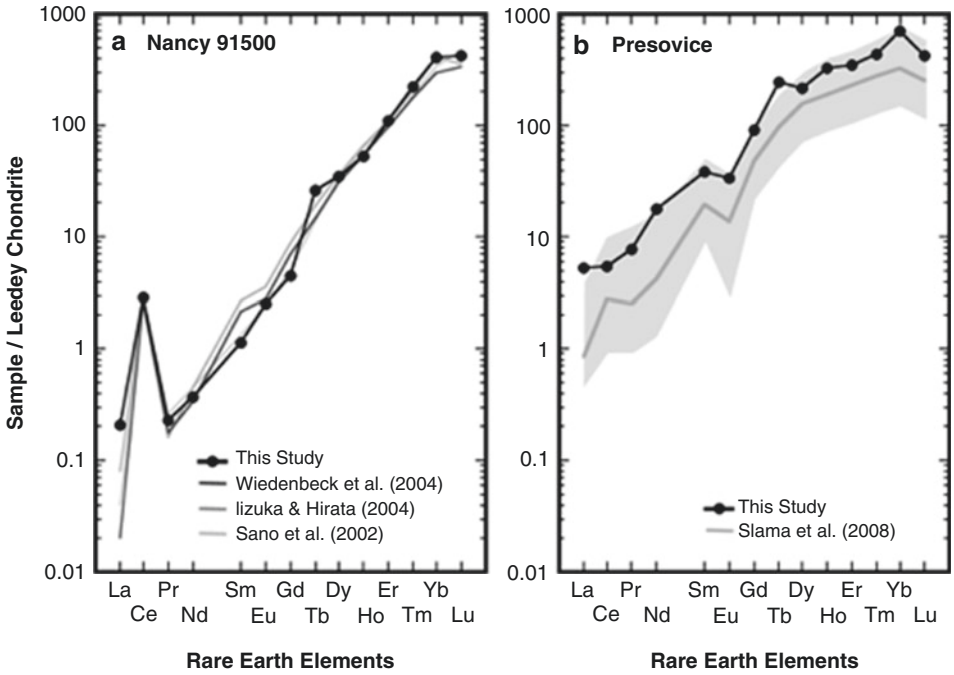

Laser Ablation – Inductively Coupled Plasma Mass Spectrometry,
Fig. 4 Determination of rare earth elements (REE) in zircon samples by means of the standard addition technique. With the galvanometric optics, standard addition technique can be applied for the elemental determinations. The particles released from sample was mixed with the particles released from standard materials, and mixed particles were then introduced into the ICP ion source (Yokoyama et al. 2011)

can be obtained. The sample aerosols released from two or three samples are well mixed in the laser ablation cell, and the mixed aerosols are introduced into the ICP. Based on the signal intensity data for isotopes, the element concentrations can be defined (Fernandez et al. 2008; Heilmann et al. 2009).

With the galvanometric optics, a standard addition method can also be applied by mixing of aerosols released from sample and standard references. The mixing ratio (sample: standard) can be controlled by changing the number of laser shots for each component. Abundances of rare earth elements (REE) in natural zircon samples can be determined by the standard addition technique by mixing of REEs from glass standard material (Fig. 4) (Yokoyama et al. 2011). The galvanometric optics can provide flexible calibration protocols for elemental analysis, where no proper (matrix-matched) calibration standard is available (Fig. 4).

In Situ Isotope Ratio Measurements

Precision and accuracy in isotope ratio measurements can be dramatically improved by the multiple collector system setup adopted in the magnetic sector based ICP-mass spectrometry (MC-ICPMS) (e.g., Albarède et al. 2004; Walczyk 2004). Combination of LA and MC-ICPMS techniques (LA-MC-ICPMS) enables to detect small variations in the isotope ratios of elements in small minerals or inclusions (Iizuka and Hirata 2005; Horn and Blanckenburg 2007; Nishizawa et al. 2010). For in situ isotope ratio measurements, several key parameters, such as size distribution of the aerosols, aspect ratios, aerosol transport efficiencies, ionization efficiencies in the plasma and/or laser-induced isotope fractionation, must be considered to obtain reliable isotope ratio data (Jackson and Günther 2003; Hirata 2012).

Similar to the elemental analysis, advances in laser ablation utilizing shorter wavelength and shorter pulse duration lasers (i.e., femtosecond lasers) provide better analytical results (Guillong et al. 2003; Koch et al. 2006; Russo et al. 2013). With the UV wavelength laser ablation, particle size distribution can be modified toward smaller, and therefore, stable signal intensity profiles. Smoother signal intensity profile is essential for isotope ratio measurements using Faraday collectors caused by slow response of the Faraday amplifier. With unstable or transient signals, the measured isotope ratios can deviate from the accurate ratios (Hirata 2012). To overcome this, analysis of smaller size distribution of the sample particle is important (Guillong and Günther 2002). Introduction of smaller particles results in smaller changes in the plasma conditions, such as kinetic temperature, electron density, or plasma potential. Moreover, with a femtosecond laser ablation, the efficiency of energy transfer from laser photons to electrons in solid samples can be dramatically improved (Hirata and Kon 2008; Poitrasson et al. 2003; Russo et al. 2002). This leads the release of smaller particles from samples. This results in both a stable signal intensity profile and smaller changes in elemental sensitivity and/or mass bias factors for the isotope ratio measurements. With the combination of fs-laser ablation and MC-ICP-MS, a precision of better than 0.1‰ can be achieved for most Fe and Cu-rich materials (e.g., metal, oxide, or sulfide). The resulting precision of the isotope ratio measurements is significantly better than the natural variations in the $^{56}Fe/^{54}Fe$, $^{65}Cu/^{63}Cu$

or $^{98}Mo/^{95}Mo$ ratios (e.g., Horn et al. 2000; Ikehata et al. 2008). The major advantage to use the LA-MC-ICPMS is the reliable and inherent isotopic signature that can be derived from a specific small sample area, avoiding the risk of analysis from secondary growth regions or contaminated areas (e.g., Nishizawa et al. 2010; Yoshiya et al. 2015a, 2015b) (Fig. 5).

In Situ Dating

Applications of several isotope chronometers have been developed by the MC-ICPMS technique comprising the Lu-Hf, Hf-W, and U-Pb isotope chronometers. High ionization efficiency can be achieved by the ICP ion source, and precise and accurate isotopic analyses from small sample size can be obtained by the MC-ICPMS (Thirlwall and Walder 1995; Tiepolo 2003; Iizuka and Hirata 2004, 2005; Snow and Friedrich 2005). Even for more conventional isotope chronometers, such as Rb-Sr, Sm-Nd, and U-Pb dating by TIMS analysis, the MC-ICPMS technique has become a major tool for the measurements as the MC-ICPMS enables a higher sample throughput and simpler chemical separation procedures. In fact, MC-ICPMS has been widely applied for the fast and precise Nd and Hf isotope ratio measurements (e.g., Woodhead 2002; Sims et al. 2008; Be'eri-Shlevin et al. 2010). The ICP-MS technique is now one of the principal methods for isotope analysis for geochronological studies.

For the U-Pb dating method, the isotopic composition of Pb can vary widely due to contribution of radioactive decay of ^{232}Th, ^{235}U, and ^{238}U, by reflecting both the Pb/U and Pb/Th ratios and the age of the samples. Because of small contribution of mass spectrometric interferences onto the Pb, Th, and U isotopes, single collector-based ICP-MS instrument were widely used for the U-Th-Pb age determinations (Hirata and Nesbitt 1995; Crowley et al. 2005; Tiepolo 2003; Simonetti et al. 2005; Cottle et al. 2009; Woodhead et al. 2009; Schaltegger et al. 2015). The resulting precision and accuracy of the U-Th-Pb age determinations can be further improved by a multiple-collector system setup (Jackson et al. 2004). The MC-ICPMS instruments, equipped with a multiple ion counting system setup, can improve the precision of the age determination (Fig. 6), and the data quality achieved by the LA-ICPMS technique is comparable or enhanced compared to those obtained by secondary ion mass spectrometry (SIMS), including SHRIMP-type instruments (Ireland and Williams 2003; Rasmussen et al. 2004; Holden et al. 2009). Moreover, the analysis time for U-Th-Pb age determinations can be significantly reduced by a multiple ion counting system setup to 1–10 sec/spot with shorter analysis time enabling to obtain an age distribution of the zircons collected from a sample (Hattori et al. 2017; O-bayashi et al.

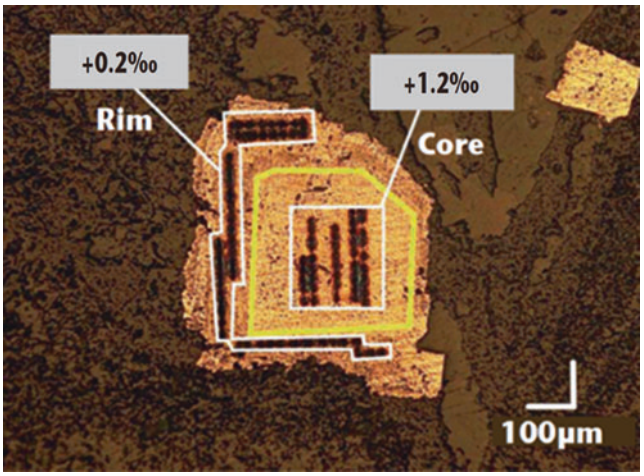

Laser Ablation – Inductively Coupled Plasma Mass Spectrometry, Fig. 5 In situ $^{56}Fe/^{54}Fe$ isotope ratio data obtained from core and rim of the single pyrite grain. Pyrite grain shown here consists of two domains: core and rim. With the LA-MC-ICPMS technique, Fe isotope signature from distinguished can be derived (Nishizawa et al. 2010)

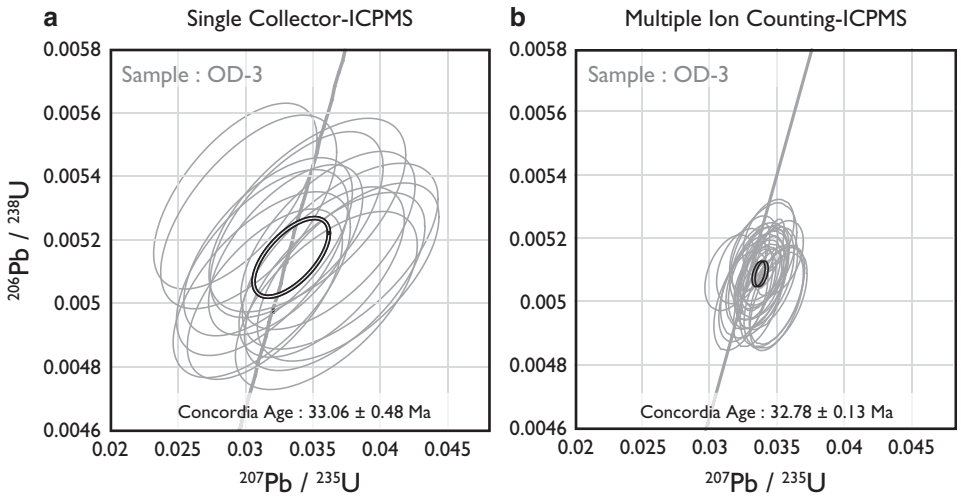

Laser Ablation – Inductively Coupled Plasma Mass Spectrometry, Fig. 6 Comparison in the resulting precision of the Pb/U ratio measurements between single collector-ICPMS and multiple ion counting-ICPMS. With the LA-ICPMS technique combined with multiple ion counting technique, the resulting precision of the U-Pb ages can be dramatically improved. Moreover, total analysis time can be shortened, obviating the laser sampling with high aspect ratio (i.e., deep drilling). Sample is OD-3 standard zircon (Iwano et al. 2013)

2017). This analytical approach allows to decipher the contribution of multiple geological events or multiple sources of the zircons. The "age distribution" is a useful and conventional approach to understand the geological sequence underlying the sample formation. Advantage of the age distribution analysis can be well demonstrated by the growth rate of the continental crust based on the U-Pb ages and Lu-Hf isotope systematics derived from >500 to 20,000 zircon grains (Rino et al. 2004; Iizuka et al. 2006).

With shorter duration time for the laser ablation, the resulting depth of the ablation pit can be smaller than 1 μm, and therefore, age determinations from thin-layer rim of zircon crystal can be made. Schmitt (2011) reported that the U-Th-Pb age derived from the outer rim (<5 μm) of the zircon crystals can reflect the timing of overgrowth through eruption processes (Schmitt 2011). This means that multiple chronological information can be derived from a single zircon grain. With the shorter ablation time achieved by the MC-ICPMS system setup, precise U-Th-Pb ages can be derived from the depth of shallower than 1 μm. This technique can be applied for geochemical evolution processes within magma chambers by determining the difference between crystallization of the zircons and timing of eruption, and thus the U-Th-Pb ages obtained from the rim of zircon crystals can reflect low-temperature geological events (e.g., Rasmussen et al. 2004; Schmitt 2011; Sakata et al. 2017).

Imaging

Images of trace elements or isotopes can provide key information to evaluate the contribution of metamorphic events or movements of elements through secondary heating events. The LA-ICPMS technique is a useful tool to obtain image data of major to trace elements from samples. Elemental and isotope images can be obtained by repeated analysis of line-scanning measurements using the LA-ICPMS technique. Time resolved-signal intensity profile obtained by laser rastering can be converted to a position based-signal intensity profile via the relationship between the rastering rate and the elapsed time. The resulting spatial resolution and the elemental sensitivity is dependent upon several key operational parameters such as size of laser beam, raster rate, and time slice of the data acquisitions (i.e., dwell time for each analytes). Typically laser beam size of 1–100 μm is used for imaging analysis. The LA-ICPMS technique is highly sensitive to determine the abundance of the trace elements (e.g., Ghazi et al. 2002; Durrant 1999; Russo et al. 2013). One of the main advantages to use the LA-ICPMS technique for imaging analysis is that the sample is located under atmospheric pressure, and neither evacuation of the sample housing nor coating with conductive materials is required. Moreover, because of both the minimum sample preparation and the postionization system configurations, the LA-ICPMS technique represents a fast and accurate method for quantitative imaging technique for trace elements from biochemical or geochemical samples (e.g., Jackson et al. 2006; Lobinski et al. 2006; Zoriy et al. 2007; Becker 2007; Becker et al. 2010; Hare et al. 2011; Gordalíza et al. 2011; Konz et al. 2011).

Another important feature of the elemental imaging using the LA-ICPMS technique is the analytical capability for large-sized samples (>10 mm). This is of crucial importance to secure a bridge between the microscopic and macroscopic realm in geochemical studies. The elemental imaging for trace elements is an essential tool to derive inherent information from samples. Figure 7 illustrates an example of the mapping image for ^{57}Fe, ^{60}Ni, ^{103}Rh, ^{178}Hf, ^{182}W, and ^{193}Ir isotopes obtained from calcium and aluminum-rich inclusion (CAIs) in chondrite material, demonstrating a clear difference of the distribution pattern for these isotopes. Difference in the distribution pattern of the isotopes can reflect the cosmochemical features of the elements. Moreover, the images suggest possible contribution of a re-distribution or secondary movement of these elements through heating or weathering. In addition, difference or similarity in the distribution pattern of the elements may provide key information concerning the status of system closure for chronologies.

Several alternative analytical techniques, such as EPMA, SIMS, or μXRF, can be applied for in situ imaging analysis. The SIMS technique allows both high sensitivity and high-spatial resolution (e.g., Chandra and Morrison 1995; McDonnell and Heeren 2007; Becker et al. 2010), whereas the μXRF technique has been recognized as one of the most reliable imaging techniques for the trace elements (Matsuyama et al. 2006; Fukuda et al. 2008; Donner et al. 2011). Despite the unique features of these techniques, they are time-consuming and therefore less suitable for the routine high throughput analysis. More importantly, these techniques are not suitable for imaging analysis for large-sized samples (> 1 mm). The LA-ICPMS technique is likely to become a significant, quantitative, and cost-effective tool for elemental and isotopic imaging, as it is highly user friendly and an efficient method for supplementary in situ imaging.

Summary and Conclusions

The laser ablation-inductively coupled plasma mass spectrometry (LA-ICPMS) technique is widely accepted as one of the most advanced, sensitive, and rapid analytical tools for elemental and isotopic analysis of solid materials. The continuous development of the LA-ICPMS techniques has provided precise elemental and isotopic data. With a better understanding of the mechanism of the laser ablation process, and with a higher elemental sensitivity of the LA-ICPMS technique, the precision of the isotopic ratio

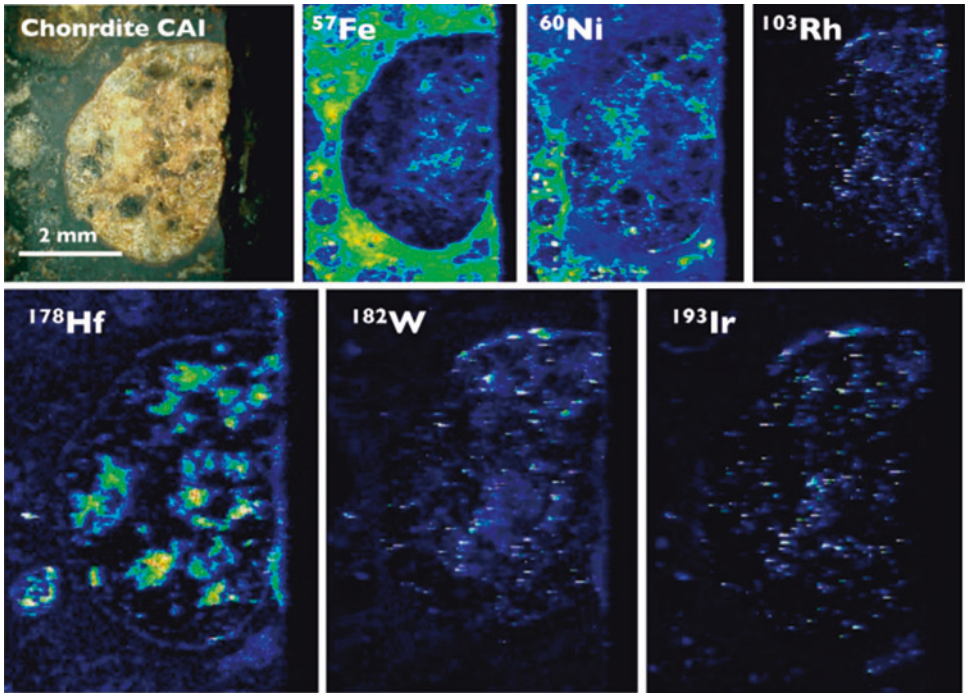

Laser Ablation – Inductively Coupled Plasma Mass Spectrometry, Fig. 7 Isotope imaging for trace elements in CAI. With the LA-ICPMS technique, the elemental and isotopic mapping analyses can be made on various geochemical materials of various sizes (μm scale to mm scale). This is very important to evaluate the contamination, secondary movement of the elements, and/or system closure of the minerals

measurement has successively improved, and new applications were developed in various research fields such as bioscience, material science, and archeological science. Despite its success, it should be noted that there still remain several possible cause for the analytical error such as elemental fractionation occurring during laser ablation, or the limited spatial resolution and elemental sensitivity for the analytes achieved by the LA-ICPMS technique. The complexity in the physical and chemical processes related to the laser ablation of solid samples has prevented a detailed understanding of the elemental and isotopic fractionation induced by laser ablation, and therefore, both the instrumental developments and understanding of further detailed mechanism for the laser ablation would be still a key issue to improve the data quality. Continuous technological developments will enable new analytical methodologies to derive geochemical information from the samples. Based on the rapid growth in analytical capabilities demonstrated in last decade, a realistic prospect is that the LA-ICPMS technique has immediate potential as a reconnaissance method for both the in situ stable isotope geochemistry or isotope chronology. Now the LA-ICPMS technique has evolved into a unique analytical approach, not the alternative choice.

Cross-References

- ▶ Chondrites
- ▶ Geochronology and Radiogenic Isotopes
- ▶ Inductively Coupled Plasma Mass Spectrometry (ICP-MS)
- ▶ Refractory Inclusions in Chondritic Meteorites
- ▶ Stable Isotope Geochemistry
- ▶ Zirconium

References

Albarède F, Telouk P, Blichert-Toft J, Boyet M, Agranier A, Nelson B (2004) Precise and accurate isotopic measurements using multiple-collector ICPMS. Geochim Cosmochim Acta 68:2725–2744

Be'eri-Shlevin Y, Katzir Y, Blichert-Toft J, Kleinhanns IC, Whitehouse MJ (2010) Nd–Sr–Hf–O isotope provinciality in the northernmost Arabian–Nubian shield: implications for crustal evolution. Contrib Mineral Petrol 160:181–201

Becker JS (2007) Inorganic mass spectrometry: principles and applications. Wiley Blackwell and Wiley VCH, New Jersey, United states

Becker JS, Zoriy M, Becker JS, Dobrowolska J, Matusch A (2007) Laser ablation inductively coupled plasma mass spectrometry (LA-ICP-MS) in elemental imaging of biological tissues and in proteomics. J Anal At Spectrom 22:736–744

Becker JS, Breuer U, Hsieh HF, Osterholt T, Kumtabtim U, Wu B, Matusch A, Caruso JA, Qin Z (2010) Bioimaging of metals and biomolecules in mouse heart by laser ablation inductively coupled plasma mass spectrometry and secondary ion mass spectrometry. Anal Chem 82:9528–9533

Chandra S, Morrison GH (1995) Imaging ion and molecular transport at subcellular resolution by secondary ion mass spectrometry. Int J Mass Spectrom 143:161–176

Cottle JM, Hortswood MSA, Parrish RR (2009) A new approach to single shot laser ablation analysis and its application to in situ Pb/U geochronology. J Anal Atom Spectrom 24:1355–1363

Crowley JL, Myers JS, Sylvester PJ, Cox RA (2005) Detrital zircon from the Jack Hills and Mount Narryer, Western Australia: evidence for diverse 14.0 Ga source rocks. J Geol 113:239–263

Donner E, Howard DL, de Jonge MD, Paterson D, Cheah MH, Naidu R, Lombi E (2011) X-ray absorption and micro X-ray fluorescence

spectroscopy investigation of copper and zinc speciation in biosolids. Environ Sci Technol 45:7249–7257
Duckworth HE, Barber RC, Venkatasubramanian LVS (1986) Mass spectroscopy, 2nd edn. Cambridge University Press, Cambridge, MA, 74pp
Durrant JF (1999) Laser ablation inductively coupled mass spectrometry: achievements, problems, prospects. J Anal At Spectrom 12:1385–1403
Fernandez B, Claverie F, Pecheyran C, Alexis J, Donard OFX (2008) Direct determination of trace elements in powdered samples by in-cell isotope dilution femtosecond laser ablation ICPMS. Anal Chem 80:6981–6994
Fricker MB, Kutscher D, Aeschlimann B, Frommer J, Dietiker R, Bettmer J, Günther D (2011) High spatial resolution trace element analysis by LA-ICP-MS using a novel ablation cell for multiple or large samples. Int J Mass Spectrom 307:39–45
Fukuda N, Hokura A, Kitajima N, Terada Y, Saito H, Abe T, Nakai I (2008) Micro X-ray fluorescence imaging and micro X-ray absorption spectroscopy of cadmium hyper-accumulating plant, *Arabidopsis* halleri ssp. gemmifera, using high-energy synchrotron radiation. J Anal At Spectrom 23:1068–1075
Ghazi AM, Wataha CJ, O'Dell NL, Singh BB, Simmons R, Shuttleworth S (2002) Quantitative concentration profiling of nickel in tissues around metal implants: a new biomedical application of laser ablation sector field ICP-MS. J Anal At Spectrom 17:1295–1299
Gordalíza EM, Giesen C, Lázaro A, Fernández DE, Humanes B, Cañas B, Panne U, Tejedor A, Jakubowski A, Gómez-Gómez MM (2011) Elemental bioimaging in kidney by LA-ICP-MS as a tool to study nephrotoxicity and renal protective strategies in cisplatin therapies. Anal Chem 83:7933–7940
Guillong M, Günther D (2002) Effect of particle size distribution on ICP-induced elemental fractionation in laser ablation inductively coupled plasma mass spectrometry. J Anal At Spectrom 17:831–837
Guillong M, Horn I, Günther D (2003) A comparison of 266 nm, 213 nm and 193 nm produced from a single solid state Nd: YAG laser for laser ablation ICP-MS. J Anal At Spectrom 18:1224–1230
Günther D, Hattendolf B (2005) Solid sample analysis using laser ablation inductively coupled plasma mass spectrometry. Trends Anal Chem 24:255–265
Günther D, Frischknecht R, Heinrich C, Kahlert HJ (1997) Capabilities of an argon fluoride 193 nm excimer laser for laser ablation inductively coupled plasma mass spectrometry microanalysis of geological mateirals. J Anal At Spectrom 12:939–944
Hare D, Austin C, Doble P, Arora M (2011) Elemental bio-imaging of trace elements in teeth using laser ablation-inductively coupled plasma-mass spectrometry. J Dent 39:397–403
Hattendorf B, Latkoczy C, Günther D (2003) Laser ablation-ICPMS. Anal Chem 75:341A–347A
Hattori K, Sakata S, Tanaka M, Orihashi Y, Hirata T (2017) U–Pb age determination for zircons using later ablation-ICP-mass spectrometry equipped with six multiple-ion counting detectors. J Anal Atom Spectrom 32:88–95
Heilmann J, Boulyga SF, Heumann KG (2009) Development of an isotope dilution laser ablation ICP-MS method for multi-element determination in crude and fuel oil samples. J Anal At Spectrom 24:385–390
Hirata T (2012) Advances in laser ablation-multi-collector inductively coupled plasma mass spectrometry, Chapter 4. In: Vanhaecke F, Degryse P (eds) Isotopic analysis: fundamentals and applications using ICP-MS. Wiley-VCH Verlag GmbH & Co. KGaA, Somerset, pp 93–112
Hirata T, Kon Y (2008) Evaluation of the analytical capability of NIR femtosecond laser ablation–inductively coupled plasma mass spectrometry. Anal Sci 24:345–353
Hirata T, Miyazaki Z (2007) High-speed camera imaging for laser ablation process: for further reliable elemental analysis using inductively coupled plasma-mass spectrometry. Anal Chem 79:147–152
Hirata T, Nesbitt RW (1995) U–Pb isotope geochronology of zircon: evaluation of the laser probe-inductively coupled plasma mass spectrometry technique. Geochim Cosmochim Acta 59:2491–2500
Holden P, Lanc P, Ireland TR, Harrison TM, Foster JJ, Bruce Z (2009) Mass-spectrometric mining of Hadean zircons by automated SHRIMP multi-collector and single-collector U/Pb zircon age dating: the first 100,000 grains. Int J Mass Spectrom 286:53–63
Horn I, Blanckenburg F (2007) Investigation on elemental and isotopic fractionation during 196 nm femtosecond laser ablation multiple collector inductively coupled plasma mass spectrometry. Spectrochim Acta 62B:410–422
Horn I, Rudnick RL, McDonough WF (2000) Precise elemental and isotope ratio determination by simultaneous solution nebulization and laser ablation-ICP-MS: application to U–Pb geochronology. Chem Geol 164:281–301
Iizuka T, Hirata T (2004) Simultaneous determinations of U-Pb age and REE abundances for zircons using ArF excimer laser ablation-ICPMS. Geochem J 38:229–241
Iizuka T, Hirata T (2005) Improvements of precision and accuracy in in situ Hf isotope microanalysis of zircon using the laser ablation-MC-ICPMS technique. Chem Geol 220:121–137
Iizuka T, Horie K, Komiya T, Maruyama S, Hirata T, Hidaka H, Windley BF (2006) 4.2 Ga zircon xenocryst in an Acasta gneiss from northwestern Canada: evidence for early continental crust. Geology 34:245–248
Ikehata K, Notsu K, Hirata T (2008) In situ determination of Cu isotope ratios in copper-rich materials by NIR femtosecond LA-MC-ICP-MS. J Anal Atom Spectrom 23:1003–1008
Ireland TR, Williams I (2003) Considerations in zircon geochronology by SIMS. In: Hanchar JM, Hoskin PWO (eds) Zircon. Reviews in mineralogy and geochemistry, vol 53. Mineralogical Society of America, Washington, DC, 215–241 pp
Iwano H, Orihashi Y, Hirata T, Ogasawara M, Danhara T, Horie K, Hasebe N, Sueoka S, Tamura A, Hayasaka Y, Katsube A, Ito H, Tani K, Kimura K-J, Chang Q, Kouchi Y, Haruta Y, Yamamoto K (2013) An inter-laboratory evaluation of OD-3 zircon for use as a secondary U–Pb dating standard. Island Arc 22:382–394
Jackson SE, Günther D (2003) The nature and sources of laser-induced isotopic fractionation in laser ablation multicollector inductively coupled plasma mass spectrometry. J Anal At Spectrom 18:205–212
Jackson S, Pearson N, Griffin W, Belousova E (2004) The application of laser ablation-inductively coupled plasma-mass spectrometry to in situ U–Pb zircon geochronology. Chem Geol 211:47–69
Jackson B, Harper S, Smith L, Flinn J (2006) Elemental mapping and quantitative analysis of Cu, Zn, and Fe in rat brain sections by laser ablation ICP-MS. Anal Bioanal Chem 384:951–957
Jochum KP, Nohl U, Herwig K, Lammel E, Stoll B, Hofmann AW (2005) GeoReM: a new geochemical database for reference materials and isotopic standards. Geostand Geoanal Res 29:333–338. https://doi.org/10.1111/j.1751-908X.2005.tb00904.x
Jochum KP, Stoll B, Herwig K, Willbold M, Hofmann AW, Amini M, Aarburg S, Abouchami W, Hellebrand E, Mocek B, Raczek I, Stracke A, Alard O, Bouman C, Becker S, Dücking M, Brätz H, Klemd R, de Bruin D, Canil D, Cornell D, de Hoog CJ, Dalpé C, Danyushevsky L, Eisenhauer A, Gao Y, Snow JE, Groschopf N, Günther D, Latkoczy C, Guillong M, Hauri EH, Höfer HE, Lahaye Y, Horz K, Jacob DE, Kasemann SA, Kent AJR, Ludwig T, Zack T, Mason PRD, Meixner A, Rosner M, Misawa K, Nash BP, Pfänder J, Premo WR, Sun WD, Tiepolo M, Vannucci R, Vennemann T, Wayne D, Woodhead JD (2006) MPI-DING reference glasses for in situ microanalysis: new reference values for element concentrations and isotope ratios. Geochem Geophys Geosyst 7:1–44. https://doi.org/10.1029/2005GC001060

Jochum KP, Stoll B, Herwig K, Willbold M (2007) Validation of LA-ICP-MS trace element analysis of geological glasses using a new solid-state 193 nm Nd: YAG laser and matrix-matched calibration. J Anal At Spectrom 22:112–121

Koch J, Bohlen A, Hergenrer R, Niemax K (2004) Particle size distributions and compositions of aerosols produced by near-IR femto- and nanosecond laser ablation of brass. J Anal At Spectrom 19:267–272

Koch J, Walle M, Pisonero J, Günther D (2006) Performance characteristics of ultra-violet femtosecond laser ablation inductively coupled plasma mass spectrometry at similar to 265 and similar to 200 nm. J Anal At Spectrom 21:932–940

Konz I, Fernandez B, Fernandez ML, Pereiro R, Sanz-Medel A (2011) Absolute quantification of human serum transferrin by species-specific isotope dilution laser ablation ICP-MS. Anal Chem 83:5353–5360

Kozlov B, Saint A, Skroce A (2003) Elemental fractionation in the formation of particulates, as observed by simultaneous isotopes measurement using laser ablation ICP-oa-TOFMS. J Anal At Spectrom 18:1069–1075

Kuhn H, Guillong M, Günther D (2004) Size-related vaporisation and ionisation of laser-induced glass particles in the inductively coupled plasma. Anal Bioanal Chem 378:1069–1074

Lobinski R, Moulin C, Ortega R (2006) Imaging and speciation of trace elements in biological environment. Biochimie 88:1591–1604

Longerich H, Günther D, Jackson S (1996) Elemental fractionation in laser ablation inductively coupled plasma mass spectrometry. Fresenius J Anal Chem 355:538–542

Matsuyama S, Mimura H, Yumoto H, Sano Y, Yamamura K, Yabashi M, Nishino Y, Tamasaku K, Ishikawa T (2006) Development of scanning xray Fuorescence microscope with spatial resolution of 30nm using KirkpatrickBaez mirror optics. Rev Sci Instrum 77:103–102

McDonnell LA, Heeren RMA (2007) Imaging mass spectrometry. Mass Spectrom Rev 26:606–643

Myers AT, Havens RG, Niles WW (1995) Glass reference standards for trace element analysis of geologic materials. Dev Appl Spectrosc 8:132–137pp

Nishizawa M, Yamamoto H, Ueno Y, Tsuruoka S, Shibuya T, Sawaki Y, Yamamoto S, Kon Y, Kitajima K, Komiya T, Maruyama S, Hirata T (2010) Grain-scale iron isotopic distribution of pyrite from Precambrian shallow marine carbonate revealed by femtosecond laser ablation multi-collector ICP-MS technique: potential proxy for the redox state of ancient seawater. Geochim Cosmochim Acta 74:2760–2778

Niu H, Houk RS (1996) Fundamental aspects of ion extraction in inductively coupled plasma mass spectrometry. Spectrochim Acta 51B:779–815

O-bayashi H, Tanaka M, Hattori K, Sakata S, Hirata T (2017) In-situ $^{207}Pb/^{206}Pb$ isotope ratio measurement using dual-daly ion counting ICP-mass spectrometer. J Anal Atom Spectrom 32:686–691

Pearce NJG, Perkins WT, Westgate JA, Gorton MP, Jackson SE, Neal CR, Chenery SP (1997) A compilation of new and published major and trace element data for NIST SRM 610 and NIST SRM 612 glass reference materials. J Geostand Geoanal 21:115–144

Poitrasson F, Mao X, Mao SS, Freydier R, Russo RE (2003) Comparison of ultraviolet femtosecond and nanosecond laser ablation inductively coupled plasma mass spectrometry analysis in glass, monazite, and zircon. Anal Chem 75:6184–6190

Rasmussen B, Fletcher IR, Bengtson S, McNaughton NJ (2004) SHRIMP U–Pb dating of diagenetic xenotime in the Stirling Range Formation, Western Australia: 1.8 billion year minimum age for the Stirling biota. Precambrian Res 133:329–337. https://doi.org/10.1016/j.precamres.2004.05.008

Rino S, Komiya T, Windley BF, Katayama I, Motoki A, Hirata T (2004) Major episodic increases of continental crustal growth determined from zircon ages of river sands: implications for mantle overturns in the early Precambrian. Phys Earth Planet Inter 146:369–394

Russo RE, Mao XL, Gonzalez J, Mao SS (2002) Femtosecond laser ablation. J Anal Atom Spectrom 17:1072–1075

Russo RE, Mao X, Gonzalez JJ, Zorba V, Yoo J (2013) Laser ablation in analytical chemistry. Anal Chem 85:6162–6177

Sakata S, Hirakawa S, Iwano H, Danhara T, Guillong M, Hirata T (2017) A new approach for constraining the magnitude of initial disequilibrium in Quaternary zircons by coupled uranium and thorium decay series dating. Quat Geochronol 38:1–12

Schaltegger U, Schmitt K, Horstwood MSA (2015) U–Th–Pb zircon geochronology by ID-TIMS, SIMS, and laser ablation ICP-MS: recipes, interpretations, and opportunities. Chem Geol 402:89–110

Schmitt AK (2011) Uranium series accessory crystal dating of magmatic processes. Annu Rev Earth Planet Sci 39:321–349

Simonetti A, Heaman LM, Hartlaub RP, Creaser RA, MacHattie TG, Böhm C (2005) U–Pb zircon dating by laser ablation-MC-ICP-MS using a new multiple ion counting Faraday collector array. J Anal Atom Spectrom 20:677–686

Sims KWW, Blichert-Toft J, Kyle PR, Pichat S, Gauthier PJ, Blusztajn J, Kelly P, Ball L, Layne G (2008) A Sr, Nd, Hf, and Pb isotope perspective on the genesis and long-term evolution of alkaline magmas from Erebus Volcano, Antarctica. J Volcanol Geotherm Res 177:606–618

Snow JE, Friedrich JM (2005) Multiple in counting ICPMS double spike method for precise U isotopic analysis at ultra-trace levels. Int J Mass Spectrom 242:211–215

Thirlwall MF, Walder AJ (1995) In situ hafnium isotope ratio analysis of zircon by inductively coupled plasma multiple collector mass spectrometry. Chem Geol 122:241–247

Tiepolo M (2003) In situ Pb geochronology of zircon with laser ablation-inductively coupled plasma-sector field mass spectrometry. Chem Geol 199:159–177

Walczyk T (2004) TIMS versus multicollector-ICP-MS: coexistence or struggle for survival? Anal Bioanal Chem 378:229–231

Weiss Y, Griffin WL, Elhlou S, Navon O (2008) Comparison between LA-ICP-MS and EPMA analysis of trace elements in diamonds. Chem Geol 252:158–168

Wieser ME, Schwieters JB (2005) The development of multiple collector mass spectrometry for isotope ratio measurements. Int J Mass Spec 242:97–115

Woodhead JD (2002) A simple method for obtaining highly accurate, Pb isotope data by MC-ICPMS. J Anal At Spectrom 17:1381–1385

Woodhead J, Hergt J, Meffre S, Large RR, Danyushevsky L, Gilbert S (2009) In situ Pb-isotope analysis of pyrite by laser ablation (multi-collector and quadrupole) ICPMS. Chem Geol 262:344–354

Yokoyama TD, Suzuki T, Kon Y, Hirata T (2011) Determinations of REE abundance and U-Pb age of zircons using multispot laser ablation-ICP-mass spectrometry. Anal Chem 83:8892–8899

YongSheng L, ZhaoChu H, Ming L, Shan G (2013) Applications of LA-ICP-MS in the elemental analyses of geological samples. Chin Sci Bull 58:3863–3878

Yoshiya K, Sawaki Y, Hirata T, Maruyama S, Komiya T (2015a) In-situ iron isotope analyses of pyrites from 3.5 to 3.2 Ga sedimentary rocks of the Barberton Greenstone Belt, Kaapvaal craton. Chem Geol 401:126–139

Yoshiya K, Sawaki Y, Shibuya T, Yamamoto S, Komiya T, Hirata T, Maruyama S (2015b) In-situ iron isotope analyses of pyrites from 3.5 to 3.2 Ga sedimentary rocks of the Barberton Greenstone Belt, Kaapvaal Craton. Chem Geol 403:58–73

Zeng X, Mao XL, Greif R, Russo RE (2004) Experimental investigation of ablation efficiency and plasma expansion during femtosecond and nanosecond laser ablation of silicon. Appl Phys A. https://doi.org/10.1007/s00339-004-2963-9

Zoriy M, Becker JS, Dobrowolska J, Matusch A (2007) Laser ablation inductively coupled plasma mass spectrometry (LA-ICP-MS) in elemental imaging of biological tissues and in proteomics. J Anal At Spectrom 22:736–744

Lead

Dominique Weis
Pacific Centre for Isotopic and Geochemical Research, Earth, Ocean and Atmospheric Sciences, University of British Columbia, Vancouver, BC, Canada

Element Data
Atomic Symbol: Pb
Atomic Number: 82
Atomic Weight: 207.2 g/mol
Isotopes and Abundances: ^{204}Pb 1.4%, ^{206}Pb 24.1%, ^{207}Pb 22.1%, ^{208}Pb 52.10%
^{210}Pb traces, radioactive ($t_{1/2} > 22.3$ yr)
^{205}Pb synthetic
1 Atm Melting Point: 327.5 °C
1 Atm Boiling Point: 1749 °C
Common Valences: 2+, 4+
Ionic Radii: 116 pm and 129, in 6-fold and 8-fold coordination respectively
Pauling Electronegativity: 2.33
First Ionization Potential: 715.6 kj/mol
Chondritic (CI) Abundance: 1–2.4 ppm
Silicate Earth Abundance: ~0.1–0.2 ppm
Crustal Abundance: 14 ppm
Seawater Abundance: 0.03 ppb
Core Abundance: ~0.5 ppm

Properties

Because it has a "magic number" of protons (82), the lead nucleus is particularly stable and is the end product of three separate radioactive decays. The most common valence state of lead is +2, with the +4 valence state being less stable.

Lead belongs to group 14 in the periodic table that together with C, Si, Ge, and Sn shows different chemical properties.

Lead can be sometimes found free in nature, but is mostly mined from the ores galena (PbS), anglesite ($PbSO_4$), cerussite ($PbCO_3$), and minum (Pb_3O_4). Lead is easily mined and refined, and is not considered to be a rare element, even with an abundance of only about 0.0014% in the Earth's crust. Most lead has been obtained by roasting galena in hot air, although more recently, nearly one third of the lead used in the United States is derived through recycling efforts.

History and Use

Together with tin (also a member of group 14), lead has been known since the antiquity. The two letters for the symbol for lead come from the Latin name: plumbum (i.e., waterworks). It is a soft, malleable, and corrosion-resistant material, easily worked into sheets. There is evidence for its use going back almost 6000 years. Hippocrates and Pliny already documented evidence of lead poisoning (Hernberg 2000). The ancient Romans used lead to make water pipes, some of which are still in use today. Because lead is a cumulative poison, the decline of the Roman Empire has been blamed, in part, on lead in the water supply (Nriagu 1983; Delile et al. 2014).

Even if the lead abundance in the Earth's crust is relatively low, lead has been mined for centuries and disseminated throughout the environment; living organisms gradually have incorporated it in their tissues, where it accumulates.

Lead is used to line tanks that store corrosive liquids, such as sulfuric acid (H_2SO_4). Lead's high density makes it useful as a shield against X-ray and gamma-ray radiation, and it is used in X-ray machines and nuclear reactors. Lead is also used as a covering on some wires and cables to protect them from corrosion, as a material to absorb vibrations and sounds and in the manufacture of ammunition. Most of the lead used today is used in the production of lead-acid storage batteries as lead dioxide (PbO_2), such as the batteries found in automobiles.

Lead also forms alloys, several of which are widely used. Conventional solder is an alloy consisting of nearly 50% lead and 50% tin that has a relatively low melting point and is used to join electrical components, pipes, and other metallic items. Type metal is an alloy made of lead, tin, and antimony used to make the type used in printing presses and plates. Babbitt metal, another lead alloy, is used to reduce friction in bearings.

Lead forms many useful compounds that have been used extensively through the years. Litharge is lead monoxide (PbO) and a yellow solid used to make some types of glass, such as lead crystal and flint glass, in the vulcanizing of rubber and as a paint pigment. Lead compounds have been used in various types of paints. The use of lead carbonate in paints has largely been stopped in favor of titanium oxide (TiO_2).

Lead arsenate ($Pb_3(AsO_4)_2$) has been used as an insecticide although other, less harmful, substances have now largely replaced it. Lead nitrate ($Pb(NO_3)_2$) is used to make fireworks and other pyrotechnics. Lead silicate ($PbSiO_3$) is used to make some types of glass and in the production of rubber and paints.

To improve combustion, lead has been used in petrol as an antiknock additive in the form of tetraethyl lead (TEL) and tetramethyl lead (TML). This has represented one of the most

dispersive sources of lead into the environment and into humans because the tiny particle size ensures efficient pulmonary penetration and adsorption. Increased levels of petrol lead can be traced all the way into the Arctic and Antarctica. This source of lead into the environment has been drastically reduced over the years, since the introduction of catalytic converters (1975 in the United States, 1990 in France, 1993 in the United Kingdom) that could not operate with leaded gasoline.

Clair C. Patterson, while working on Pb isotope systematics to establish the absolute age of the Earth in the mid-1960s, discovered the extent of Pb pollution related to its use as an antiknock additive in gasoline (Patterson 1965). He went on a campaign, both in the United States and internationally to quantify the issue, including by coring ice sheets in Greenland and Antarctica and documenting that recent human bones had lead levels much higher (by 1000 times) than the *Homo sapiens sapiens* (Patterson et al. 1991).

Geochemical Behavior

Lead is a relatively volatile element, so it is anticipated that its concentration in the Earth is lower than in chondrites. Lead is a chalcophile element, and it is possible that if the core contains S, it might also contain some Pb. Due to lead's relatively large ionic size, it is an incompatible element, in the range of the incompatibility of the rare Earth elements and not as much as Th or U. Galena is the most common Pb mineral, whereas in silicates, Pb can substitute for K, especially in alkali feldspar.

The element concentration of Pb has been used to constrain the composition and evolution of the Earth's mantle. Most mantle-derived rocks (OIB and MORB) have uniform Ce/Pb ratios ~ 25 that are different from bulk Earth values and also significantly higher than in the continental crust. This indicates that the mantle source of OIB (and MORB) cannot be primitive (Hofmann et al. 1986).

The distribution of Pb in the oceans, together with Al, is distinctive as these two elements are depleted in deep waters relative to surface waters. Studies of the fate of Pb in the open-ocean environments can be used to model ocean metal transport and reactivity (Pb has a high particle reactivity and is scavenged onto particles). In addition, because of Pb high volatility, especially at high temperatures, anthropogenic uses have distributed Pb everywhere on the planet and also in the world oceans (Boyle et al. 2014). With Pb isotope distinctive fingerprinting capability, it is possible to trace the source of contamination and build circulation models and pollutant pathways.

Lead isotopes are extremely useful in geochronology and geochemistry. Three decay systems (^{232}Th,^{238}U, and^{235}U) end in three different Pb isotopes, respectively,^{208}Pb,^{206}Pb, and^{207}Pb. This makes the dating of zircon, a very resistant mineral on Earth, one of the powerful geochronometer available to date geological events in a distant past. With the combination of three isotopic ratios and the recent improvements in analytical techniques allowing to measure isotopic compositions with a better precision, Pb isotopes constitute a powerful tracer in mantle geochemistry, in crustal and planetary evolution.

Biological Utilization and Toxicity

Lead is the only metal, among the six principal pollutants for which the EPA has established NAAQS (National Ambient Air Quality Standards): the limit not to be exceeded is 0.15 μg/m^3. Lead has no known biological role; however, as it can accumulate in the body, it can cause serious health problems.

High lead levels in the human body have been shown to generate many negative health outcomes: (1) effects on the nervous system (decline in cognitive functions, symptoms of depressive disorder, general anxiety disorder), especially for children (low IQ, loss of memory, decrease in academic performance, hyperactivity, inattention); (2) cardiovascular effects such as hypertension and increased blood pressure and subclinical artherosclerosis; (3) effects on the hematologic system with alteration of various blood parameters including heme synthesis; (4) and developmental and reproductive effects, with early birth and associated low birth weight and delayed onset of puberty in males and females.

The major sources of lead in urban environment are: (a) Homes built before 1978 (date when lead-based paints were banned) probably contain lead-based paint. Children are especially susceptible to this source of pollution, as when the paint dries and peels, it cracks and makes lead dust that can be swallowed or inhaled by children. (b) Certain water pipes may contain lead, or are made of lead, especially in houses built before the 1970s. The main risk for contamination here depends on the hardness of the water, as it will form a layer of protective lime deposits in the pipes that will isolate the lead from the water. (c) Lead can be found in some products, such as toys and toy jewelry; recent exposures have occurred with toys produced in countries with less control. (d) Lead has been found in some traditional home remedies or makeup. (e) Certain jobs involve working with lead-based products like smelting, stain glass work, and other activities where lead cannot be replaced by another metal.

The recent crisis of Pb contamination in Flint, Michigan, was related to a change in water supply. Depending on the type of water, Pb can be remobilized from previously contaminated sites or simply from piping if the water stagnates

too long. This also leads to an investigation at the national level by *USA Today* that documented a large number of water systems with significantly too high lead contamination. The EPA stresses that there is no safe level of lead exposure.

Summary

Humans have mined, smelted, and used Pb since ancient times, but its high toxicity very much compromises its value and it is being phased out in many applications. Particularly because of its radiogenic nature and one of the end product of three decay systems, it remains among the most useful of elements in geochemistry.

Cross-References

- ▶ Chalcophile Elements
- ▶ Chondrites
- ▶ Earth's Continental Crust
- ▶ Formation and Evolution of the Earth
- ▶ Geochronology and Radiogenic Isotopes
- ▶ Incompatible Elements
- ▶ Lead Isotopes
- ▶ Mantle Geochemistry
- ▶ Thorium
- ▶ Uranium

References

Boyle EA et al (2014) Anthropogenic lead emissions in the ocean: the evolving global experiment. Oceanography 27(1):69–75. https://doi.org/10.5670/oceanog.2014.10

Delile H, Blichert-Toft J, Goiran JP, Keay S, Albarède F (2014) Lead in ancient Rome's city waters. Proc Natl Acad Sci. https://doi.org/10.1073/pnas.1400097111

EPA. Integrated science assessment for lead (Third external review draft – November 2012). EPA/600/R-10/075C

Hernberg S (2000) Lead poisoning in a historical perspective. Am J Ind Med 38:244–254

Hofmann AW, Jochum K, Seufert M, White WM (1986) Nb and Pb in oceanic basalts – new constraints on mantle evolution. Earth Planet Sci Lett 79:33–45

Nriagu JO (1983) Lead and lead poisoning in antiquity. Wiley, New York

Patterson CC (1965) Contaminated and natural lead environments of man. Arch Environ Health 11(3):344–360

Patterson C, Ericson J, Manea-Krichten M, Shirahata H (1991) Natural skeletal levels of lead in Homo sapiens sapiens uncontaminated by technological lead. Sci Total Environ 107:205–236. https://doi.org/10.1016/0048-9697(91)90260-L

USA Today

http://www.usatoday.com/story/news/2016/03/11/nearly-2000-water-systems-fail-lead-tests/81220466/; http://www.usatoday.com/story/news/nation/2016/03/16/what-lead-levels-in-water-mean/81534336/

Lead Isotopes

Dominique Weis
Pacific Centre for Isotopic and Geochemical Research, Earth, Ocean and Atmospheric Sciences, University of British Columbia, Vancouver, BC, Canada

Introduction

Isotopic ratios of Pb are key geochemical tracers for unraveling the compositional evolution of the solar system, the Earth, and the continental crust, and are an important geochronometer with many different applications.

Lead has of four naturally occurring stable isotopes, ^{204}Pb (1.4%), ^{206}Pb (24.1%), ^{207}Pb (22.1%), and ^{208}Pb (52.10%). ^{204}Pb is non-radiogenic; the latter three are the final decay products of the three decay chains from uranium (^{238}U and ^{235}U) and thorium (^{232}Th), where all the intermediate members of each series have relatively short half-lives and can be ignored on long geological timescales (tens millions of years). Some of the U decay series and ^{230}Th decay present applications for shorter time periods (i.e., volcanic eruption, sedimentation at the bottom of the oceans, coral dating).

^{238}U has a half-life comparable to the age of the Earth, i.e., 4.47 Ga, whereas ^{235}U half-life is much shorter, 0.704 Ga, and as a result, almost all the original ^{235}U present in the Earth at its formation has now decayed into ^{207}Pb. This means that there are minimal relative variations in ^{207}Pb over the last 1.5–2 Ga. ^{232}Th has a half-life (14.01 Ga) comparable to the age of the universe. In addition, ^{210}Pb is a member of the ^{238}U decay chain and has a half-life of 22.2 years.

Lead isotopes were used very early in the development of isotopic analyses to determine the age of the meteorites and the Earth (Patterson 1956). It is also while measuring lead isotopic compositions of various Earth materials that Patterson discovered the extent of Pb contamination the Pb tetraethyl added to gasoline as an antiknock agent (e.g. Patterson 1965). From the human health perspective, this was a very important discovery as Pb accumulates in organisms and has many negative health outcomes, especially on the neurological system. His work eventually led to the removal of Pb from gasoline, paints, and other products.

Pb Isotope Ratio Determinations

Lead is chemically isolated from other elements by cation exchange chromatography, except when it is extracted from galena where it represents 82% of the mineral. Lead isotope ratios have been measured by thermal ionization mass

spectrometry (TIMS) or by multi-collector inductively coupled mass spectrometry (MC-ICPMS). During ionization and transmission through the mass spectrometer, as observed for other isotopic systems, the lead isotope ratios fractionate differentially from the true value as a function of the relative isotope masses. In contrast to other radiogenic systems, such as Sr, Nd, and Hf isotopes, where a stable isotope ratio is available to measure the extent of fractionation, only one isotope is not radiogenic in the case of the Pb system. Lead isotopic compositions have been measured on TIMS instruments for about half a century, and fractionation is monitored by repeated analysis of a Pb standard, such as SRM-981 or SRM-982 (Catazanro et al. 1969) under conditions comparable to those of the samples (especially temperature). This led to precision of about 1.2–1.5 permil for $^{208}Pb/^{204}Pb$, $^{207}Pb/^{204}Pb$, and $^{206}Pb/^{204}Pb$. With time, the addition of double or triple spike allowed for better precision to be achieved (e.g., Galer 1999), but it is only with the development of MC-ICP-MS that precision could be improved by a factor of 10, with doping with a Tl standard allowing for fractionation correction on the basis of $^{205}Tl/^{203}Tl$ (White et al. 2000). Depending on the matrix of the samples, typically two separations through columns are necessary (Nobre Silva et al. 2009). When data from different laboratories are compared, care should be taken that measurements are normalized to the same standard value to avoid interlaboratory bias, and when MC-ICP-MS instruments are used, it is also important to analyze reference materials with comparable matrix (Weis et al. 2006; Fourny et al. 2016).

Geochronology

When discussing Pb isotopic compositions, one usually distinguishes two systems: (a) radiogenic-rich system where the mineral (zircon, titanite, monazite, apatite) has high U and/or Th concentrations and where (b) decay through time generates very radiogenic Pb isotopic compositions (i.e., very high $^{208}Pb/^{204}Pb$, $^{207}Pb/^{204}Pb$, $^{206}Pb/^{204}Pb$) and "common lead" when the Pb isotopic compositions are representative of the source of the rock or mineral, with minimal growth by radioactive decay. These two systems represent two very different applications of Pb isotopic compositions: the radiogenic systems represent a powerful dating tool, providing in many cases the most accurate and precise ages, while common lead has proved extremely useful in tracer geochemistry to model the evolution of Earth's reservoirs.

The ^{238}U-^{206}Pb, ^{235}U-^{207}Pb, and ^{232}Th-^{208}Pb decay systems

For a closed system where the parent and daughter isotopes remain undisturbed from any process other than radioactive decay, the Pb ratios will increase over time due to the decay of ^{238}U, ^{235}U, and ^{232}Th to ^{206}Pb, ^{207}Pb, and ^{208}Pb, respectively, according to the decay equation:

$$\frac{^{206}Pb}{^{204}Pb} = \left(\frac{^{206}Pb}{^{204}Pb}\right)_i + \frac{^{238}U}{^{204}Pb}\left(e^{\lambda_{238U}t} - 1\right), \quad (1)$$

where $^{206}Pb/^{204}Pb$ is the measured isotope ratio of the sample (so-called present-day), $^{238}U/^{204}Pb$ is the measured parent-daughter ratio, $(^{206}Pb/^{204}Pb)_i$ is the initial ratio of the sample at the time where the U-Th-Pb system became closed to elemental and mass exchange, t is the time since system closure, and $\lambda^{238}U$ is the decay constant of ^{238}U.

Comparable equations can be written for both the ^{235}U-^{207}Pb (Eq. 2) and ^{232}Th-^{208}Pb (Eq. 3) decay systems and three isotopic ratios can then be combined.

Uranium- and Thorium-rich ystems

In this case, the initial "common" Pb, if not negligible, is much less abundant than the radiogenic Pb and can be subtracted from the radiogenic Pb. One can then write

$$\frac{^{206}Pb*}{^{238}U} = e^{\lambda_{238U}t} - 1 \quad (4)$$

$$\text{where } \frac{^{206}Pb*}{^{238}U} = \frac{^{206}Pb/^{204}Pb - \left(^{206}Pb/^{204}Pb\right)_0}{^{238}U/^{204}Pb} \quad (5)$$

and the asterisk denotes only the radiogenic Pb produced since time t.

A comparable equation can be written for ^{235}U and ^{207}Pb (Eq. 5).

In the case of U-bearing mineral that behaved as a closed system (for U and all its intermediate decay products) since its crystallization, it will provide a "concordant" age in the two U-Pb systems, which is to say that the ^{238}U-^{206}Pb age equals the ^{235}U-^{207}Pb age. In addition, one can also calculate a 207-206 age by combining the two systems (Eqs. 4 and 5):

$$\frac{^{207}Pb/^{204}Pb - \left(^{207}Pb/^{204}Pb\right)_0}{^{206}Pb/^{204}Pb - \left(^{206}Pb/^{204}Pb\right)_0} = \frac{^{207}Pb*}{^{206}Pb*} = \left(\frac{^{235}U}{^{238}U}\right)\frac{e^{\lambda_{235U}t} - 1}{e^{\lambda_{238U}t} - 1}, \quad (6)$$

The age obtained from this equation will be concordant with those of Eqs. (4 and 5) in the case of a closed system and in a diagram of $^{206}Pb^*/^{238}U$ vs $^{207}Pb^*/^{235}U$, where all concordant ages plot along a curve that Wetherill (1956) called "concordia."

Recently, the potential of in situ U-Pb dating by laser ablation, coupled to either an ICP-MS (HR-ICP-MS or quadrupole) or an MC-ICP-MS, has opened new avenues of research and allowed for a expansion of applications of this robust dating technique, especially on the mineral zircon.

Uranium-poor Systems

When the natural system lacks U and Th, as does the mineral galena (PbS), the Pb isotopic composition of the mineral does not change after crystallization of the mineral and corresponds to the initial composition. In such systems, one can apply the "common lead" method, based on the evolution of Pb in a given system since the origin of the Earth (age T) until the time (t) where Pb is extracted and separated from its radiogenic parents U and Th.

The method was developed by Nier (1938, 1939) who reported systematic variations of Pb isotopic compositions in galena from different geological settings, and Gerling (1942), Holmes (1946), and Houtermans (1946) developed independently models for the evolution of Pb at the scale of the Earth.

$$\begin{aligned}\left(\frac{^{206}Pb}{^{204}Pb}\right)_t &= \left(\frac{^{206}Pb}{^{204}Pb}\right)_0 + \frac{^{238}U}{^{204}Pb}\left(e^{\lambda_{238U}T} - 1\right) \\ &\quad - \frac{^{238}U}{^{204}Pb}\left(e^{\lambda_{238U}t} - 1\right) \\ &= \left(\frac{^{206}Pb}{^{204}Pb}\right)_0 + \frac{^{238}U}{^{204}Pb}\left(e^{\lambda_{238U}T} - e^{\lambda_{238U}t}\right), \qquad (7)\end{aligned}$$

The same equations can be developed for ^{207}Pb and ^{208}Pb. In these equations, T is the age of the Earth, and t corresponds to the time elapsed since removal of a common Pb sample from its source.

Combining these equations leads to very interesting applications, including the first absolute value for the age of the Earth (Patterson 1956) or the common lead dating method: modern single-stage leads in Earth and meteorites (with $t = 0$) define a line, called the geochron, that originates from the Canyon Diablo troilite composition, the primordial Pb isotopic composition of the Earth. Patterson had the brilliant idea to analyze a series of meteorites (three stony meteorites, two iron meteorites with the Canyon Diablo troilite being the least radiogenic compositions measured) and a sample of recent oceanic sediment (representative of the bulk Earth Pb isotopic composition); they all plotted on one Pb-Pb line, giving an age of 4.55 Ga.

All single-stage leads that were removed from their sources at the same time t will lie on a straight line (isochron) in the Pb-Pb diagram.

In nature, there are also intermediary systems, where both U and Th decay into their relative Pb isotopes through time, however in case of a closed system, in a Pb-Pb plot, the equation of the slope will always be proportional to t.

In such a diagram, and because such a diagram and because we are dealing with only one chemical element, mixing between two end-members with different and homogeneous isotopic compositions will also generate a straight line.

Dating of Ancient Rocks

Pb-Pb whole rock dating methods depend only on isotopic compositions and are therefore less sensitive to element mobility compared to other dating methods. Extensive use of Pb-Pb dating was therefore applied to Archean rocks, especially in the North Atlantic Province (Taylor et al. 1980).

Dating of Meteorites

Lead isotope dating systematics have also been applied to extraterrestrial material, such as meteorites (pioneer work of Patterson 1956), and more recently to other planetary bodies such as Mars and the Moon (e.g., Bouvier et al. 2009).

Crust-Mantle Evolution

Typical lower continental crust and upper continental crust are represented by lower crustal xenoliths and modern marine sediments, respectively (these somewhat underestimate the total variance in these reservoirs). MORB and oceanic islands represent the isotopic composition of upper mantle and deep mantle, respectively (Fig. 1).

Lead Isotope Applications

Oceanic Basalts, Implications for Mantle Evolution

In 1964, the analyses of basalts from Gough and Ascension islands provided the first evidence of heterogeneity of the oceanic mantle (Gast et al. 1964). This represented an important milestone in geochemistry as, conventional wisdom was that the mantle was homogeneous. Further work (e.g., Tastumoto 1978), on other oceanic islands, also provided another fundamental observation; most of their Pb isotopic compositions were more radiogenic than the geochron (i.e., had future ages in single-stage history) (Fig. 1). This led to the so-called "Pb paradox" (e.g., Hofmann 2003). Recent volcanic rocks from various areas, including those from subduction zones, define linear trends in Pb isotopic diagrams; these trends have been interpreted as mixing trends between two end-members (among different reservoirs in the Earth's mantle, the mantle and oceanic crust, the mantle and the continental crust), as the age corresponding to the slope of these trends does not have direct age significance. Pb isotopic systematics in mantle-derived rocks also formed the basis, together with Sr and Nd, for the model by Hofmann and

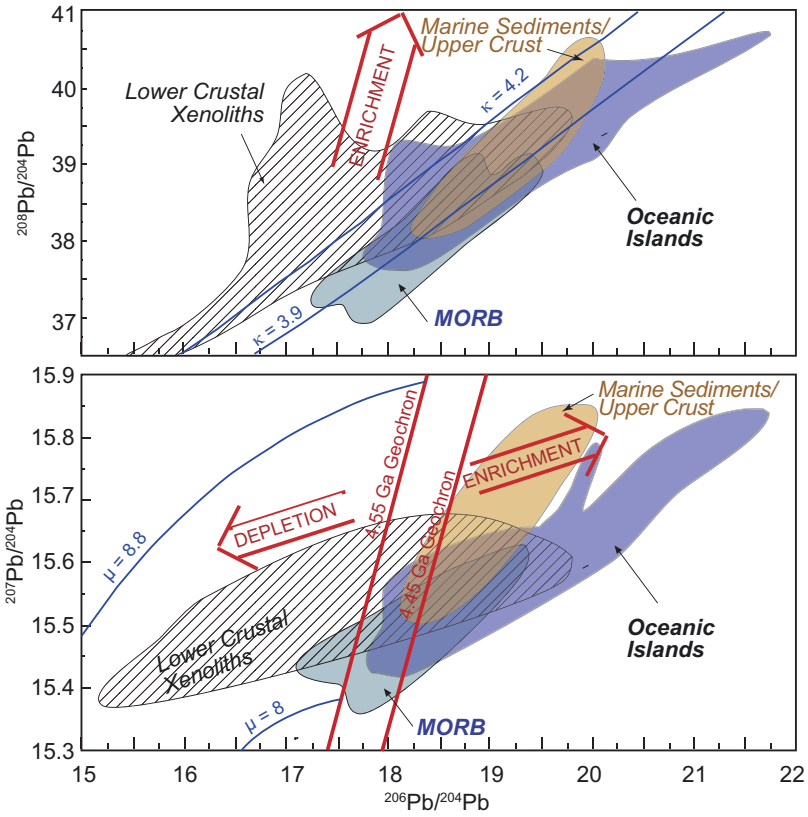

Lead Isotopes, Fig. 1 Pb isotope ratios in major terrestrial reservoirs (Modified from W.M. White 2013). The evolution *blue* curves correspond to the values of κ ($^{232}Th/^{238}U$) and μ ($^{238}U/^{204}Pb$), respectively. All points having evolved in a closed system since the origin of the Earth lie on the geochron

White (1980) suggesting that recycled subducted oceanic crust plays a role in mantle evolution. Recent work on oceanic islands with much improved precision (e.g., Abouchami et al. 2005; Weis et al. 2011) or with in situ techniques (Saal et al. 2005) document much finer scale variations in Pb isotopic compositions that are tentatively attributed to the presence of different reservoirs deep in the Earth mantle, at the core-mantle boundary, with material brought to the surface via a mantle plume.

Continental Crust Growth, Episodic or Recycling

One of the first applications of Pb isotopes was through the analyses of galena, a Pb sulfide where there is no U, and as a result, the Pb isotopic composition is frozen at the time of crystallization of the mineral. This is where Eq. 7 comes into play.

Initially, single-stage models were developed (e.g., Holmes-Houtermans model), however scientists quickly realized that in light of the complexity of the Earth's evolution, it was physically impossible for the host rocks of galena to have been a closed system since the formation of the Earth. More complex systems were developed, with either evolving U/Pb ratios different between the crust and the mantle, or with continental crust evolution in two stages with a major event at 3.7 Ga (Stacey and Kramers 1975). The 1970s and 1980s showed the development of numerous models of crust evolution, with the involvement of various reservoirs with a given U/Pb ratio. There were also strong debates about the role of recycling of Pb between the crust and the mantle (see Armstrong 1968). Doe and Zartman (1979) developed a computer model for the Pb evolution of the Earth with three reservoirs: the upper crust with the highest U/Pb ratio, the lower crust with the lowest U/Pb ratio, and the upper mantle (with an intermediate U/Pb ratio). They argued that crustal accretion began earlier in the Earth evolution and that orogenies mixed mantle and crustal sources, with a U/Pb ratio in between the upper crust and the mantle.

The mineral galena is very common in various rock types. Galena Pb isotopic compositions have been used over the past four or five decades, in models of continental growth, in the sourcing of metals in mineral deposits, and as a geochemical "fingerprint" for distinguishing between different styles of mineralization in a district.

Environmental Applications

Tracing Pb Pollution

Tetraethyl Pb has been used since the early part of the twentieth century as an antiknock additive in gasoline. The amount of Pb that has been released into the atmosphere and then deposited into the environment reached astronomical levels (by 1965, up to 2.6 M tons). Patterson (1980) is the scientist who alerted the world to the widespread distribution of Pb into the environment as well as to the dangers of long-term exposure to Pb. Patterson and colleagues worked for decades

to document the source of anthropogenic Pb via isotopic analyses of soils, seawater, and snow/ice. The fingerprinting was relatively straightforward as the source of the Pb added to gasoline had very distinctive isotopic compositions. In the USA, Pb was extracted from galena-sphalerite depositions of the Mississippi Valley (Heyl et al. 1974); in Europe and Australia, Pb was extracted from the Broken Hill ore deposit characterized by very unradiogenic isotopic compositions.

Anthropogenic contributions of Pb also came from paint, lead smelters, metal manufacturing plants, waste incinerators, and batteries. See element Pb entry.

Seawater

When it became possible to isolate natural Pb from anthropogenic Pb (see review in Boyle et al. 2014), some fundamental applications were developed for Pb isotopes in seawater (i.e., Paul et al. 2015) and other reservoirs where Pb concentrations are very low.

Summary

Lead is present in detectable (i.e., measurable) quantities in many common rocks and minerals. Lead has four isotopes, three of these are radiogenic derived by radioactive decay of uranium and thorium. The isotopic composition of Pb evolves with time in most environments and has been used extensively for dating applications and fingerprinting sources of minerals, lavas, and also pollutants in the environment.

Cross-References

- Chondrites
- Earth's Continental Crust
- Formation and Evolution of the Earth
- Geochronology and Radiogenic Isotopes
- Lead
- Lithophile Elements
- Mantle Geochemistry
- Mid-Ocean Ridge Basalts (MORB)
- Ocean Biochemical Cycling and Trace Elements
- Oceanic Island Basalts
- Thorium
- Uranium
- Uranium Decay Series

References

Abouchami W, Hofmann AW, Galer SJG, Frey FA, Eisele J, Feigenson MD (2005) Lead isotopes reveal bilateral asymmetry and vertical continuity in the Hawaiian mantle plume. Nature 434(7035):851–856

Armstrong RL (1968) A model for Pb and Sr isotope evolution in a dynamic earth. Rev Geophys 6:175–199

Bouvier A, Blichert-Toft J, Albarède F (2009) Martian meteorite chronology and the evolution of the interior of Mars. Earth Planet Sci Lett 280:285–295

Boyle EA et al (2014) Anthropogenic lead emissions in the ocean: the evolving global experiment. Oceanography 27(1):69–75. https://doi.org/10.5670/oceanog.2014.10

Catanzaro EJ, Murphy TJ, Garner EL, Shields WR (1969) Absolute isotopic abundance ratio and atomic weight of terrestrial rubidium. J Res Natl Bur Stand 73A:511–516

Doe BR, Zartman RE (1979) Chapter 2. Plumbotectonics I, the Phanerozoic. In: Barnes HL (ed) Geochemistry of hydrothermal ore deposits, 2nd edn. Wiley-Interscience, New York, pp 22–70

Fourny A, Weis D, Scoates JS (2016) Comprehensive Pb-Sr-Nd-Hf isotopic, trace element, and mineralogical characterization of mafic to ultramafic rock reference materials. Geochem Geophys Geosyst 17(3):739–773. https://doi.org/10.1002/2015GC006181

Galer SJG (1999) Optimal double and triple spiking for high precision lead isotopic measurement. Chem Geol 157(3–4):255–274

Gast PW, Tilton GR, Hedge C (1964) Isotopic composition of lead and strontium from Ascension and Gough Islands. Science 145(3637):1181–1185

Gerling EK (1942) Age of the Earth according to radioactive data. Dokl Acad Sci URSS 24:259–261

Heyl AV, Landis GP, Zartman RE (1974) Isotopic evidence for the origin of Mississippi Valley-type mineral deposits: a review. Econ Geol 69(7):1025–1059

Hofmann AW, White WM (1980) The role of subducted oceanic crust in mantle evolution. Year B Carnegie Inst Wash 79:477–483

Hofmann AW (2003) Sampling mantle heterogeneity through oceanic basalts: isotopes and trace elements. In: Carlson R (ed) Treatise on geochemistry, vol 3, 2nd edn. Elsevier, Amsterdam, pp 67–101

Holmès A (1946) An estimate of the age of the earth. Nature 157:680–684

Houtermans FG (1946) Die Isotopenhäufigkeiten im natürlichen Blei und das Alter des Urans. Naturwissenschaften 33(6):185–186

Nier AO (1938) Variations in the relative abundances of the isotopes of common lead from various sources. J Am Chem Soc 60:1571

Nier AO (1939) The isotopic constitution of radiogenic leads and the measurement of geological times II. Phys Rev 55:153

Nobre Silva IGN, Weis D, Barling J, Scoates JS (2009) Leaching systematics and matrix elimination for the determination of high-precision Pb isotope compositions of ocean island basalts. Geochem Geophys Geosyst 10. https://doi.org/10.1029/2009GC002537

Patterson C (1956) Age of meteorites and the Earth. Geochim Cosmochim Acta 10(4):230–237

Patterson CC (1965) Contaminated and natural lead environments of man. Arch Environ Health 11(3):344–366

Patterson CC (1980) An alternate perspective—lead pollution in the human environment: origin, extent, and significance. In: Lead in the human environment. National Academy of Sciences, Washington, D.C., pp 265–349

Paul M, van de Flierdt T, Rehkämper M, Khondoker R, Weiss D, Lohan MC, Homoky WB (2015) Tracing the Agulhas leakage with lead isotopes. Geophys Res Lett 42(20):8515–8521. https://doi.org/10.1002/2015GL065625

Saal AE, Hart SR, Shimizu N, Hauri EH, Layne GD, Eiler JM (2005) Pb isotopic variability in melt inclusions from the EMI-EMII-HIMU mantle end-members and the role of the oceanic lithosphere. Earth Planet Sci Lett 240(3–4):605–620

Stacey JS, Kramers J (1975) Approximation of terrestrial lead isotope evolution by a two-stage model. Earth Planet Sci Lett 26(2):207–221

Tatsumoto M (1978) Isotopic composition of lead in oceanic basalt and its implication to mantle evolution. Earth Planet Sci Lett 38:63–87

Taylor PN, Moorbath S, Goodwin R, Petrykowski AC (1980) Crustal contamination as an indicator of the extent of early Archaean continental crust: Pb isotopic evidence from the late Archaean gneisses of West Greenland. Geochim Cosmochim Acta 44(10):1437–1453
Weis D, Kieffer B, Maerschalk C, Barling J, de Jong J, Williams GA et al (2006) High-precision isotopic characterization of USGS reference materials by TIMS and MC-ICP-MS. Geochem Geophys Geosyst 7 (8). https://doi.org/10.1029/2006GC001283
Weis D, Garcia MO, Rhodes JM, Jellinek M, Scoates JS (2011) Role of the deep mantle in generating the compositional asymmetry of the Hawaiian mantle plume. Nat Geosci 4(12):831–838
Wetherill GW (1956) Discordant uranium-lead ages, I. EOS Trans Am Geophys Union 37(3):320–326
White WM, Albarède F, Télouk P (2000) High-precision analysis of Pb isotope ratios by multi-collector ICP-MS. Chem Geol 167(3–4):257–270
White WM (2013) Geochemistry. Wiley-Blackwell, Oxford. 660 pp

Lipids (Bacteria and Archaea)

Ann Pearson
Department of Earth and Planetary Sciences, Harvard University, Cambridge, MA, USA

Definition

Lipids are fundamental biochemical constituents of all cells. Membrane lipids form bilayer or monolayer structures and provide physical and energetic barriers between intracellular processes and the external environment. Accessory lipids such as pigments and small-molecule metabolites also are important for cell function. In geosciences, the study of these lipids – known as "biomarkers" – takes advantage of two critical properties: (i) lipids are more resistant to degradation than other molecular classes (e.g., proteins, nucleic acids), allowing long-term preservation in the geologic record; and (ii) lipids have a large variety of chemical structures that can be taxonomically and physiologically diagnostic. Applications of lipid biomarker analysis range widely and tackle questions of recent and ancient Earth history and environmental processes.

Introduction

Geochemical approaches to reconstructing the history of the Earth and its ecosystems rely on a variety of proxies. Lipid biomarkers preserved in sedimentary rocks are an important part of this toolbox, providing records of community composition and the operation of specific metabolic pathways (Brocks and Pearson 2005; Grice and Eiserbeck 2014; Peters et al. 2005). The most valuable biomarkers are taxonomically specific and can be traced to organisms that perform specific functions, e.g., sulfide-oxidizing photosynthesis or anaerobic oxidation of ammonia (Anammox). The biomarker record can reveal information about the redox state of ancient oceans (e.g., Brocks et al. 2005), sources of sediments to continental margins (e.g., Prahl et al. 1992), past thermal histories of the surface ocean (e.g., Sluijs et al. 2006), dynamics of mass extinctions (e.g., Sepúlveda et al. 2009), and the operation of specific biogeochemical cycles (e.g., Rush et al. 2012).

Key to the utility of lipid studies is the fact that these molecules are inherently resistant to degradation. Although most biologically synthesized lipids contain one or more oxygen-, nitrogen-, and/or sulfur-containing groups, diagenesis often removes only these groups, leaving the parent structure largely intact (although with stereochemical and/or other minor structural rearrangements). The resulting molecules are the hydrocarbon skeletons of the original products, and they can persist in low-maturity sedimentary rocks for millions of years (Peters et al. 2005).

Siliciclastic sedimentary rocks (e.g., shales, mudstones) are the major reservoirs of biomarker molecules, although organic-rich marls and carbonate and silicic sediments (oozes) also contain extractible lipids. Records of biomarker lipids date back to at least the Mesoproterozoic ($\geq$1.6 Ga); but lipids previously identified in samples from 2.7 Ga (Brocks et al. 1999) now are known to be contaminants; i.e., at present, there is no confirmed biomarker record of life in the Archean (French et al. 2015a).

Biomarker analyses in recent time or in modern analogue environments often investigate lipids in their original, biological form, called "intact polar lipids" (IPLs; e.g., Schubotz et al. 2009). Ancient sediments typically contain only the hydrocarbon diagenetic products, albeit with some exceptions (Melendez et al. 2013). Analysis of hydrocarbons usually is done by gas chromatography-mass spectrometry (GC/MS), while analysis of biomarkers in IPL form usually is done by liquid chromatography-mass spectrometry (LC/MS). Many advanced technologies exist for both types of analyses (Grice 2014). In all cases, the fundamental goal is to identify diagnostic structures and relate them to their source organisms and environmental processes.

Lipid Structural Classes

The two major structural families of lipids are called ***acetogenic*** and ***isoprenoid*** based on their biosynthetic origins as polymers of acetate (two carbons, C_2) and isoprene (five carbons, C_5), respectively. Bacteria synthesize their major membrane structures from acetogenic lipids, while archaeal membranes are composed of isoprenoid lipids. Most other geochemically useful lipids of both bacterial and archaeal cells (e.g., carotenoid pigments, quinones) are isoprenoids.

Common bacterial and archaeal lipid classes used in geochemical studies are (Fig. 1; parent compound/geologic hydrocarbon):

Fatty acids/n-alkyl lipids – hydrophobic component of bacterial and eukaryotic membrane lipids

Sterols/steranes – polycyclic isoprenoid lipids, generally diagnostic for eukaryotes

Bacteriohopanepolyols (*BHPs*)/*hopanes* – polycyclic isoprenoid lipids, analogues of eukaryotic sterols

Phytol/phytane (*and pristane*) – isoprenoid sidechain of chlorophyll pigments

Carotenoids – isoprenoid accessory pigments for photosynthesis and energy metabolism

Archaeal diethers/phytanes – glycerol dialkyl diether lipids of archaeal bilayer membranes (also called archaeols)

Archaeal tetraethers/biphytanes – glycerol dialkyl glycerol tetraether (GDGT) lipids of archaeal monolayer membranes (also called caldarchaeols)

Bacterial tetraethers – branched, but not isoprenoid, glycerol dialkyl glycerol tetraether (brGDGT) lipids of bacterial monolayer membranes

Ladderanes – cyclobutane chain lipids of Anammox bacteria

Membrane bilayers of bacteria are composed of acetogenic lipids, typically containing a polar (often phospho- or glyco- (***i, ii***)) head group, glycerol backbone, and two esterified alkyl tails (***1***). Hydrolysis of these lipids yields biomarker fatty acids, and subsequent diagenesis ultimately yields alkanes (***2***). Numerous structural variations, including terminal branching (*iso-* or *anteiso-*; Kaneda 1991), unsaturation (always with *cis-* configuration), and mid-chain cyclopropyl versions, all are common and in some cases can provide taxonomic or metabolic information (Bodelier et al. 2009).

Polycyclic isoprenoid lipids such as the eukaryotic compound cholesterol (***3***) are membrane-rigidifying structures. The bacteriohopanepolyols (BHPs) (***4***) are analogous to sterols and share a common biochemical ancestry. Their corresponding hydrocarbons are called hopanes (***5***) and are among the most widely studied lipid biomarkers in geologic investigations (Newman et al. 2016; Ourisson et al. 1987; Summons et al. 1999).

Pigment molecules provide records of photosynthetic life. Lysis of the esterified C_{20} isoprenoid side chains of bacteriochlorophylls and chlorophyll *a* yields phytol (***6***), which during oxic and anoxic diagenesis degrades to pristane (***7***, C_{19}) and phytane (C_{20}), respectively (Didyk et al. 1978). Accessory C_{40} carotenoid pigments, often with terminal aromatic groups (aryl-, e.g., okenone; or diaryl-, e.g., isorenieratene (***8***)), are sufficiently taxonomically specific to reveal different types of photosynthesis in past environments (Brocks et al. 2005; French et al. 2015b; Sinninghe Damsté et al. 1993).

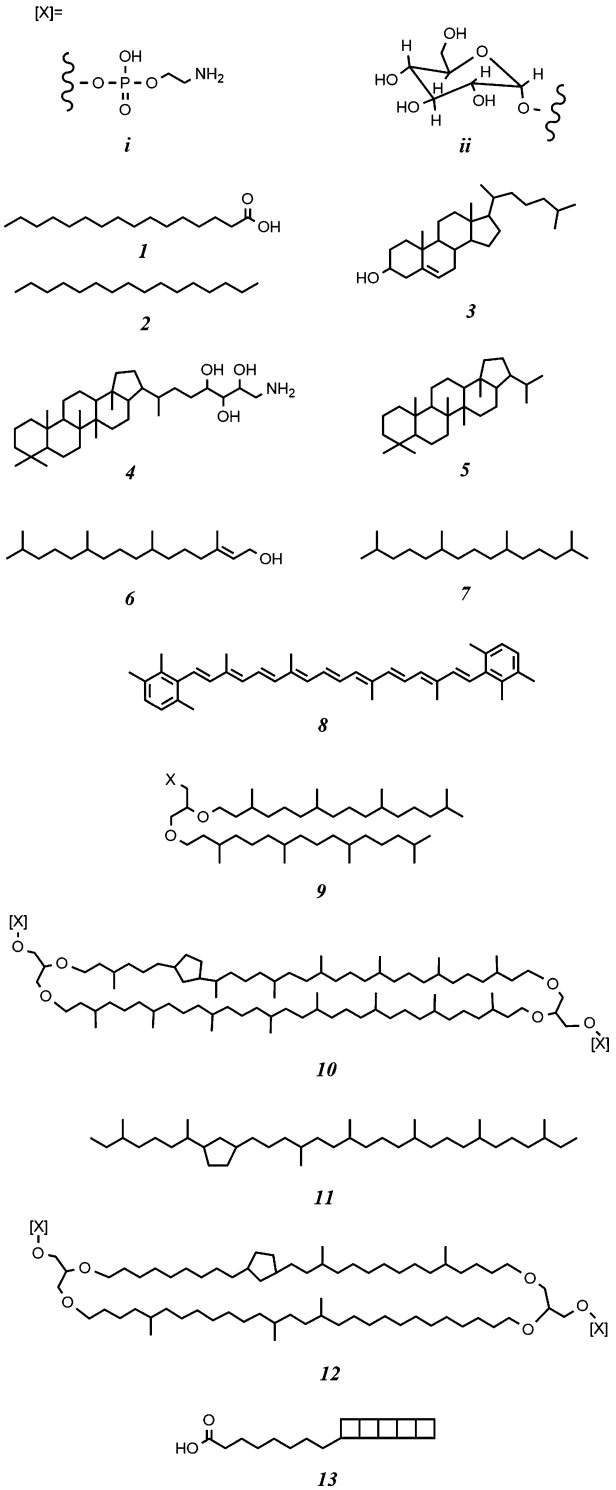

Lipids (Bacteria and Archaea), Fig. 1 Examples of lipid structures commonly used for geochemical studies: (***i, ii***), phospho- and glyco- head groups (many other structures are possible; e.g., Schubotz et al. 2009); (***1***), $C_{16:0}$ fatty acid; (***2***), *n*-C_{16} alkane; (***3***), cholesterol; (***4***), aminobacteriohopanetriol; (***5***), hopane; (***6***), phytol; (***7***), pristane; (***8***), isorenieratene; (***9***), archaeol; (***10***), GDGT-1, containing one cyclopentane ring; (***11***), $C_{40:1}$ biphytane; (***12***), brGDGT IIIb, containing one cyclopentane ring and 5 methyl groups; (***13***), C_{20} [5]-ladderane fatty acid

Lipids of archaea are invariably isoprenoid (Kates 1992). Archaeal membranes are composed of bilayers of diether lipids (***9***) or monolayers of tetraether lipids (***10***; GDGT), also with polar head groups (e.g., ***i, ii***). Due to the ether bonds linking the hydrocarbon side chains to the glycerol moieties, archaeal lipids are highly resistant to degradation. Diagenesis of GDGTs yields biphytanes (***11***), although intact (known as "core," i.e., without polar head groups) tetraether lipids are preserved at least as far back as the Jurassic; Jenkyns et al. 2012). Biphytanes can contain up to four or more internal cyclopentane rings and/or a single cyclohexane ring (Sinninghe Damsté et al. 2002a).

Tetraether lipids also are found in bacteria, although their taxonomic sources remain poorly understood (Weijers et al. 2006, 2009). These lipids resemble archaeal GDGTs, but their hydrocarbon centers are acetogenic (***12***) and contain up to six methyl branches and/or cyclopentane rings in a variety of structural positions (De Jonge et al. 2014). Collectively, they are regarded as "branched" (brGDGTs), even when containing cyclopentane rings; they persist in the geologic record at least since the Eocene (Inglis et al. 2017).

Ladderanes are a class of unusual lipids having concatenated chains of cyclobutane rings (***13***) (Sinninghe Damsté et al. 2002b). They are produced exclusively by the divisions of *Planctomycetes* bacteria that mediate the anaerobic oxidation of ammonia (Strous et al. 1999), where they are thought to provide an impermeable barrier to the toxic intermediate hydrazine. Their resulting diagenetic hydrocarbons are not yet known, although intact ladderanes in ocean waters and sediments provide records of Anammox in the recent past (e.g., Rush et al. 2012).

Selected Applications in Geosciences

Sources of bacteriohopanepolyols (*BHPs*) – Hopanoids are synthesized by a minority of bacteria and are not found in any archaea (Pearson 2014). The high resistance of hopane skeletons (***5***) to biotic and abiotic degradation makes hopanoids excellent tracers for ancient bacterial communities, resulting in several important applications. The ratio of total hopanes to total steranes has been used to interpret changes in the fraction of bacterial versus algal input (Moldowan et al. 1985). Hopane chain length proxies such as the C_{35} homohopane index, defined as $[C_{35}/(\Sigma C_{31}\text{-}C_{35})]$, record the extent of degradation of hopanoids. A higher index, denoting less degradation, is believed to indicate anoxia (Peters et al. 2005).

Some intact BHPs are believed to correspond to specific metabolisms. For example, aminobacteriohopanetriol (***4***) is found in methanotrophs and is observed in environments mediating aerobic methane oxidation (Talbot et al. 2003). The 2-methylhopanoids, previously regarded as markers for Cyanobacteria (Summons et al. 1999), now are regarded also as products of Alphaproteobacteria and perhaps other taxa (Welander et al. 2010). In general, the relatively greater occurrence of hopanoids in terrestrial ecosystems and the physiological association of hopanoids with microbial stress responses indicate they may be important biomarkers for terrestrial and/or benthic microbial activity (Newman et al. 2016).

Carotenoid distributions over time – Carotenoids provide a record of bacterial and algal photosynthesis. The detection of isorenieratane, an early diagenetic product of isorenieratene (***8***), in mid-Holocene sediments of the Black Sea (Sinninghe Damsté et al. 1993), provided evidence that photic-zone euxinia (anoxic, sulfide-containing surface water) predates human influence on the region; isorenieratene is only produced by photosynthetic green sulfur bacteria.

Recent improvements in the detection of a wide variety of carotenoids (French et al. 2015b) allowed their reassessment in geologic sediments dating back to the Proterozoic. This work confirms the extinction of the pigment paleorenieratane at the Permo-Triassic boundary, perhaps associated with the loss of unknown photosynthetic taxa. Conversely, the pigment okenone – found in purple sulfur bacteria (Brocks and Schaeffer 2008) – was shown to be more common than previously believed.

Paleotemperatures from GDGTs and brGDGTs – Accurate reconstruction of past sea surface temperatures (SSTs) and continental mean annual air temperatures (MAATs) is fundamental to a better understanding of paleoclimate. GDGTs of archaea (***10***) are used in the SST proxy known as the TEX_{86} index (Schouten et al. 2002). These compounds are believed to be produced primarily by ammonia-oxidizing, planktonic archaea that are critical and ubiquitous players in the global nitrogen cycle (c.f., Schouten et al. 2013). The distribution of GDGTs in marine surface sediments is calibrated to modern overlying waters (e.g., Tierney and Tingley 2014), and this calibration is subsequently applied to generate paleorecords from sediments. Such records have been fundamental tools for understanding SSTs over Cenozoic and Mesozoic timescales.

The analogous bacterial compounds, brGDGTs, have found utility as MAAT proxies (Weijers et al. 2007). Some of these compounds may be produced by the phylum *Acidobacteria*, although their sources remain generally unknown (Sinninghe Damsté et al. 2014). Calibrations show that brGDGTs are influenced by both temperature and pH and that soils and lakes require separate (region-specific) calibrations (Loomis et al. 2014; Peterse et al. 2012; Tierney et al. 2010). Records generated from brGDGTs have been important for studies of changes in Pleistocene/Quaternary climate patterns, especially over Africa, Asia, and the Caribbean.

Summary

Lipid biomarkers have broad utility in studies of historical geobiology, paleoclimate, and ecosystem reconstruction. Their structural diversity and high potential for preservation make them a critical tool in geochemical investigations of modern and ancient systems.

Cross-References

- ▶ Biogeochemistry
- ▶ Biomarkers: Petroleum
- ▶ Gas Chromatography–Mass Spectrometry (GC–MS)
- ▶ Hydrocarbons
- ▶ Organic Geochemistry
- ▶ Paleoenvironments

Acknowledgments AP is supported by the NASA Astrobiology Institute, the Gordon and Betty Moore Foundation, and the US National Science Foundation.

References

Bodelier PLE, Bär Gillisen MJ, Hordijk K, Sinninghe Damsté JS, Rijpstra WIC, Geenevasen JAJ, Dunfield PF (2009) A reanalysis of phospholipid fatty acids as ecological biomarkers for methanotrophic bacteria. ISME J 3:606–617

Brocks JJ, Pearson A (2005) Building the biomarker tree of life. In: Banfield J (ed) Molecular geomicrobiology. Reviews in mineralogy and geochemistry, vol 59. The Mineralogical Society of America, Chantilly, pp 233–258

Brocks JJ, Schaeffer P (2008) Okenane, a biomarker for purple sulfur bacteria (Chromatiaceae), and other new carotenoid derivatives from the 1640 Ma Barney Creek formation. Geochim Cosmochim Acta 72:1396–1414

Brocks JJ, Logan GA, Buick R, Summons RE (1999) Archean molecular fossils and the early rise of eukaryotes. Science 285:1033–1036

Brocks JJ, Love GD, Summons RE, Knoll AH, Logan GA, Bowden SA (2005) Biomarker evidence for green and purple sulphur bacteria in a stratified Palaeoproterozoic sea. Nature 437:866–870

De Jonge C, Hopmans EC, Zell CI et al (2014) Occurrence and abundance of 6-methyl branched glycerol dialkyl glycerol tetraethers in soils: implications for palaeoclimate reconstruction. Geochim Cosmochim Acta 141:97–112

Didyk BM, Simoneit BRT, Brassell SC, Eglinton G (1978) Organic geochemical indicators of paleoenvironmental conditions of sedimentation. Nature 272:216–222

French KL, Hallmann C, Hope JM, Schoon PL, Zumberge JA, Hoshino Y et al (2015a) Reappraisal of hydrocarbon biomarkers in Archean rocks. Proc Nat Acad Sci USA 112:5915–5920

French KL, Rocher D, Zumberge JE, Summons RE (2015b) Assessing the distribution of sedimentary C_{40} carotenoids through time. Geobiology 13:139–151

Grice K (2014) Principles and practice of analytical techniques in the geosciences. R Soc Chem, UK

Grice K, Eiserbeck C (2014) The analysis and application of biomarkers. In: Holland H, Turekian K (eds) Treatise on geochemistry, vol 12, 2nd edn. Elsevier, Boston, pp 47–78

Inglis GN, Collinson ME, Riegel W, Wilde V, Farnsworth A, Lunt DJ, Valdes P et al (2017) Mid-latitude continental temperatures through the early Eocene in western Europe. Earth Planet Sci Lett 460:86–96

Jenkyns H, Schouten-Huibers L, Schouten S, Sinninghe Damsté JS (2012) Warm middle Jurassic-early cretaceous high-latitude sea surface temperature from the Southern Ocean. Clim Past 8:215–226

Kaneda T (1991) Iso- and anteiso-fatty acids in bacteria: biosynthesis, function, and taxonomic significance. Microbiol Rev 55:288–302

Kates M (1992) Archaebacterial lipids: structure, biosynthesis and function. Biochem Soc Symp 58:51–72

Loomis SE, Russell JM, Eggermont H et al (2014) Effects of temperature, pH and nutrient concentration on branched GDGT distributions in East African lakes: implications for paleoenvironmental reconstruction. Org Geochem 66:25–37

Melendez I, Grice K, Schwark L (2013) Exceptional preservation of Palaeozoic steroids in a diagenetic continuum. Sci Rep 3. https://doi.org/10.1038/srep02768

Moldowan JM, Seifert WK, Gallegos EJ (1985) Relationship between petroleum composition and depositional environment of petroleum source rocks. AAPG Bull 69:1255–1268

Newman DK, Neubauer C, Ricci JN, Wu C-H, Pearson A (2016) Cellular and molecular biological approaches to interpreting ancient biomarkers. Ann Rev Earth Planet Sci 44:493–522

Ourisson G, Rohmer M, Poralla K (1987) Prokaryotic hopanoids and other polyterpenoid sterol surrogates. Annu Rev Microbiol 41:301–333

Pearson A (2014) Lipidomics for geochemistry. In: Holland H, Turekian K (eds) Treatise on geochemistry, vol 12, 2nd edn. Elsevier, Boston, pp 291–336

Peters KE, Walters CC, Moldowan JM (2005) The biomarker guide. Cambridge University Press, Cambridge

Peterse F, van der Meer J, Schouten S, Weijers JWH, Fierer N, Jackson RB, Kim JH, Sinninghe Damsté JS (2012) Revised calibration of the MBT–CBT paleotemperature proxy based on branched tetraether membrane lipids in surface soils. Geochim Cosmochim Acta 96:215–229

Prahl FG, Hayes JM, Xie TM (1992) Diploptene – an indicator of terrigenous organic carbon in Washington coastal sediments. Limnol Oceanogr 37:1290–1300

Rush D, Hopmans EC, Wakeham SG, Villanueva L, Schouten S, Sinninghe Damsté JS (2012) Occurrence and distribution of ladderane oxidation products in different oceanic regimes. Biogeosciences 9:2407–2418

Schouten S, Hopmans EC, Schefuß E, Sinninghe Damsté JS (2002) Distributional variations in marine crenarchaeotal membrane lipids: a new tool for reconstructing ancient sea water temperatures? Earth Planet Sci Lett 204:265–274

Schouten S, Hopmans EC, Sinninghe Damsté JS (2013) The organic geochemistry of glycerol dialkyl glycerol tetraether lipids: a review. Org Geochem 54:19–61

Schubotz F, Wakeham SG, Lipp JS, Fredricks HF, Hinrichs KU (2009) Detection of microbial biomass by intact polar membrane lipid analysis in the water column and surface sediments of the Black Sea. Environ Microbiol 11:2720–2734

Sepúlveda J, Wendler PV, Summons RE, Hinrichs KU (2009) Rapid resurgence of marine productivity after the Cretaceous-Paleogene mass extinction. Science 326:129–132

Sinninghe Damsté JS, Wakeham SG, Kohnen MEL, Hayes JM, de Leeuw JW (1993) A 6,000–year sedimentary molecular record of chemocline excursions in the Black Sea. Nature 362:827–829

Sinninghe Damsté JS, Schouten S, Hopmans EC, van Duin ACT, Geenevasen JAJ (2002a) Crenarchaeol: the characteristic core glycerol dibiphytanyl glycerol tetraether membrane lipid of cosmopolitan pelagic crenarchaeota. J Lipid Res 43:1641–1651

Sinninghe Damsté JS, Strous M, Rijpstra WIC et al (2002b) Linearly concatenated cyclobutane lipids form a dense bacterial membrane. Nature 419:708–712
Sinninghe Damsté JS, Rijpstra WIC, Hopmans EC, Foesel BU, Wüst PK, Overmann J, Tank M, Bryant DA, Dunfield PF, Houghton K, Stotte MB (2014) Ether- and ester-bound iso-diabolic acid and other lipids in members of Acidobacteria subdivision 4. Appl Environ Microbiol 80:5207–5218
Sluijs A, Schouten S, Pagani M, Woltering M, Brinkhuis H, Damsté JSS, Dickens GR, Huber M, Reichart GJ, Stein R, Matthiessen J, Lourens LJ, Pedentchouk N, Backman J, Moran K (2006) Subtropical Arctic Ocean temperatures during the Palaeocene/Eocene thermal maximum. Nature 441:610–613
Strous M, Fuerst JA, Kramer EHM, Logemann S, Muyzer G, van de Pas-Scoonen KT, Webb R, Kuenen JG, Jetten MSM (1999) Missing lithotroph identified as new planctomycete. Nature 400:446–449
Summons RE, Jahnke LL, Hope JM, Logan GA (1999) 2-Methylhopanoids as biomarkers for cyanobacterial oxygenic photosynthesis. Nature 400:554–557
Talbot HM, Watson DF, Pearson EJ, Farrimond P (2003) Diverse biohopanoid compositions of non-marine sediments. Org Geochem 34:1353–1371
Tierney JE, Russell JM, Eggermont H, Hopmans EC, Verschuren D, Sinninghe Damsté JS (2010) Environmental controls on branched tetraether lipid distributions in tropical East African lake sediments. Geochim Cosmochim Acta 74:4902–4918
Tierney JE, Tingley MP (2014) A Bayesian, spatially-varying calibration model for the TEX86 proxy. Geochim Cosmochim Acta 127:83–106
Weijers JWH, Schouten S, Hopmans EC et al (2006) Membrane lipids of mesophilic anaerobic bacteria thriving in peats have typical archaeal traits. Environ Microbiol 8:648–657
Weijers JWH, Schouten S, van den Donker JC, Hopmans EC, Sinninghe Damsté JS (2007) Environmental controls on bacterial tetraether membrane lipid distribution in soils. Geochim Cosmochim Acta 71:703–713
Weijers JWH, Panoto E, van Bleijswijk J et al (2009) Constraints on the biological source(s) of the orphan branched tetraether membrane lipids. Geomicrobiol J 26:402–414
Welander PV, Coleman ML, Sessions AL, Summons RE, Newman DK (2010) Identification of a methylase required for 2-methylhopanoid production and implications for the interpretation of sedimentary hopanes. Proc Nat Acad Sci USA 107:8537–8542

Lithium

Jeffrey G. Ryan
School of Geosciences, University of South Florida, Tampa, FL, USA

Element Data
Atomic Symbol: Li
Atomic Number: 3
Atomic Weight: 6.941
Isotopes and Abundances: ^{6}Li, 7.5%; ^{7}Li, 92.5%
1 Atm Melting Point: 180.5 °C
(*continued*)

1 Atm Boiling Point: 1342 °C
Common Valences: +1
Ionic Radii: 0.76 Å
Pauling Electronegativity: 0.98
First Ionization Energy: 520.2 kJ/mol
Chondritic (CI) Abundance: 1.49 ppm
Silicate Earth Abundance: 1.6 ppm
Crustal Abundance: 17 ppm
Seawater Abundance: 0.18 ppm
Core Abundance: ~0

Properties

Lithium is a low-density (0.5 × H_2O), silvery-white metal, which, while somewhat less reactive in water than sodium or other alkali metals, is nonetheless highly reactive and found in nature only in compounds or as a trace-level constituent in rocks.

History and Use

Johan August Arfvedson isolated lithium from the mineral petalite in 1817 and subsequently identified Li in both lepidolite and spodumene. Today lithium is extracted from brines (from LiCl) and is as well mined from large spodumene-bearing pegmatites. Lithium forms a range of silicate and evaporitic minerals, including Li-variants on micas and sheet silicates (lepidolite, zinnwaldite), inosilicates (spodumene), and tectosilicates (petalite), and a number of lithium-bearing phosphates (amblygdonite, triphilite, lithiophilite). Lithium has a wide range of industrial uses: as the key electrochemical agent in Li-ion batteries, in lubricants, and in medicine (Trujillo et al. 2011). Hiddenite, a green variant of the Li-mineral spodumene, and kunzite, a pink/lavender variant, are sought as gemstones.

Geochemical Behavior

In terms of nucleosynthesis, a portion of available ^{7}Li is thought to have been formed during the Big Bang (Stegman and Walker 1992), but Li is unstable in stellar interiors. Most Li (and nearly all ^{6}Li) forms at low abundances via spallation processes on CNO nuclei in interstellar medium (Stegman and Walker 1992; Vangione-Flam et al. 1999). Cosmochemically lithium is a moderately depleted element that largely follows Mg during nebular condensation (Dreibus et al. 1976). Li abundances in chondritic meteorites range from 1 to 2 ppm (Nichiporuk and Moore 1970, 1974), while

eucrites and lunar basalts range from 2 to 20 ppm Li (Dreibus et al. 1976; Shearer et al. 1994).

The ionic radius of Li^{1+}, at 0.76 Å, is close to that of Mg^{2+} (Shannon 1976), and as such the element substitutes at a $D^{mineral/melt}$ value of 0.1–0.3 into the M1 cation sites in many mafic minerals, in particular olivine, pyroxenes, and amphiboles; into alkali sites in plagioclase; and strongly ($D^{mineral/melt} \approx 0.3 -> 1.0$) into sheet silicate minerals, including micas and (in particular) Mg-bearing sheet silicates like serpentine (e.g., Brenan et al. 1998; Earthref.org 2016; Tomascak et al. 2016). Lithium concentrations are comparatively high in mantle rocks, with abundances in peridotites ranging from 1 to 4 ppm Li (Ryan and Langmuir 1987; Seitz and Woodland 2000). Lithium abundances are consistently low in mafic volcanic rocks, with basalts from all tectonic settings ranging between 2 and 10 ppm Li (Ryan and Langmuir 1987; Ryan and Kyle 2004). Li/Yb ratios are essentially constant in ocean-ridge basalts at ≈1.8, while Li/Dy ratios are constant in ocean island and intraplate lavas (Ryan and Langmuir 1987). This apparent tectonic setting-related difference in Li behavior results from the distinctive pattern of Li mineral-melt partitioning, in that Li, unlike all other commonly studied lithophile elements, substitutes into nearly all mafic silicate mineral phases with $D^{mineral/melt}$ values of similar magnitude.

Differentiated lavas and granitic rocks are higher in Li and can reach values of over 100 ppm, though most are in the range of 10–50 ppm Li, consistent with overall estimates for the continental crust (Teng et al. 2004, 2006; Rudnick and Gao 2014). Li is a conservative species in the oceans at 0.18 ppm, varying with Cl content, while seafloor hydrothermal fluids can have Li contents up to 50 times seawater values (Von Damm et al. 1985). Li is adsorbed by clays during marine alteration, and marine sediments typically contain 30–50 ppm Li (Plank 2014), while altered oceanic basalts can locally reach very high contents but overall are probably around 10 ppm (Donnelly et al. 1980).

During hydrothermal fluid-rock exchanges, Li tends to be mobilized to only a limited degree, even at temperatures as high as 375 °C (Seyfried et al. 1984). During metamorphism, Li concentrations increase slightly with grade (implying Li retention while fluids and other species are lost) until reaching the highest grade (granulite) conditions, where Li shows depletions suggestive of metasomatic removal (Sighinolfi and Gorgoni 1978). Metasediments from greenschist/blueschist to amphibolite facies metamorphic conditions thus largely preserve their original lithium contents, albeit with extensive isotopic re-equilibration (Sighinolfi and Gorgoni 1978; Penniston-Dorland et al. 2012).

With its high charge-to-mass ratio, lithium has the highest chemical diffusivity of any non-gaseous element, with diffusion coefficients several orders of magnitude higher than other alkalies and nearly all other lithophile trace elements (Cunningham et al. 1983; Lundstrom et al. 2005). This unique chemical characteristic of Li can result in comparatively rapid Li isotopic and abundance homogenization of mantle domains, and in the development of marked isotopic heterogeneities across interfaces with strong Li abundance gradients (Richter et al. 2003; Lundstrom et al. 2005).

Biological Utilization and Toxicity

Lithium is not biologically utilized in humans, though it seems to afford some benefit in plant growth. Natural human intake of Li in foods ranges between 0.6 and 3 mg/day, though in areas with high natural Li abundances these values may be >3 times higher without apparent negative effects (Aral and Vecchio-Sadus 2008). Li metal is toxic in high doses, as it can negatively impact neurological function. Li_2CO_3, to a serum level of up to 10 mg/l (close to its toxity level), is a traditional pharmacological treatment for bipolar disorder, though the specifics of how it impacts mood and mental state are still not clearly understood (Aral and Vecchio-Sadus 2008).

Cross-References

- Alkali and Alkaline Earth Metals
- Lithium Isotopes
- Lithophile Elements
- Nucleosynthesis
- Partitioning and Partition Coefficients
- Trace Elements

References

Aral H, Vecchio-Sadus A (2008) Toxicity of lithium to humans and the environment – a literature review. Ecotoxicol Environ Saf 70:349–356

Brenan JM, Neroda E, Lundstrom CC, Shaw HF, Ryerson FJ, Phinney DL (1998) Behavior of boron, beryllium and lithium during melting and crystallization: constraints from mineral-melt partitioning experiments. Geochim Cosmochim Acta 62:2129–2141

Cunningham GJ, Henderson P, Lowry RK, Nolan J, Reed SJB, Long JVP (1983) Lithium diffusion in silicate melts. Earth Planet Sci Lett 65:203–205

Donnelly TW, Thompson G, Salisbury MH (1980) The chemistry of altered basalts at site 417, Deep Sea Drilling Project leg 51. In: Powell R, Laughter F (eds) Initial reports of the Deep Sea Drilling Project, vol 51–53, pp 1319–l330. https://doi.org/10.2973/dsdp.proc.515253.1980

Dreibus G, Spettel B, Wanke H (1976) Lithium as a correlated element, its condensation behaviour, and its use to estimate the bulk composition of the moon and the eucrite parent body. In: Proceedings of the 7th Lunar science conference, pp 3383–3396

Earthref.org (2016) Geochemical Earth Reference Model (GERM). https://earthref.org/GERM/

Lundstrom CC, Chaussidon M, Hsui AT, Kelemen P, Zimmerman M (2005) Observations of Li isotopic variations in the Trinity Ophiolite: evidence for isotopic fractionation by diffusion during mantle melting. Geochim Cosmochim Acta 69:735–751
Nichiporuk W, Moore CB (1970) Lithium in chondritic meteorites. Earth Planet Sci Lett 19:280–286
Nichiporuk W, Moore CB (1974) Lithium, sodium, and potassium abundances in carbonaceous chondrites. Geochim Cosmochim Acta 38:1691–1701
Penniston-Dorland SC, Bebout GE, Pogge von Strandmann PAE, Elliott T, Sorensen SS (2012) Lithium and its isotopes as tracers of subduction zone fluids and metasomatic processes: evidence from the Catalina Schist, California, USA. Geochim Cosmochim Acta 77:530–545
Plank T (2014) The chemical composition of subducting sediments. In: Treatise on geochemistry, 2nd edn. Elsevier. Chap. 4: the crust, pp 607–629
Richter FM, Davis AM, DePaolo DJ, Watson EB (2003) Isotope fractionation by chemical diffusion between molten basalt and rhyolite. Geochim Cosmochim Acta 67:3905–3923
Rudnick RL, Gao S (2014) Composition of the continental crust, Chap. 4.13. In: Holland HD, Turekian KK (eds) Treatise on geochemistry. Elsevier, Amsterdam, pp 1–51
Ryan JG, Kyle PR (2004) Lithium and lithium isotope variations in intraplate mantle sources: insights from McMurdo Group lavas (Mt. Erebus) and other intraplate volcanic rocks. Chem Geol 212:125–142
Ryan JG, Langmuir CH (1987) The systematics of lithium abundances in young volcanic rocks. Geochim Cosmochim Acta 51:1727–1741
Seitz H-M, Woodland AB (2000) The distribution of lithium in peridotitic and pyroxenitic mantle lithologies: and indicator of magmatic and metasomatic processes. Chem Geol 166:47–64
Seyfried WE, Janecky DR, Mottl MJ (1984) Alteration of the oceanic crust: implications for chemical cycles of lithium and boron. Geochim Cosmochim Acta 48:557–569
Shannon RD (1976) Revised effective ionic radii and systematic studies of interatomic distance in halides and chalcogenides. Acta Crystallogr A32:751–767
Shearer CK, Layne GD, Papike JJ (1994) The systematics of light lithophile elements (Li, Be, and B) in lunar picritic glasses: implications for basaltic magmatism on the Moon and the origin of the Moon. Geochim Cosmochim Acta 58:5349–5362
Sighinolfi GP, Gorgoni C (1978) Chemical evolution of high grade metamorphic rocks-anatexis and remotion of material from granulite terranes. Chem Geol 22:157–176
Stegman G, Walker TP (1992) Production of Li, Be, and B in the early galaxy. Astrophys J 385:L13–L16
Teng F-Z, McDonough WF, Rudnick RL, Dalpe C, Tomascak PB, Chappell BW, Gao S (2004) Lithium isotopic composition and concentration of the upper continental crust. Geochim Cosmochim Acta 68:4167–4178
Teng F-Z, McDonough WF, Rudnick RL, Walker RJ, Sirbescu M-LC (2006) Lithium isotopic systematics of granites and pegmatites from the Black Hills, South Dakota. Am Mineral 91:1488–1498
Tomascak PB, Magna T, Dohmen R (2016) Advances in Lithium isotope geochemistry. Springer International Publishing, New York. https://doi.org/10.1007/978-3-319-01430-2
Trujillo M, Hobart D, Smith J (2011) Lithium. In: Periodic table of the elements. Online resource, Los Alamos National Laboratory. http://periodic.lanl.gov/3.shtml
Vangione-Flam E, Casse M, Audouze J (1999) Lithium-beryllium-boron: origin and evolution. Astro-ph/9907171, 1–30
Von Damm KL, Edmond JM, Grant B, Measures CI, Walden B, Weisser F (1985) Chemistry of submarine hydrothermal solutions at 21° N, East Pacific Rise. Geochim Cosmochim Acta 49:2197–2220

Lithium Isotopes

Jeffrey G. Ryan
School of Geosciences, University of South Florida, Tampa, FL, USA

Definition

The large relative mass difference between the lithium isotopes (^{7}Li (~92.5%) and ^{6}Li (~7.5%)) leads to isotopic fractionations of Li during equilibrium and kinetic reactions in Earth systems. Substantial (20–30‰) δ^7Li differences exist between natural waters and rocks. Mafic igneous rocks from all tectonic settings range in δ^7Li from +2‰ to +6‰, suggesting a uniform mantle reservoir, though mantle-derived samples may show variable δ^7Li due to its high chemical diffusivity. Weathering processes lower δ^7Li in surface rocks, with continental δ^7Li at ~0‰. While subduction processes do not usually lead to strong Li isotope shifts, in places where subduction is ceasing, large δ^7Li variations have been observed in lavas.

Introduction

Lithium has two naturally occurring stable isotopes which occur in the Earth at approximately the ^{7}Li/^{6}Li ratio of ~12 encountered in primitive meteorites (Tomascak et al. 2016). The large relative mass difference between its isotopes makes lithium highly susceptible to chemically induced isotopic fractionation. Successful chemical separation of Li and thermal ionization mass spectrometric determinations of Li isotopes on geological samples was first reported by Chan (1987) and Chan and Edmond (1988). Tomascak et al. (1999) presented results using solution multicollector ICP-MS analysis with sample-standard bracketing, and this advance has led to a wealth of new Li isotopic data on a wide range of geological materials and a better understanding of the Li isotopic system overall.

Natural Waters

In aqueous solutions, Li generally exists as an $Li([H_2O]_N)+$ complex coordinated with four oxygens (Jahn and Wunder 2009; Kowalski and Jahn 2011), while in minerals, it can coordinate both octahedrally and tetrahedrally, largely substituting for Mg in silicate phases. ^{7}Li is preferentially concentrated in hydrous fluids, and as such δ^7Li $((({}^7Li/{}^6Li_{sample} - {}^7Li/{}^6Li_{L\text{-}SVEC})/({}^7Li/{}^6Li_{L\text{-}SVEC}))\times 1000$, where L-SVEC is the NIST Li_2CO_3 isotopic reference material) values in the oceans and natural freshwater bodies are 20–30‰ higher than in minerals and rocks. δ^7Li in modern

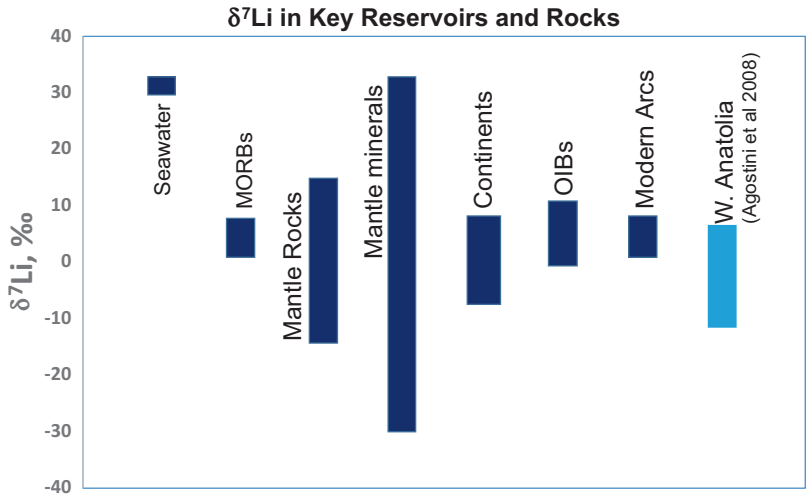

Lithium Isotopes, Fig. 1 δ^7Li variation in key rocks and reservoirs. *Dark bars* based on data compiled in Tomascak et al. (2016); Western Anatolia is from Agostini et al. (2008)

seawater is ~+31‰ (Fig. 1), though evidence from foraminiferal tests suggests a secular variation in the seawater reservoir in the Cenozoic that likely relates to changes in continental Li inputs (Misra and Froelich 2012; Pogge von Strandmann et al. 2013). River water δ^7Li signatures in the dissolved load are elevated, while suspended and bed load signatures verge closer to the value of entrained sediments (Huh et al. 2001). Hydrothermal fluids are typically closer in their δ^7Li to the rocks they interact with, largely ranging between 2‰ and 15‰ in the oceans (Chan et al. 1993, 1994).

Mafic Rocks and the Mantle

Basaltic igneous rocks have largely uniform δ^7Li signatures, with MORBs ranging between +2‰ to +6‰ (Tomascak et al. 2008). Oceanic intraplate basalts show evidence for somewhat greater δ^7Li variability (e.g., higher δ^7Li in HIMU and South Pacific lavas: Ryan and Kyle 2004; Nishio et al. 2005; see also Tomascak et al. 2016). The comparatively limited δ^7Li range in mafic lavas contrasts with the large range in ultramafic samples (−12‰ to +12‰: Brooker et al. 2004; Rudnick and Ionov 2007; Ackerman et al. 2013) and an even larger range in minerals from mantle-derived samples (+30‰ to −28‰: Tomascak et al. 2016). The high overall chemical diffusivity of Li, specifically the substantial relative diffusivity difference between the Li isotopes, is responsible for much of the Li isotopic variability observed in mantle samples, as strong Li isotopic gradients can develop, even in subsolidus conditions, across any boundary where there is a Li abundance gradient (Richter et al. 2003, 2014; Lundstrom et al. 2005). Li diffusivity is likely also responsible for the apparent isotopic homogeneity of mantle sources as sampled by basaltic magmas, as solid-state diffusive homogenization of Li isotopic anomalies in the mantle is possible on a ~10^7–10^8 year scale (Richter et al. 2003). Under low temperature conditions, Li isotopic heterogeneities can develop during the alteration of mafic and ultramafic lithologies by progressive fluid-rock exchanges where Li is taken up in Mg-rich phyllosilicate phases, such as serpentine, in which it is compatible (Decitre et al. 2002; Benton et al. 2004).

Sediments, Metamorphic Rocks and the Continents

Rudnick et al. (2004) and subsequent workers have documented that surficial weathering and alteration processes reduce Li contents and the δ^7Li in soils and sediments. Marine sedimentary sections as well show an overall shift to lower δ^7Li, although both on land and in the oceans, some materials recording very high δ^7Li are preserved. Sediment δ^7Li signatures are reflected in both sedimentary rocks and in metamorphic and granitic igneous rocks formed from sedimentary protoliths (Teng et al. 2004; Chan et al. 2006; Penniston-Dorland et al. 2012; see also Tomascak et al. 2016). Teng et al. (2004) estimated that the δ^7Li of the upper continental crust is 0 ± 2‰, reflecting the influence of weathering-related Li isotopic fractionations. High-pressure metamorphic rocks often record δ^7Li < than 0‰, based on which, some have suggested substantial subduction-related Li isotopic fractionations, though experimental results have argued against this (Zack et al. 2003; Marschall et al. 2007: see below). Current thinking is that fluid-rock diffusive and chemical exchanges associated with the uplift and unroofing of high-P rock suites may be primarily responsible for anomalously low δ^7Li in some samples (Tomascak et al. 2016).

Subduction Cycling of the Li Isotopes

While some early studies of volcanic arc lavas and subduction-related metamorphic rocks have been suggestive of large Li isotopic fractionations during subduction zone processes (e.g., Moriguti and Nakamura 1998; Zack et al. 2003), broader-based studies have not turned up clear evidence for such systematics: Tomascak et al. (2002) and Chan et al. (2002) found that mafic volcanic arc lavas have δ^7Li similar to MORBs, and Marschall et al. (2007) showed both

analytically and experimentally that the potential change in δ^7Li during subduction zone fluid-rock exchanges is likely not more than ±3‰. Benton et al. (2004) found that under forearc P-T conditions, eruptive serpentinites from the Mariana forearc preserve a δ^7Li of only +6‰ to + 7‰, pointing to comparatively modest slab-related increases in δ^7Li, as compared to large increases in δ^{11}B (up to +18‰; Benton et al. 2001). Given that the upper mantle has Li abundances of 1–2 ppm and (thanks to Li diffusivity) a relatively uniform δ^7Li value, slab-derived Li additions may not be sufficient to produce a Li isotopic anomaly in arc source regions, even though Li shows enrichments in arc lavas (Ryan and Langmuir 1987). Interestingly, Agostini et al. (2008), in a time series study of volcanic rocks spanning the transition from subduction to extension in Western Anatolia, found strong, paired Li and B isotopic declines as subduction shut down, followed by a rapid recovery to prevalent mantle values with the onset of extension. They hypothesized that the shutdown of mantle wedge convection and extreme distillation of a slowing downgoing plate permitted the ephemeral development of a highly fractionated δ^7Li reservoir, which quickly became homogenized with the onset of extension.

Conclusions

Thanks in equal parts to high Li solubility in fluids at low temperatures and its high chemical diffusivity at higher temperatures, δ^7Li signatures are relatively uniform at the scales of melting in the mantle and crust but can be highly diverse on a finer scale. Many of the more promising applications of the Li isotopes (deep Earth fluid-rock exchanges, secular variation in the oceans) leverage this finer scale diversity.

Cross-References

- ▶ Boron Stable Isotopes
- ▶ Chemical Weathering
- ▶ Diffusion
- ▶ Lithium
- ▶ Ocean Biochemical Cycling and Trace Elements
- ▶ Stable Isotope Geochemistry
- ▶ Subduction Zone Geochemistry

References

Ackerman L, Špaček P, Magna T, Ulrych J, Svojtka M, Hegner E, Balogh K (2013) Alkaline and carbonate-rich melt metasomatism and melting of subcontinental Lithospheric mantle: evidence from mantle Xenoliths, NE Bavaria, Bohemian Massif. J Petrol 54:2597–2633

Agostini S, Ryan JG, Tonarini S, Innocenti F (2008) Drying and dying of a subducted slab: coupled Li and B isotope variations in Western Anatolia Cenozoic Volcanism. Earth Planet Sci Lett 272:139–147

Benton LD, Ryan JG, Tera F (2001) Boron isotope systematics of slab fluids as inferred from a serpentinite seamount, Mariana forearc. Earth Planet Sci Lett 187:273–282

Benton LD, Ryan JG, Savov IP (2004) Lithium abundance and isotope systematics of forearc serpentinites, Conical Seamount, Mariana forearc: insights into the mechanics of slab-mantle exchange during subduction. Geochem Geophys Geosyst 5:Q08J12. https://doi.org/10.1029/2004GC000708

Brooker RA, James RH, Blundy JD (2004) Trace elements and Li isotope systematics in Zabargad peridotites: evidence of ancient subduction processes in the Red Sea mantle. Chem Geol 212:179–204

Chan LH (1987) Lithium isotope analysis by thermal ionization mass spectrometry of lithium tetraborate. Anal Chem 59:2662–2665

Chan LH, Edmond JM (1988) Variation of lithium isotope composition in the marine environment: a preliminary report. Geochim Cosmochim Acta 52:1711–1717

Chan LH, Edmond JM, Thompson G (1993) A lithium isotope study of hot springs and metabasalts from mid-ocean ridge hydrothermal systems. J Geophys Res 98:9653–9659

Chan LH, Gieskes JM, You CF, Edmond JM (1994) Lithium isotope geochemistry of sediments and hydrothermal fluids of the Guaymas Basin, Gulf of California. Geochim Cosmochim Acta 58:4443–4454

Chan L-H, Leeman WP, You C-F (2002) Lithium isotopic composition of Central American Volcanic Arc lavas: implications for modification of subarc mantle by slab-derived fluids: correction. Chem Geol 182:293–300

Chan L-H, Leeman WP, Plank T (2006) Lithium isotopic composition of marine sediments. Geochem Geophys Geosyst 7:Q06005. https://doi.org/10.1029/2005GC001202

Decitre S, Deloule E, Reisberg L, James RH, Agrinier P, Mével C (2002) Behavior of Li and its isotopes during serpentinization of oceanic peridotites. Geochem Geophys Geosyst 3:1–20. https://doi.org/10.1029/2001GC000178

Huh Y, Chan LH, Edmond JM (2001) Lithium isotopes as a probe of weathering processes: Orinoco River. Earth Planet Sci Lett 194:189–199

Jahn S, Wunder B (2009) Lithium speciation in aqueous fluids at high P and T studied by ab initio molecular dynamics and consequences for Li-isotope fractionation between minerals and fluids. Geochim Cosmochim Acta 73:5428–5434

Kowalski PM, Jahn S (2011) Prediction of equilibrium Li isotope fractionation between minerals and aqueous solutions at high P and T: an efficient ab initio approach. Geochim Cosmochim Acta 75:6112–6123

Lundstrom CC, Chaussidon M, Hsui AT, Kelemen P, Zimmerman M (2005) Observations of Li isotopic variations in the Trinity Ophiolite: evidence for isotopic fractionation by diffusion during mantle melting. Geochim Cosmochim Acta 69:735–751

Marschall HR, Pogge von Strandmann PAE, Seitz H-M, Elliott T, Niu Y (2007) The lithium isotopic composition of orogenic eclogites and deep subducted slabs. Earth Planet Sci Lett 262:563–580

Misra S, Froelich PN (2012) Lithium isotope history of Cenozoic seawater: changes in silicate weathering and reverse weathering. Science 335:818–823

Moriguti T, Nakamura E (1998) Across-arc variation of Li isotopes in lavas and implication for crust/mantle recycling at subduction zones. Earth Planet Sci Lett 163:167–174

Nishio Y, Nakai S, Kogiso T, Barsczus HG (2005) Lithium, strontium, and neodymium isotopic compositions of oceanic island basalts in the Polynesian region: constraints on a Polynesian HIMU origin. Geochem J 39:91–103

Penniston-Dorland SC, Bebout GE, Pogge von Strandmann PA, Elliott T, Sorensen SS (2012) Lithium and its isotopes as tracers of subduction zone fluids and metasomatic processes: evidence from the Catalina Schist, California, USA. Geochim Cosmochim Acta 77:530–545

Pogge von Strandmann PAE, Jenkyns HC, Woodfine RG (2013) Lithium isotope evidence for enhanced weathering during Oceanic Anoxic Event 2. Nat Geosci 6:668–672

Richter FM, Davis AM, DePaolo DJ, Watson EB (2003) Isotope fractionation by chemical diffusion between molten basalt and rhyolite. Geochim Cosmochim Acta 67:3905–3923
Richter F, Watson B, Chaussidon M, Mendybaev R, Ruscitto D (2014) Lithium isotope fractionation by diffusion in minerals. Part 1: pyroxenes. Geochim Cosmochim Acta 126:352–370
Rudnick RL, Ionov DA (2007) Lithium elemental and isotopic disequilibrium in minerals from peridotite xenoliths from far-east Russia: product of recent melt/fluid–rock reaction. Earth Planet Sci Lett 256:278–293
Rudnick RL, Tomascak PB, Njo HB, Gardner LR (2004) Extreme lithium isotopic fractionation during continental weathering revealed in saprolites from South Carolina. Chem Geol 212:45–57
Ryan JG, Kyle PR (2004) Lithium abundance and lithium isotope variations in the mantle sources: insights from intraplate volcanic rocks from Ross Island and Marie Byrd Land (Antarctica) and other oceanic islands. Chem Geol 212:125–142
Ryan JG, Langmuir CH (1987) The systematics of lithium abundances in young volcanic rocks. Geochim Cosmochim Acta 51:1727–1741
Teng F-Z, McDonough WF, Rudnick RL, Dalpé C, Tomascak PB, Chappell BW, Gao S (2004) Lithium isotopic composition and concentration of the upper continental crust. Geochim Cosmochim Acta 68:4167–4178
Tomascak PB, Carlson RW, Shirey SB (1999) Accurate and precise determination of Li isotopic compositions by multi-collector sector ICP-MS. Chem Geol 158:145–154
Tomascak PB, Widom E, Benton LD, Goldstein SL, Ryan JG (2002) The control of lithium budgets in island arcs. Earth Planet Sci Lett 196:227–238
Tomascak PB, Langmuir CH, le Roux PJ, Shirey SB (2008) Lithium isotopes in global mid-ocean ridge basalts. Geochim Cosmochim Acta 72:1626–1637
Tomascak PB, Magna T, Dohmen R (2016) Advances in Lithium Isotope Geochemistry. Springer International Publishing, New York. https://doi.org/10.1007/978-3-319-01430-2
Zack T, Tomascak PB, Rudnick RL, Dalpé C, McDonough WF (2003) Extremely light Li in orogenic eclogites: the role of isotope fractionation during dehydration in subducted oceanic crust. Earth Planet Sci Lett 208:279–290

Lithophile Elements

Frances E. Jenner[1] and Hugh StC O'Neill[2]
[1]Department of Environment, Earth and Ecosystems, The Open University, Milton Keynes, Buckinghamshire, UK
[2]Research School of Earth Sciences, Australian National University, Canberra, Australia

Definition

Lithophile is a term used to refer to elements that are preferentially partitioned into silicate minerals as opposed to sulfides or metals.

The Goldschmidt Classification of the Elements

Goldschmidt (1929; 1937) used various chemical considerations to classify elements as *lithophile* (coined from the Greek for "rock-loving," indicating it is found in silicates), *siderophile* ("iron-loving," therefore partitioning into the Fe-rich metal of planetary cores), *chalcophile* ("copper-loving," meaning it is found in sulfides, like Cu), and *atmophile* (gas-loving). The *Goldschmidt classification* of the elements derived predominantly from the distribution of elements between the various mineral phases that make up *meteorites*, but it can be predicted to a large extent from the standard-state Gibbs free energies of formation of the oxide ($\Delta_f G^\circ_{(Ox)}$) and sulfide ($\Delta_f G^\circ_{(sulf)}$) of the element in its lowest commonly encountered nonzero valence state. These quantities reflect the element's fundamental chemical properties in the chemical environment relevant to most geological processes. For metals (i.e., electropositive elements, meaning elements whose common valence state is positive), a large negative $\Delta_f G^\circ_{(Ox)}$ indicates lithophile tendencies, a positive or small negative difference ($\Delta_f G^\circ_{(Ox)} - \Delta_f G^\circ_{(sulf)}$) indicates chalcophile tendencies, and elements having neither $\Delta_f G^\circ_{(Ox)}$ nor $\Delta_f G^\circ_{(sulf)}$ very negative are likely to be siderophile. The behavior of Fe as summarized in the Gibbs free energies of formation of FeO and FeS can be taken as the benchmark. Electronegative elements are either lithophile or atmophile. The distinction between siderophile and chalcophile elements is not as clear-cut as that between lithophiles on one hand and siderophiles plus chalcophiles on the other, since sulfides are miscible in molten Fe-rich metal. So in the context of core-forming processes in planets, the term "siderophile" is often used to cover both siderophile and chalcophile elements.

The lithophile elements are typically subdivided according to their cosmochemical volatility, a property that is quantified using a theoretical concept, the element's "condensation temperature," Tc, defined as the calculated temperature at which 50% of the element would be condensed out of a cooling gas of solar composition, assuming a constant pressure (traditionally, 10^{-4} bars) and chemical equilibrium (Lodders 2003). With this classification:

Refractory lithophile elements (T_c = 1850–1355 K): a group of 28 elements with Tc greater than the condensation temperatures of the main planet-forming elements Mg, Si, and Fe. The group consists of Be, Al, Ca, Sc, Ti, Sr, Y, Zr, Nb, Ba, the 14 *lanthanide rare earth elements* (REE), Hf, Ta, Th, and U. In the past, V often used to be included, but this element is now usually classified as *siderophile*. Two of these elements, Ca and Al, are major elements in rocky planets and, together with Ti, are essential for forming refractory phases such as hibonite (ideally, $CaAl_{12}O_{19}$) and perovskite ($CaTiO_3$) that host the other refractory lithophile elements in Ca-Al-rich inclusions (CAIs) in unmetamorphosed, hence texturally primitive chondritic meteorites. The relative proportions of the refractory lithophile elements are approximately the same in nearly all groups of *chondrites*, and these proportions match those of the solar composition, as deduced from spectroscopic measurements of the solar photosphere, within uncertainty. Until recently it was widely assumed that the

refractory lithophile elements occur in the bulk silicate Earth in the solar proportions (e.g., Palme and O'Neill 2014), but this assumption is now being questioned (e.g., O'Neill and Palme 2008).

Main group lithophile elements (T_c = 1355–1250 K): Mg and Si. These elements are calculated to condense out of the solar nebular (initially as forsterite, Mg_2SiO_4) at a similar temperature to the most abundant *siderophile* elements, Fe, Ni, and Co. Mg and Si with their associated *oxygen* plus Fe are the main constituents of the rocky planets.

Moderately volatile lithophile elements (T_c = ≥1250 K): *alkali earth metals* (Li, Na, K, Rb, and Cs), *halogens* (F, Cl, Br, and I), and B. These elements are depleted relative to Mg and their solar proportions in all chondritic *meteorites*, except for the CI carbonaceous *chondrites*. They are also depleted in the bulk silicate Earth composition, but with a quite different pattern of depletion compared to any of the depletion patterns recorded in the chondrites (O'Neill and Palme 2008).

Summary and Conclusion

The Goldschmidt classification scheme should be viewed as a guide rather than a definitive classification scheme, because the chemical affiliation of elements is sensitive to differences in temperature, pressure, redox conditions, and sulfur contents. For example, in aubrites (enstatite achondrites), the REEs are almost entirely chalcophile, being held in oldhamite (CaS). Similarly some Si occurs in the metal phase of enstatite chondrites, and it is commonly supposed that the low Si/Mg of the bulk silicate Earth is due to some Si partitioning into **Earth's core** (Palme and O'Neill 2014). There may also be a small deficit of Nb in the bulk silicate Earth, which could be similarly explained (e.g., Wood et al. 2008), as Nb is the refractory lithophile element with the greatest **siderophile** tendency. Hence, whether an element is classified as "lithophile" or not depends on the geochemical process that is being documented.

Cross-References

- ▶ Alkali and Alkaline Earth Metals
- ▶ Chalcophile Elements
- ▶ Chondrites
- ▶ Earth's Core
- ▶ Lanthanide Rare Earths
- ▶ Meteorites
- ▶ Oxygen
- ▶ Periodic Table
- ▶ Refractory Inclusions in Chondritic Meteorites
- ▶ Siderophile Elements

References

Goldschmidt VM (1929) The distribution of the chemical elements. Nature 124:15–17

Goldschmidt VM (1937) The principles of distribution of chemical elements in minerals and rocks. The seventh Hugo Muller Lecture, delivered before the chemical society on 17 Mar 1937. J Chem Soc (Resumed), 655–673

Lodders K (2003) Solar system abundances and condensation temperatures of the elements. Astrophys J 591:1220–1247

O'Neill HSC, Palme H (2008) Collisional erosion and the non-chondritic composition of the terrestrial planets. Phil Trans R Soc A Math Phys Eng Sci 366:4205–4238

Palme H, and St.C O'Neill H (2014) Compositional estimates of mantle composition. In: Carlson RW (ed) Treatise on Geochemistry: The Mantle and Core. Elsevier-Pergamon, Oxford

Wood BJ, Wade J, Kilburn MR (2008) Core formation and the oxidation state of the earth: additional constraints from Nb, V and Cr partitioning. Geochimica et Cosmochimica Acta 72:1415–1426

Low-Temperature Geochemistry

Tori Z. Forbes
Department of Chemistry, University of Iowa, Iowa City, IA, USA

Synonyms

Environmental Geochemistry

Definition

Low-temperature or environmental geochemistry is the study of chemical processes that occur in the earth's surficial environments. While basic aqueous chemistry principles, including acid-base equilibrium, reduction-oxidation reactions, and solubility, are the driving force behind most phenomena, interconnections between geology, hydrology, biology, and atmospheric science require an interdisciplinary approach to investigating these systems. Low-temperature geochemistry is a broad field, but major areas of study include mineral precipitation, chemical weathering, soil chemistry, sedimentary processes and diagenesis, biogeochemical cycles, and contaminant transport.

Introduction to Low-Temperature Geochemistry

In general, geochemistry can be defined as the study of the chemical composition and changes of the earth and other celestial bodies. We further define the subject based upon the overall geologic environment, pressure, or temperature. While the delineations in temperature are somewhat vague, the most

accepted definition for low-temperature geochemistry describes the chemistry of minerals, rocks, solid, water, and atmosphere when the temperature is below 200 °C (Guangzhi 1996). This temperature range typically occurs on the earth's surface or within the first few km of the lithosphere. Surface water, soils, exposed rock formations, groundwater, aquifers, and hydrothermal vents can all be considered systems that are regulated by low-temperature geochemical processes.

Due to the relationship between geochemistry and natural processes that occur within the environment, low-temperature geochemistry is often presented within the context of environmental geochemistry (Ryan 2014). No region on the surface of the earth can be considered a closed system so there are continuous interactions taking place between the various components. Understanding complex environmental systems requires thinking about phenomenon on molecular, regional, and global scales. In addition, it requires using an interdisciplinary approach due to the deep and complex relationship between atmospheric, hydrologic, biotic, and geologic systems (Fig. 1).

Low-temperature geochemistry is also intimately tied to human society because our activities have significant impacts on the processes that are happening on the earth's surface. Sometimes these activities are direct, such as the release of chemical waste form a mine and milling piles. Other times, the connections are less direct, such as the release of small amounts of a compound that undergo chemical transformations that result in a new compound that has much greater detrimental effects on the ecosystem. Thus a major thrust of low-temperature geochemistry is to understand the impact of humans on these processes on the molecular, regional, and global scales.

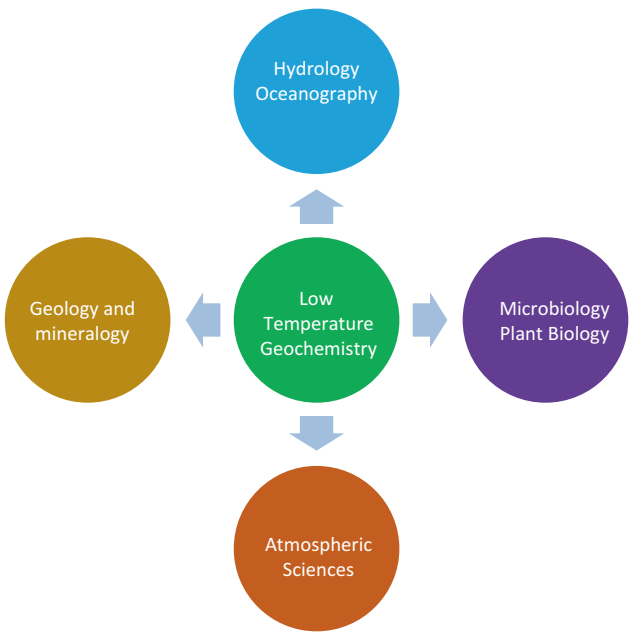

Low-Temperature Geochemistry, Fig. 1 Low-temperature geochemistry requires interdisciplinary thinking due to the interconnections between geology, biology, hydrology, and atmospheric sciences

History and Basic Principles

Low-temperature geochemistry is a relatively new subdiscipline of geology, developing from the molecular scale before encompassing global phenomena. The Norwegian scientist, Victor M. Goldschmidt is often considered to be the founder of geochemistry with his important contributions to mineral reactivity and his guiding principles on elemental substitutions in crystalline phases (Reinhardt 2001). The idea of geochemistry was broadened by the work of Vladimir I. Vernadsky, who determined that chemical reactions resulted in the formation of minerals and more specifically that living organisms could reshape geological systems or even planets (Ryan 2014). Investigations regarding the consequences of anthropogenic activities on environmental and geochemical systems began in the 1960s with concerns regarding contamination of the air, water, and soil. Seminal work during this period found that pesticides were a significant threat to ecosystem health (Carson 1962), acid rain was caused by industrial emissions (Likens and Bormann 1974), and humans were impacting the global climate through emissions of greenhouse gasses (Hansen et al. 1981). Current investigations in low-temperature geochemistry span the range of topics and scale that was laid down by the leaders in this area.

At the most basic level, low-temperature geochemical processes are controlled by fundamental chemical principles that control reactions in aqueous systems (Fig. 2). A major factor in the formation and dissolution of minerals and rocks is acid-base equilibrium and hydrogen ion activity (pH). In water, the hydrogen ion activity (pH) is the driver for many geochemical properties including dissolution, precipitation, crystallization, gas solubilities, and biochemical reactions. The pH of the solution can also be influenced by inorganic constituents, most notably the equilibrium between dissolved carbon dioxide and the carbonate anion (Drever 1997). Reduction and oxidation (redox) reactions are also of importance for elements that can access multiple oxidation states. Hydrogen, nitrogen, oxygen, sulfur, iron, and manganese are abundant and important redox active elements in geochemical systems (Drever 1997). These elements typically control the redox conditions within aqueous solutions, which in turn can determine the speciation, mobility, and toxicity of trace metals and organic compounds. Organisms, such as microbes and fungi, also play an important role in harnessing the chemical energy within geochemical systems to control the redox conditions, molecular speciation, and precipitation of mineral phases. Equilibria between the various inorganic and organic components and their overall energetics and stability (thermodynamics) ultimately determine the overall chemical

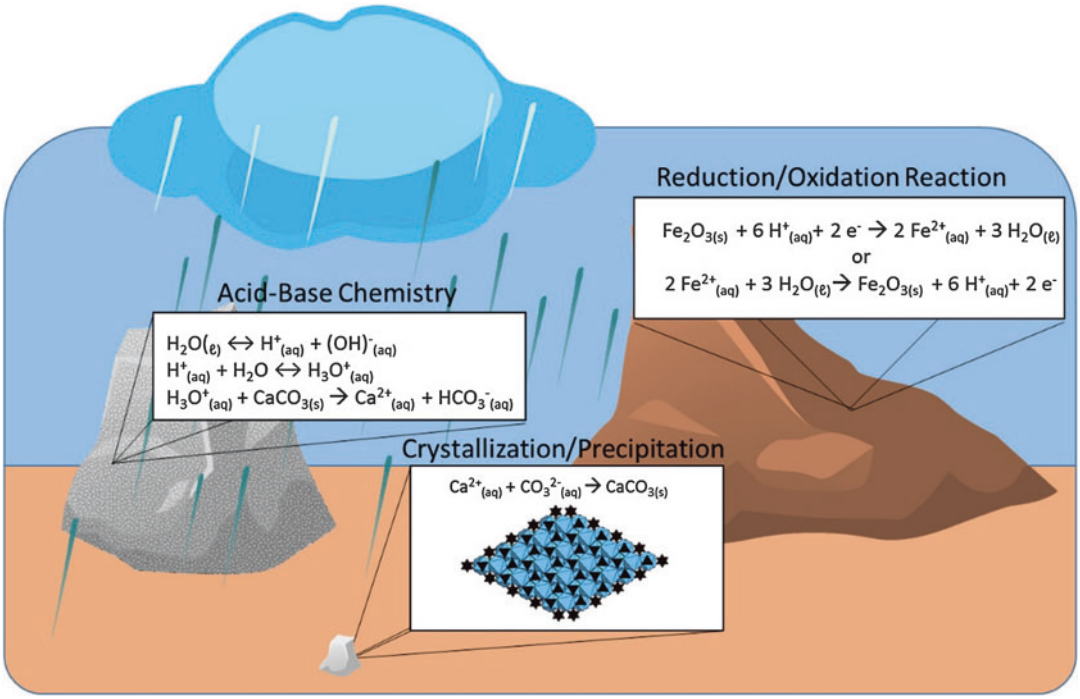

Low-Temperature Geochemistry, Fig. 2 Fundamental chemical reactions, such as acid-base, reduction-oxidation, and crystallization/precipitation, control low-temperature geochemical processes

Low-Temperature Geochemistry, Table 1 Common mineral classes and phases formed from low-temperature geochemistry processes

Hydroxides	**Carbonates**	**Sulfates**
Brucite ($Mg(OH)_2$)	Calcite or aragonite ($CaCO_3$)	Gypsum ($CaSO_4 \cdot 2\,H_2O$)
Manganite MnO(OH)	Magnesite ($MgCO_3$)	Anhydrite ($CaSO_4$)
Goethite (α-FeO(OH)	Siderite ($FeCO_3$)	Cessurite ($SrSO_4$)
Ferrihydrite	Cerussite ($PbCO_3$)	Anglesite ($PbSO_4$)
Bauxite[a]	Malachite $Cu_2CO_3(OH)_2$	
	Dolomite ($MgCa(CO^3)_2$	**Borates**
Clays		Kernite ($Na_2B_4O_6(OH)_2 \cdot 3H_2O$)
Kaolinite ($Al_2Si_2O5(OH)_4$)	**Halides**	Borax ($Na_2B_4O_5(OH)_4 \cdot 8\,H_2O$)
Illite ($K, H_3O)(Al, Mg, Fe)_2(Si, Al)_4O_{10}[(OH)_2, (H_2O)]$	Halite (NaCl)	Ulexite ($NaCaB_5O_6(OH)_6 \cdot 5H_2O$)
	Sylvite (KCl)	Colemanite ($CaB_3O_4(OH)_3 \cdot H_2O$)

[a]Mixture of diaspore, gibbsite, and boehmite

reactions and products within the environment (Drever 1997). These basic chemical principles can be applied to a wide range of geologic media, environments, and processes, and the broad categories of low-temperature geochemistry will be described in the following sections.

Major Topics in Low-Temperature Geochemistry

Mineral Precipitation/Crystallization and Chemical Weathering

A wide range of common mineral phases is formed under low-temperature geochemical conditions by precipitation and crystallization reactions. Precipitation is the direct result of reaching the solubility limit of an aqueous species that leads to the formation of a solid phase (Jarvinen 2009). Crystallization can be considered a precipitation reaction, but more specifically, one that has long-range ordering of the chemical constituents within the crystalline lattice. Amorphous phases may form from precipitation reactions, but minerals must have some degree of crystallinity (Jarvinen 2009). Table 1 provides a summary of common mineral classes and phases that form under low-temperature geochemical environments, although there are a number of less abundant minerals that form under similar conditions. The major mineral types that typically form in surficial or hydrothermal environments include hydroxides, borates, carbonates, halides, sulfides, and clays (Klein 2002).

Changes in chemical equilibria related to pH or redox conditions or through the evaporation of water can result in the precipitation of aqueous species into a solid mineral. Acidic waters can dissolve metal cations, such as Fe(III) and Al(III) and upon mixing with more neutral freshwater, causes the formation of hydrolysis products. These hydrolysis products have low solubility in water and cause the precipitation of hydroxide phases (Stumm and Morgan 1981). In some cases, the metal cation is present in the reduced form, and initial oxidation is required for the precipitation reaction to occur. Such is the case for dissolved Fe (II) oxidizing in the presence of O_2 to form Fe(III), which is then followed by the hydrolysis and precipitation reaction (Stumm and Morgan 1981; Cornell and Schwertmann 2004). Evaporite minerals are formed when saline lakes or restricted sea bodies evaporate, creating extensive deposits in arid regions (Schreiber and Tabakh 2000; Klein 2002). Halides and sulfates are the most common evaporite mineral classes, with gypsum and halite deposits constituting the most common mineral species within the natural deposits (Spencer 2000; Screiber and Tabakh 2000). Carbonates can be marine in origin, and over the history of the earth there has been a shift from low-temperature chemical precipitation to biogenic sources, such as benthic and pelagic organisms (Morse et al. 2007). Calcium carbonate is also a major constituent in freshwater systems and is widely observed in sedimentary rocks and as the building blocks of cave formations (Drever 1997; Klein 2002; Kotz et al. 2006; James and Jones 2015). Borate mineral deposits can be found in marine basins, but the largest known deposits originated as chemical precipitates from thermal springs or hydrothermal solutions associated with volcanic activities (Kistler and Smith 1975; Argust 1998).

Chemical weathering is the change in the composition of the original geologic media, often in the presences of water that occur because of oxidation, hydrolysis, and dissolution of the elements present in the parent rock (Carroll 1962). Some hydroxide phases, like bauxite, form in surficial or low-temperature supergene environments by leaching of silica from aluminum-bearing rocks (Schellmann 1994). The leaching process occurs through initial dissolution of the mineral lattice by the slightly acidic rainwater, followed by hydrolysis and precipitation of the insoluble hydroxide phase upon an increase in the pH of the pore water (Whittington and Muir 2000). Hydrolysis reactions occur when anhydrous mineral absorbs water and water dissociates to H^+ and OH^- ions, which interact with the cations present in the solid and result in structural changes to the solid-state material (Reaction Scheme 1). Overall the reaction causes the formation of a secondary mineral phase from the parent rock, plus soluble species that are removed as the water flows over the surface. Other hydroxide phases, such as goethite and ferrihydrite, can form from an initial oxidation step, such as the oxidation both sulfur and iron in pyrite, followed by hydrolysis and precipitation (Lowson 1982; Nordstrom 1982). Dissolution reactions result in the breakdown of the solid-state mineral into soluble aqueous species. One of the most common mechanisms for dissolution occurs when CO_2 in the atmosphere is dissolved in rainwater to form carbonic acid, which is also referred to as carbonation reactions (Reaction Scheme 3) (Ryan 2014).

Reaction Scheme 1 (Hydrolysis)

$$2\,KAlSi_3O_8(s) + 2\,H^+(aq) + 9\,H_2O_{(\ell)} \rightarrow H_4Al_2Si_2O_{9(s)} + 4\,H_4SiO_{4(aq)} + 2\,K^+{}_{(aq)}$$

Reaction Scheme 2 (Oxidation)

$$FeS_{2(s)} + 15/4\,O_{2(aq)} + 7/2\,H_2O_{(\ell)} \rightarrow Fe(OH)_{3(s)} + 2\,H_2SO_{4(aq)}$$

Reaction Scheme 3 (Dissolution/Carbonation)

$$CO_{2(aq)} + H_2O_{(\ell)} \rightarrow H_2CO_{3(aq)}$$

$$CaCO_{3(s)} + H_2CO_{3(aq)} \rightarrow Ca^{2+}{}_{(aq)} + 2\,H_2CO_{3(aq)}$$

Sedimentary Processes and Diagenesis

Chemical weathering results in the breakdown of rocks and formation of soils, but sedimentation processes utilize geochemical reactions to create new geologic deposits. Sedimentary rocks are formed by the accumulation of sediments (small particles of gravel, sand, silts, and clays) that are held together through lithification (West 1995). Early diagenesis or lithification is the process by which unconsolidated sediments are converted into solid rock and can occur via mechanical (compaction), geochemical (cementing or crystallization), or a combination of both processes. Cementation involves filling the pore space between the individual sediment grains with a binding agent. Under low-temperature regimes, calcium carbonate or iron hydroxides can precipitate from water seeping through the sediments, resulting cementation and lithification to occur (West 1995). Crystallization processes typically focus on the transformation of amorphous or colloidal substances into crystalline mineral phases and generally occur after deposition and even in some cases after lithification of the sedimentary rock.

Changes in the sedimentary rocks at temperatures and pressures lower than the formation of metamorphic rocks is considered late diagenesis (Teodorovich 1961). It is important to point out that late diagenensis is a different process than chemical weathering described above. Recrystallization processes can occur during later diagenesis, most notably in limestones, where aragonite in contact with freshwater can convert into calcite crystals within the solid sedimentary rock. Burial of organic matter within sedimentary rocks results in the chemical transformations of lipids, proteins, carbohydrates, and lignin-humic compounds into hydrocarbons,

which are the major constituents of methane, petroleum, and coal deposits (Singer and Muller 1983).

Chemistry of Soils

Low-temperature geochemical processes are the driving force for the formation and evolution of soils in the surficial environments. Soils are porous media created at the surface by weathering processes and differ from weather rocks because they show a vertical stratification (Sposito 1989). Mechanical weathering processes can result in the breakdown of bulk rock into smaller particles and is combined with chemical weathering processes to form the inorganic components of soils (Sposito 1989). Given the presence of water and dissolved chemical components, soils are excellent environments for microbes and fungi that can control redox reactions and breakdown organic matter (Ehlrich and Newman 2009). This leads to a complex mixture of organic components that are hospitable to plants and larger organisms and a rich and diverse biogeochemical system.

Soils are in continuous flux and exchange both matter and energy with the surrounding air, water, and biome (Sposito 1989). Meteoric water is continually percolating through soils, dissolving soluble chemical species, and transporting it through the soil column. Atmospheric gasses can easily penetrate this porous media, resulting in additional weathering and oxidation reactions (Sposito 1989). Microbial communities can continuously evolve through changes in the chemical and physical conditions of the soil (Ehlrich and Newman 2009). Humans can also influence the soil environment, either directly (intensive agricultural efforts) or indirectly (acid rain), and in turn the soil quality has impacts on overall health of the population (Locke and Zablotowicz 2004; Singh and Agrawal 2008; Brevik and Sauer 2015).

Biogeochemical Cycling

The surficial environment can be considered an open system with continual chemical fluxes between the various components; thus there is continuous movement of elements throughout the global system (Schlesinger 1997). As discussed in the previous sections, meteoric water moves through soils and porous rocks, picking up various chemical components through weathering processes. Some of the chemical constituents in the water can undergo precipitation reactions within the soil or porous rock, resulting in a sink or removal of that particular element from the solution. Interactions with plants and organisms can also cause elements to either remain in the soil or biome or be transported with the hydrologic flux. Other elements can remain dissolved in the water, where it is transferred through the subsurface system and can then be recharged into surface water through seeps and springs. Additional precipitation or redox reactions can occur within the surface water either resulting in precipitation or dissolution of the chemical component, where there can again be interactions with biological systems or dispersion into the atmosphere. Once in the atmosphere, additional chemical reactions can occur that result in addition global dispersion or wet/dry deposition. The impact of human activities must also be accounted for when considering the flux of elements between the biological, geological, hydrological, and atmospheric systems. It is the chemical reactions that occur within these systems combined with the flow and mass balance of elements of interest within these different domains that constitutes the study of biogeochemistry (Schlesinger 1997).

A well-known biogeochemical cycle as illustrated in Fig. 3, which describes the different chemical processes that control the flux of nitrogen throughout the soil, ocean, and atmosphere (Schlesinger 1997). A portion of the nitrogen is

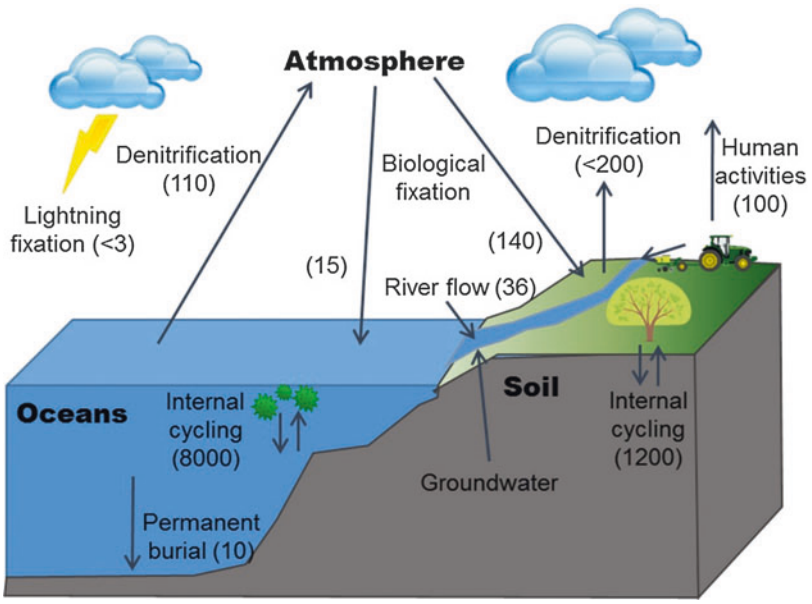

Low-Temperature Geochemistry, Fig. 3 The biogeochemical cycle for nitrogen. Values are provided by Schlesinger (1997) and are in units of 10^{12} g N per year

stored as a reservoir within the organic matter of the soil that can undergo chemical reactions, such as mineralization (Reaction Scheme 4) and nitrification (Reaction Scheme 5). Within the soil column, nitrogen is also involved with an internal cycle of uptake and release within terrestrial plants and additional mass is added to the soil through biological fixation (Reaction Scheme 6). Removal of nitrogen from the soil can occur through denitrification (Reaction Scheme 7) and release to the atmosphere. A second pathway for release is the dissolution of the nitrogen in the form of $NO_3^-{}_{(aq)}$ or $NH_4^+{}_{(aq)}$ that can be transported either by the subsurface groundwater or as run-off into freshwater streams, rivers, and lakes. Eventually the water from the surface and subsurface sources flow into the ocean where there is a large reservoir of dissolved nitrogen species. An internal cycle also occurs in the ocean with the uptake and release of nitrogen by phytoplankton and marine organisms and burial in the ocean sediments. Flux to the ocean can also occur through nitrogenase-catalyzed biological fixation, and removal of nitrogen to the atmosphere occurs through denitrification processes (Kim and Reese 1994). Within the atmosphere, nitrogen can be converted to different forms through fixation by lightning or photocatalyzed redox reactions. Humans can also add to the global nitrogen cycle through release of NO_x gasses or through the overfertilization of agricultural lands (Fields 2004). Changes in the amount of nitrogen in the air or freshwater systems that is the result of human activity can cause significant changes in the nitrogen reservoirs for these systems. This has impacts on the state of these systems as evidenced by the production of acid rain or the eutrophication of the coastal regions, particularly the Gulf of Mexico (Schlesinger 1997; Fields 2004).

Reaction Scheme 4 (mineralization)

$$R - NH_2 + H_2O \rightarrow NH_3 + R - OH$$

Reaction Scheme 5 (nitrification)

$$NH_3 + \frac{1}{2}O_2 + 2e^- \rightarrow NH_2OH + H_2O \rightarrow NO_2^- + 5\,H^+ + 2\,e^-$$

Reaction Scheme 6 (nitrogen fixation)

$$N_2 + 8H^+ + 6e^- \rightarrow 2NH_4^+$$

Reaction Scheme 7 (denitrification)

$$2\,NO_3^- + 12H^+ + 10\,e^- \rightarrow N_2 + 6H_2O$$

Changes that human activity has on global biogeochemical cycles for a wide range of elements are a major area of current scientific investigations. Global warming is the direct result of changes in the carbon cycle, and understanding the details of the chemical reactions that result in fluxes between the different systems is important for more accurate climate models and means for combating climate change (Hansen et al. 1981). As described above, overfertilization of agricultural lands causes an influx of elements that are then washed into freshwater rivers in lakes. While excess nitrogen causes problems in marine environment, the high influx of phosphorus results in the eutrophication of freshwater systems (Correll 1998). Human activity can also influence the global cycling of trace metals due to their use in industrial applications or modern living and then release through improper disposal. Lead (Pb) is an example a trace metal that was impacted by anthropogenic effects when it was added as a fuel additive in the 1970s (Shotyk and Le Roux 2005). During the combustion process, lead was released into the atmosphere through exhaust systems that resulted in dry and wet deposition into surface waters and land. Increased concentrations of lead were observed in soils and the human population until polices were adopted that minimized the use of lead as an additive and in industrial processes (Shotyk and Le Roux 2005).

Contaminant Transport

Low-temperature geochemical processes control the oxidation state and speciation of elements that are harmful to human and ecosystem health, which in turn determines the mobility and fate of contaminants in the environment. Release of contaminants into the environment can be through natural processes or through human activities that catalyze the release of toxic elements and compounds into the environment (McCarthy and Zachara 1989; Brown and Calas 2011). For example, weathering and dissolution of host rocks can occur either through natural ore deposits that are exposed to the atmosphere or groundwater or the leaching from mine and milling tailings. Typically this process is controlled both by the acid-base chemistry of the meteoric water and redox reactions when the rocks are exposed to oxygen present in the atmosphere. Mobility of the contaminant phases in surface or subsurface waters depends on the aqueous speciation and water-rock interactions. Surface interactions typically involve adsorption and binding of the contaminant to mineral phases, which can limit its mobility in the environment (McCarthy and Zachara 1989; Brown and Parks 2001). Contaminant adsorption on mineral surfaces can be reversible and again controlled by the low-temperature geochemical parameters. Interactions with the microbial community can also impact the fate of contaminants in soils and sediments, typically by control of redox parameters and precipitation reactions (McCarthy and Zachara 1989; Ehrilich and Newman 2006). Ultimately the chemical speciation controls the mobility of the contaminant in water, uptake by biological organisms, and the overall public health risk.

Inorganic elements that are of concern for public and ecosystem health include heavy metals, radioactive isotopes, and problematic main group elements. Heavy metals, such as mercury, are naturally occurring elements that become contaminants in the environment due to natural processes (redox, microbial activity) but can also be caused by human activities,

such as mining, release from industrial processes, or accidental dispersion. Speciation of mercury is a major factor in determining health risk, with methylation by bacterial communities resulting in increased uptake and bioaccumulation (Boening 2000). Arsenic is an example of a problematic main group element that occurs naturally and becomes soluble when in the reduce form (arsenite, AsO_3^{3-}) (Bowell et al. 2015). Countries such as Bangladesh, India, China, Mexico, and Argentina have significant arsenic contamination in water sources due to formation of strongly reducing aquifers or closed basins in arid or semiarid climates (Smedley and Kinniburg 2002). Uranium is a naturally occurring radioactive element that has health risks when ingested through drinking water or food sources due to its chemical and radiological toxicity (Brugge et al. 2005). Redox conditions also drive the mobility of uranium in environmental systems, with the oxidize uranyl (UO_2^{2+}) moiety forming soluble complexes over a range of environmentally relevant pH values (Maher et al. 2013).

Organic contaminants are typically the result of human activities and can be controlled by natural geochemical processes that are often utilized by environmental remediation. Volatile organic compounds, plasticizers, pesticides, and chlorinated compounds are the most common organic pollutants in drinking waters (Olson 2003). Due to concerns over the presence of hormones and endocrine disruptors, the USGS comprehensive survey conducted in 2002 also that found steroids (coprostanol, cholesterol), insect repellant (*N*,*N*-diethyltoluamide), caffeine, antimicrobial agents (triclosan), fire retardant (tri(2-chloroehtyl)phosphate), and detergent residues (4-nonylpentol) can be detected in surface waters and are now considered emerging contaminants (Kolpin et al. 2002; Lapworth et al. 2012). Sunlight can cause photochemical reactions that transform natural organic matter into other compounds, such as halogenated species (Mendez-Diaz et al. 2014). Some of these transformations can yield degradation products that are less harmful than the initial material, but some of these reactions were reported to be reversible. An endocrine disruptor, 17α-trembolone has been shown to degrade in the presence of light but then reform in the dark (Qu et al. 2013). Chemical spills of hydrocarbons or chlorinated compounds present in groundwater can be remediated through microbial degradation processes that utilize these compounds as an energy source. For example, tetrachloroethane and trichloroethane are common contaminants in water, but under anerobic conditions microbial communities can be transformed to less chlorinated dichloroethane and vinyl ethane for natural attenuation (Bradley et al. 2005).

Summary

Low-temperature geochemistry is the study of chemical processes that occur in a complex and ever changing environment. It requires understanding fundamental chemical principles applied to geology, hydrology, biology, and atmospheric systems to understand some of the most important processes on the surface of the earth. Mineral precipitation, chemical weathering, sedimentation, diagenesis, soil science, biogeochemical cycling, and contaminant transport impact natural ecosystems and human society. Low-temperature geochemistry also provides a means to understand how interconnected we are with natural processes and our actions can cause significant impacts on global processes.

Beginning with fundamental elemental processes that occur within solid-state minerals and branching out into global topic, low-temperature geochemistry continues to be an important area of scientific study. Continued interest in combating climate change requires advanced understanding of how rocks, soils, natural bodies of water, and the atmosphere are connected through chemical, physical, and biological processes. As we continue to change the landscape and release new chemicals into the environment, there is increased efforts to determine the impact of these emerging contaminants on the ecosystem. Given our relationship and reliance on the natural world, understanding the geochemical processes that occur in low-temperature, surficial environments will continue to be a key research focus for human and global health.

Cross-References

- Biogeochemistry
- Carbon Cycle
- Chemical Weathering
- Diagenesis
- Soils

References

Argust P (1998) Distribution of boron in the environment. Biol Trace Elem Res 66:131–143

Boening DW (2000) Ecological effects, transport, and fate of mercury: a general review. Chemosphere 40:1335–1351

Bowell RJ, Alpers CN, Jamieson HE, Nordstrom DE, Majzlan J (2015) Arsenic: environmental geochemistry, mineralogy, and microbiology, Reviews in mineralogy and geochemistry, vol 79. American Mineralogical Society of America, Washington, DC

Bradley PM, Carr SA, Baird RB, Chapelle FH (2005) Microbial degradation of chloroethenes in groundwater systems. Hydrogeol J 8:104–111

Brevik EC, Sauer TJ (2015) The past, present, and future of soils and human health studies. Soil 1:35–46

Brown GE, Calas G (2011) Environmental mineralogy – understanding element behavior in ecosystems. Compt Rendus Geosci 343:90–112

Brown GE, Parks GA (2001) Sorption of trace elements on mineral surfaces: modern perspectives from spectroscopic studies, and comments on sorption in the marine environment. Int Geol Rev 43:963–1073

Brugge D, deLemos JL, Oldmixon B (2005) Exposure pathways and health effects associated with chemical and radiological toxicity of natural uranium: a review. Rev Environ Health 20:173–199
Carroll D (1962) Rainwater as a chemical agent of geologic processes. A review geological survey water supply paper, vol 1535-G. pp 1–16
Carson R (1962) Silent spring Houghton Mifflin Harcourt, Boston
Cornell RM, Schwertmann U (2004) The Iron oxides: structure, properties, reactions, occurrences, and uses, 2nd edn. Wiley, Berlin
Correll DL (1998) The role of phosphorus in the eutrophication of receiving waters: a review. J Environ Qual 27:263–266
Drever JI (1997) The geochemistry of natural waters: surface and Roundwater environments, 3rd edn. Princeton Hall Publishing, Upper Saddle River
Ehlrich HL, Newman DK (2009) Geomicrobiology, 5th edn. CRC Press, Boca Raton
Ehrilich HL, Newman DK (2006) Geomicrobiology, 5th edn. Taylor and Francis Group, LLC., Boca Raton
Fields S (2004) Global nitrogen: cycling out of control. Environ Health Perspect 112:A556–A563
Guangzhi T (1996) Low temperature geochemistry. Science Press, Beijing
Hansen J, Johnson A, Lacis S, Lebedeff S, Lee P, Rind D, Russell G (1981) Climate impact of increasing atmospheric carbon dioxide. Science 213:957–966
James NP, Jones B (2015) Origins of carbonate sedimentary rocks. Wiley VCH, Berlin
Jarvinen G (2009) Precipitation and crystallization processes. Los Alamos National Laboratory, Los Alamos
Kim J, Reese DC (1994) Nitrogenase and nitrogen fixation. Biochemistry 33:389–397
Kistler RB, Smith W (1975) Boron and borates. In: Lefond SJ (ed) Industrial rocks and minerals. American Institute of Mining, Metallurgical and Petroleum Engineers, Englewood
Klein C (2002) Mineral science. Wiley, New York
Kolpin DW, Furlong ET, Meyer MT, Thurman EM, Zaugg SD, Barber LB, Buxton HT (2002) Pharmaceuticals, hormones, and other organic wastewater contaminants in U.S. streams, 1999–2000: a national reconnaissance. Environ Sci Technol 36:1202–1211
Kotz JC, Treichel PM, Weaver GC (2006) Chemistry and chemical reactivity. Thomson Learning Inc., Belmont
Lapworth DL, Baran N, Stuart ME, Ward RS (2012) Emerging organic contaminants in groundwater: a review of sources, fate and occurrence. Environ Pollut 163:287–303
Likens GE, Bormann FH (1974) Acid rain: a serious regional environmental problem. Science 184:1176–1179
Locke MA, Zablotowicz RM (2004) Pesticides in soil – benefits and limitations to soil health. In: Schjonning P, Elmholt S, Christensen BT (eds) Managing soil quality: challenges in modern agriculture. CABI Publishing, Wallingford
Lowson RT (1982) Aqueous oxidation of pyrite by molecular oxygen. Chem Rev 82:461–497
Maher K, Bargar JL, Brown GE (2013) Environmental speciation of actinides. Inorg Chem 52:3510–3532
McCarthy JF, Zachara JM (1989) Subsurface transport of contaminants. Environ Sci Technol 23:496–502
Mendez-Diaz JD, Shimabuku KK, Ma J, Ennumah ZO, Pignatello JJ, Mitch WA, Dodd MC (2014) Sunlight-driven photochemical halogenation of dissolved organic matter in seawater: a natural abiotic source of organobromine and organoiodine. Environ Sci Technol 48:7418–7427
Morse JW, Arvidson RS, Luttg A (2007) Calcium carbonate formation and dissolution. Chem Rev 107:342–381
Nordstrom DK (1982) Aqueous pyrite oxidation and the consequent formation of secondary iron minerals. In: Kittrick JA, Fanning DS, Hossner LR (eds) Acid sulfate weathering. Soil Science Society of America, Madison
Olson E (2003) What's on tap: grading drinking water in U.S. cities. Natural Resource Defense Council, Washington, DC
Qu S, Kolodziej EP, Long SA, Gloer JB, Patterson EV, Baltrusaitis J, Jones GD, Benchetler PV, Cole EA, Kimbrough KC, Tarnoff MD, Cwiertny DM (2013) Product-to-parent reversion of Trenbolone: unrecognized risks for endocrine disruption. Science 341:1441–1443
Reinhardt C (2001) Chemical sciences in the 21st century: bridging boundaries. Wiley VCH, Berlin
Ryan P (2014) Environmental and low-temperature geochemistry. Wiley, New York
Schellmann W (1994) Geochemical differentiation in laterite and bauxite formation. Can Underwrit 21:131–143
Schlesinger WH (1997) Biogeochemistry: an analysis of global change. Academic, San Diego
Schreiber BC, Tabakh ME (2000) Deposition and early alteration of evaporates. Sedimentology 47:215–238
Shotyk W, Le Roux G (2005) Biogeochemistry and cycling of lead. Met Ions Biol Syst 43:239–275
Singer A, Muller G (1983) Diagenesis in agrillaceous sediments. In: Larsen G, Chilingar GV (eds) Diagenesis in sediments and sedimentary rocks, vol 2. Elsevier Scientific Publishing, Amsterdam
Singh A, Agrawal M (2008) Acid rain and its ecological consequence. J Environ Biol 29:15–24
Smedley PL, Kinniburgh DL (2002) A review of the source, behavior and distribution of arsenic in natural waters. Appl Geochem 17:517–568
Spencer RJ (2000) Sulfate minerals in evaporite deposits. In: Alpers CN, Jambor JL, Nordstron DK (eds) Sulfate minerals: crystallography, geochemistry, and environmental significance, Reviews in mineralogy and geochemistry, vol 40. Mineralogical Society of America, Washington, DC, pp 173–192
Sposito G (1989) The chemistry of soils. Oxford University Press, Oxford, UK
Stumm M, Morgan JJ (1981) Aquatic chemistry. Wiley, New York
Teodorovich GI (1961) Authigenic mineral in sedimentary rocks. Springer Science, New York
West T (1995) Geology applied to engineering. Prentice Hall, Upper Saddle River
Whittington BI, Muir D (2000) Pressure acid leaching of nickel laterites: a review. Miner Process Extr Metall Rev Int J 21:527–599

Luminescence

Tori Z. Forbes
Department of Chemistry, University of Iowa, Iowa City, IA, USA

Definition

Luminescence is the creation of light by chemical or physical processes that does not involve heat. Photoluminescence, which uses light as the excitation source, can be observed in minerals and provides information regarding the presence of trace metals, formation of defect sites, growth conditions, and sample age. Spectroscopic methods can be utilized to determine chemical and physical properties of the mineral specimen, and dating of geologic media can be achieved through thermoluminescence techniques.

Basics of Luminescence

When an electron within a molecule or solid compound is promoted to an excited state through the absorption of energy, there are two possible processes that will return the electron to the ground state. Non-radiative transfer mechanism allows the energy to dissipate through translation, rotational, or vibrational motion of the atoms and occurs on the order of 10^{-11} to 10^{-10} s. Radiation processes release energy through the emission of a photon and are generally classified as luminescence (Ingle and Crouch 1988).

The process of luminescence can be further classified as either fluorescence or phosphorescence depending on the transfer of the electron within the excited state. After energy absorption and promotion, the electron can move between excited singlet states (where the spin of the electrons is still paired) through internal conversion and undergo vibrational relaxation until it reaches the lowest energy excited singlet state. Fluorescence occurs when a radiational transition between the excited singlet state and the ground singlet state results in the release of a photon and occurs on time scales of 10^{-10} to 10^{-6} s. When an electron absorbs energy, it can only be promoted to singlet states, but intersystem crossing can result in the formation of triplet states (where the spin of the electrons is not paired). Additional vibrational relaxation transfers the electron to the lowest energy triplet excited state, followed by radiational deactivation that occurs through the release of a photon. This process is called phosphorescence and takes place on slower time scales (10^{-4} to 10^{4} s) because of the need for intersystem crossing. Different categories of luminescence are distinguished through the excitation energy source (Fig. 1).

Photoluminescence is the most common category of luminescence and describes emission of photons after excitation by electromagnetic radiation. It often occurs through the absorption of ultraviolet or visible light, but some materials may absorb X-rays (X-ray excited luminescence). For both fluorescence and phosphorescence, resulting wavelength of released photon is longer than the absorbed light because the electron is promoted to higher energy excited states (Ingle and Crouch 1988). Energy of the photon released through photoluminescence is typically in the visible range but can also occur in the ultraviolet or infrared regions (Geake and Walker 1975; Rakovan and Waychunas 1996).

Luminescence can also occur when the electron is excited or released by other mechanisms. Cathodoluminescence is caused by promotion of the electron to the excited state with an electron beam (Gotze 2012). If a mechanical action (crushing, tricking, scratching, or rubbing) triggers an electrical excitation, then it can cause phosphorescence and is referred to as triboluminescence, mechanoluminescence, piezoluminescence, or fractoluminescence (Zink 1978; Sweeting 2001). In thermoluminescence, the electron was originally promoted by electromagnetic radiation or some other energy source and then trapped in the excited state (Wintle and Huntley 1982; Forman 1989). The trapping centers are generally defect sites caused by radioactive or stacking faults, but they can also be caused by ion substitution. Upon exposure to heat, the trapped electrons are released and fall back to the ground state, releasing a photon in the process (Wintle and Huntley 1982; Forman 1989).

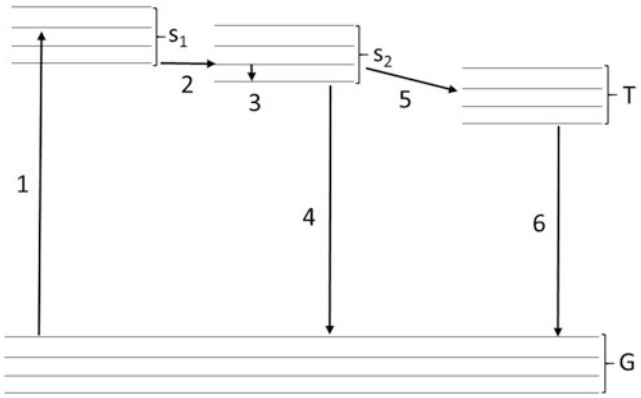

Luminescence, Fig. 1 Diagram of the luminescence process. (*1*) An electron is promoted from the ground state (*G*) to a singlet excited state (S_1) and can (*2*) transfer to a different singlet excited state (S_2). (*3*) Vibrational relaxation lowers the energy until (*4*) the electron moves to the ground state and releases a photon to create fluorescence. Alternatively, intersystem crossing (*5*) results in movement of the electron into an excited triplet state (*T*). (*6*) Phosphorescence occurs with electron transfer from the excited triplet state back to the ground state, which results in the release of a photon

Luminescence in Minerals

In most mineral phases that exhibit photoluminescence, there are atoms present with the correct separation of the energy levels to emit a photon in the visible or ultraviolet region (Rakovan and Waychunas 1996). These atoms are called activators and can be present in either bulk compositions or trace levels. A related process involves absorption of electromagnetic radiation or an electron beam by one atom (the sensitizer) which can then be transferred to the excited state of a second atom (the activator) before the release of a photon (Rakovan and Waychunas 1996). Common activators and sensitizers are manganese (II), chromium (III), tungstates, titanates, molybdates, zirconates, sulfide, uranyl, some hydrocarbons, and rare earth elements (Rakovan and Waychunas 1996; Gaft et al. 2005).

A less common mechanism for photoluminescence occurs through defect centers within the solid-state crystalline lattice. The luminescence mechanisms for defect sites are not

completely understood; however, a well-known type is the Frenkel defect or F-center (Rakovan and Waychunas 1996). This type of defect can occur in halite where the displacement of the Cl^- anion will leave a vacancy and an electron will inhabit the site as a means for overall charge balancing (Rodriguez-Lazcano et al. 2012). Within the vacancy, the electron can be present in an excited state, and photoluminescence occurs when transitions result in the release of a photon in the visible region.

In 1989, Dr. Gerhard Henkel published an exhaustive list of minerals that undergo luminescence and includes 566 mineral species and 59 related substances (Henkel 1989). Only a handful of minerals undergo fluorescence when pure phase, including scheelite ($CaWO_4$) and secondary hexavalent uranium minerals (autinite ($Ca(UO_2)_2(PO_4)_2 \cdot 10–12\ H_2O$)) (Gorobets and Sidorenko 1974; Nikl et al. 2000). Other common minerals such as calcite, fluorite, and apatite will fluoresce when trace amounts of activators (generally Mn^{2+} or UO_2^{2+}) are present in the solid-state materials (Machel et al. 1991; Calderon et al. 1992; Waychunas 2002). The Franklin mine (New Jersey, USA) is home to the largest number of fluorescent mineral specimens observed from one site, including some spectacular specimens that contain bright fluorescence and unusual crystal habits (Wilkerson 1962).

Other types of luminescence are rarer, but can be observed in a handful of mineral species. Thermoluminescence has been observed in apatite, calcite, fluorite, quartz, zircon, lepidolite, and some feldspars (McKeever 1985). In each of these cases, there must be activators present and the luminescence of the specimen is removed after heating. Triboluminescence has been reported in some minerals, but is generally not consistent between specimens. This is the case for calcite, feldspars, sphalerite fluorite, micas, and quartz (Walton 1977; Chapman and Walton 1983). Sphalerite samples are typically the most consistent, and the light associated with the triboluminescence can be observed in the dark.

Luminescence Zoning

Luminescence can be used as a tool for identifying different minerals within a specimen. Intercrystalline luminescence describes the difference in fluorescence for different mineral phases within the same host rock (Rakovan and Waychunas 1996). Typically this will be observed through difference in the color of the resulting fluorescence when the sample is placed underneath ultraviolet radiation. This type of luminescence can be used to distinguish minerals that may look similar in visible light or aid in the isolation of individual crystallites within the matrix. It is important to point out that luminescence may aid in identification, but cannot be used as the only method because certain mineral from the same species may fluoresce different colors from different locations due to difference in the trace element chemistry. Once a mineral has been identified, the specific fluorescent wavelength that it emits can sometimes be helpful to identify its place of origin (Rakovan and Waychunas 1996).

Intracrystalline zoning is defined as variations that occur within individual crystallites. Zoning within minerals occurs when there is a spatial difference in a particular chemical or physical property and provides information regarding the morphological history of the crystal, changes in the deposition environment, growth mechanism, and atomic-level structure. Zoning of the luminescence signal is caused by changes in the activator concentration and is usually the result of the growth process (Rakovan and Waychunas 1996). Zoning can occur as concentric rings or as defects on specific crystal phases (sectoral and intrasectoral zoning) and provides wealth of information regarding the deposition environment and growth of the mineral sample.

Luminescence Spectroscopy

Photoluminescent properties of a mineral specimen can be measured using a spectrometer and can provide information regarding the chemical and physical properties that result in the release of a photon (Waychunas 2014). The energy levels of the ground and excited states are dependent on the identity of the element, oxidation state, coordination geometry, and local site symmetry. Thus, luminescence spectroscopy can determine the presence and identity of the activator, even at trace levels within the sample.

The absorption, excitation, and emission processes can all be probed using this technique. Absorption spectra measure the amount of light absorbed or transmitted by a sample, while the wavelength of the incident radiation is varied to provide information on the energy of the electronic transmission in the ground states to multiple excited states of the activator or luminescence center. Excitation spectroscopy scans the wavelength of the incident beam while monitoring emitted light to impart information regarding the energies that produce luminescence when they are absorbed by the sample. By comparing the absorption and excitation spectra, the exact wavelengths required for luminescence can be determined. The emission spectra are collected by fixing the incident wavelength and scanning through the emitted energy, which shows the transition from that specific excited state that releases the photon (Waychunas 2014). This can provide details regarding the identity of the activator because those specific energy levels can be probed by scanning through the emission spectra. The spectra of both absorption and emission

spectroscopy of unknown activators can be compared to standards to provide identification of the elements in the sample.

Cathodoluminescence spectra can also be collected using an electron-beam instrument like a scanning electron microscopy or an electron microprobe (MacRae et al. 2005; Gotze 2012). The energy from the electron beam can promote electrons from the ground state to the excited state for most activators, so identification of the element responsible for luminescence can be difficult to identify using this technique. However, high-resolution spatial mapping can be obtained for mineral specimens and provide information regarding growth, zoning, impurities, and the crystallization environment (Waychunas 2014).

Luminescence Dating

Soils and sediment may contain thermoluminescence minerals which can be used to determine the geologic age of the sample (Singhvi and Mejdahl 1982; Wintle and Huntley 1982). Minerals, such as calcite, quartz, or zircon, present within the sample matrix, are heated under an inert atmosphere or vacuum, and the emitted light is recorded using a photon sensitive detector (Huntley et al. 1988; Rendell et al. 1993). Electrons are trapped at different depths, and thus, the variation in temperature is related to the irradiation history of the sample, which occurs due to exposure to naturally occurring radioactivity. The spectra of the mineral will change as a result of crystal purity, radiation dose, dose rate, and thermal history. The age is determined by dividing the equivalent dose determined through thermoluminescence by the overall dose rate of the sample (obtained through gamma spectrometry) (Wintle and Huntley 1982; Duller 2004). This technique is particularly useful when dating samples from the quaternary period, but given that the thermal history or impurities may impact the overall emission, thermoluminescence dating is often combined with other methods, such as U-series dating or stratigraphy (Forman 1989; Duller 2004).

Summary

Luminescence in geologic samples can occur through a variety of pathways, but photoluminescence is the most commonly observed form. Luminescence signals can provide information on the presence of trace elements in the sample, crystallite growth, and deposition environment. Spectroscopic techniques can be used to understand the chemical characteristics of the mineral phase, and thermoluminescence is utilized in geochronological studies of soils and sediments.

References

Calderon T, Khanlary M-R, Rendell HM, Townsend PD (1992) Luminescence from natural fluorite crystals. Int J Rad Appl Instrum Part D 20:475–485

Chapman GN, Walton AJ (1983) Triboluminescence of glasses and quartz. J Appl Phys 54:5961–5965

Duller GAT (2004) Luminescence dating of quaternary sediments: recent advances. J Quat Sci 19:183–192

Forman SL (1989) Applications and limitations of thermoluminescence to date quaternary sediments. Quat Int 1:47–59

Gaft M, Reisfeld R, Panczer G (2005) Modern luminescence spectroscopy of minerals and materials. Springer Publishing, Berlin

Geake JE, Walker G (1975) Luminescence of minerals in the near-infrared. In: Karr C Jr (ed) Infrared and Raman spectroscopy of lunar and terrestrial minerals. Academic, New York

Gorobets BS, Sidorenko GA (1974) Luminescence of secondary uranium minerals at low temperatures. Sov At Energy 36:5–12

Gotze J (2012) Application of cathodoluminescence microscopy and spectroscopy in geosciences. Microsc Microanal 18:1270–1284

Henkel G (1989) The Henkel glossary of fluorescence minerals. Fluorescence Mineral Society, Tarzana

Huntley DJ, Godfrey-Smith DI, Thewalt ML, Berger GW (1988) Thermoluminescence spectra of some mineral samples relevant to thermoluminescence dating. J Lumin 39:123–136

Ingle JD Jr, Crouch SR (1988) Spectrochemical analysis. Prentice Hall Publishing, Upper Saddle River

Machel HG, Mason RA, Mariano AN, Mucci A (1991) A causes and emission of luminescence in calcite and dolomite. In: Baker CE, Kopp OE (eds) Luminesce microscopy and spectroscopy: qualitative and quantitative applications. Society for Sedimentary Geology, Tulsa

MacRae CM, Wilson NC, Johnson SA, Phillips PL, Otsuki M (2005) Hyperspectral mapping – combining cathodoluminescence and X-ray collection in an electron microprobe. Microsc Res Tech 67:271–277

McKeever SWS (1985) Thermoluminescence of solids. Cambridge University Press, Cambridge

Nikl M, Bohacek P, Mihokova E, Kobayshi M, Ishii M, Usuki Y, Babin V, Stolovich A, Zazubovich S, Bacci M (2000) Excitonic emission of scheelite tungstates AWO_4(A = Pb, Ca, Ba, Sr). J Lumin 87–89:1136–1139

Rakovan J, Waychunas G (1996) Luminescence in minerals. Mineral Rec 27:7–19

Rendell HM, Khanlary M-R, Townsend PD, Calderon T, Luff BJ (1993) Thermoluminescence spectra of minerals. Mineral Mag 57:217–222

Rodriguez-Lazcano Y, Correcher V, Garcia-Guinea J (2012) Luminescence emission of natural NaCl. Radiat Phys Chem 81:126–130

Singhvi AK, Mejdahl V (1982) Thermoluminescence dating of sediments. Nucl Tracks Radiat Meas 10:137–161

Sweeting L (2001) Triboluminescence with and without air. Chem Mater 13:854–870

Walton AJ (1977) Triboluminescence. Adv Phys 26:887–948

Waychunas G (2002) Apatite. In: Kohn MJ, Rakovan J, Hughes JM (eds) Phosphates: geochemical, Geobiological, and materials importance, Luminescence in reviews in mineralogy and geochemistry, vol 48. Mineralogical Society of America, Washington, DC

Waychunas G (2014) Luminescence spectroscopy. In: Henderson GS, Neuville DR, Downs RT (eds) Spectroscopic methods, Reviews in mineralogy and geochemistry, vol 78. Mineralogical Society of America, Washington, DC

Wilkerson AS (1962) The minerals of Franklin and Sterling Hill, New Jersey, vol 65. The New Jersey Geological Survey, Trenton

Wintle AC, Huntley AG (1982) Thermoluminescence dating of sediments. Quat Sci Rev 1:31–53

Zink JI (1978) Triboluminescence. Acc Chem Res 11:289–295

Lutetium

Scott M. McLennan
Department of Geosciences, Stony Brook University, Stony Brook, NY, USA

Element Data
Atomic Symbol: Lu
Atomic Number: 71
Atomic Weight: 174.9668(1)
Isotopes and Abundances: ^{175}Lu, 97.401(13)% and ^{176}Lu, 2.599(13)%
1 Atm Melting Point: 1663 °C
1 Atm Boiling Point: 3402 °C
Common Valences: +3
Ionic Radii: 86.1 pm (CN6), 97.7 pm (CN8), and 119.4 pm (CN12)
Pauling Electronegativity: 1.27
First Ionization Energy: 523.52 kJ mol^{-1}
Chondritic (CI) Abundance: 0.0254 ppm
Silicate Earth Abundance: 0.057 ppm
Crustal Abundance: 0.30 ppm
Seawater Abundance: 0.227 ppt
Core Abundance: ~0

Properties

Lutetium (Lu), named after *Lutetia*, the Latin name for Paris, is a soft, malleable, ductile, dense (9.841 g cm^{-3}), bright silvery metal. Its electronic configuration is [Xe]4f^{14}5d^{1}6s^{2}. It is relatively stable in air and readily dissolves in mineral acids. It is a group 3 or IIIB inner transition element, with +3 being its only valence state in geological environments, and is one of the lanthanide rare earth elements (REE). In geochemical terminology, it is grouped with heavy rare earth elements (HREE; Gd-Lu). Lutetium has one natural, stable isotope and one long-lived radioisotope (^{176}Lu; $t_{1/2} = 3.713 \times 10^{10}$ year; beta decaying to ^{176}Hf) occurring in nature, listed above with their abundances.

More than 270 minerals contain lanthanides as essential structural constituents, but those with Lu as a significant component are restricted to minerals such as gadolinite-Y [$Y_2FeBe_2(Si_2O_{10})$], xenotime [$Y(PO_4)$], bastnäsite [REE(CO_3)F], allanite [$(REE,Ca,Y)_2(Al,Fe^{2+},Fe^{3+})_3(SiO_4)_3(OH)$], and britholite [$(REE,Ca)_5(SiO_4,PO_4)_3(OH,F)$].

Details of properties, mineralogy, history, and uses of Lu were compiled from Goonan (2011), Chakhmouradian and Wall (2012), Zaimes et al. (2015), Gschneidner (2016), Hammond (2016), and Meija et al. (2016a, b).

History and Use

The early history of Lu was controversial, being identified independently by three workers (Urbain, von Weisbach, James) in 1907, with final attribution of discovery (and naming) going to Georges Urbain in 1909. Lutetium metal was first produced in 1953. Being the rarest of the naturally occurring REE in the Earth, Lu is also the most valuable but has limited commercial use. It has been used as a catalyst in petroleum cracking, and due to its very high density, $LuTaO_4$ has been used in X-ray phosphors. Lu is also used in Tm:LuYAG lasers, PET medical imaging detectors, and LED lights.

Geochemical Behavior

The fundamental importance of Lu in geochemistry is that it is one of the small trivalent rare earth elements, among the most useful trace elements in all areas of geochemistry and cosmochemistry due to their coherent and systematic behavior as a group, largely a consequence of the "lanthanide contraction." The ^{176}Lu/^{176}Hf decay system is an important geochronometer and isotope tracer in a wide variety of geological settings (e.g., Wu et al. 2007).

Lutetium is typically a trace element in most rocks and minerals. It is classified geochemically and cosmochemically as a highly refractory lithophile element, with a 50% $T_{condensation}$ of 1659 K at 10^{-4} bars (Lodders 2003). In most igneous systems, Lu is incompatible with bulk partition coefficients, $D < 1$. In aqueous systems, Lu normally has very low fluid/rock partition coefficients ($\ll 1$). As a result, Lu contents of clastic sediments typically reflect their average provenance.

In seawater, Lu has very low concentrations (sub-ppt) and residence times (~2890 year) with speciation dominated by Lu^{3+}, $LuCO_3^+$, and $Lu(CO_3)_2^-$. In other aqueous systems (e.g., magmatic, hydrothermal), Lu can reach ppm levels due to elevated temperatures, pH effects, and complexing with various ligands (e.g., F^-, Cl^-, OH^-).

Concentration and residence time data are from compilations in Taylor and McLennan (2009) and Nozaki (2001).

Biological Utilization and Toxicity

There are no documented biological uses for Lu. REE (including Lu^{3+}) likely substitute for Ca^{2+} in biological materials and processes. REE concentrations (including Lu) in human tissues and fluids are very low (~ppb to <ppb levels, respectively) due to very low concentrations in natural waters and low uptake rates throughout the food chain (Bulman 2003). At low levels of ingestion, there are no established toxic effects that pose a threat to human health.

Cross-References

- ▶ Incompatible Elements
- ▶ Lanthanide Rare Earths
- ▶ Lithophile Elements
- ▶ Trace Elements
- ▶ Transition Elements

References

Bulman RA (2003) Metabolism and toxicity of the lanthanides. In: Sigel A, Sigel H (eds) Metal ions in biological systems, vol 40, The lanthanides and their interrelations and Biosystems. Marcel Dekker, Basel, pp 683–703

Chakhmouradian AR, Wall F (eds) (2012) Rare earth elements. Elements 8:333–376

Goonan TG (2011) Rare earth elements – end use and recyclability. US Geol Surv Sci Invest Rpt 2011–5094, 15pp

Gschneidner KA Jr (2016) Physical properties of the rare earth metals. In: Haynes WM (ed) CRC handbook of chemistry and physics, 96th edn. CRC Press, Boca Raton, pp 4-115–4-120

Hammond CR (2016) The elements. In: Haynes WM (ed) CRC handbook of chemistry and physics, 96th edn. CRC Press, Boca Raton, pp 4-1–4-42

Lodders K (2003) Solar system abundances and condensation temperatures of the elements. Astrophys J 591:1220–1247

Meija J, Coplen TB, Berglund M, Brand WA, De Bièvre P, Gröning M, Holden NE, Irrgeher J, Loss RD, Walczyk T, Prohaska T (2016a) Atomic weights of the elements 2013. Pure Appl Chem 88:265–291. (IUPAC Technical Report)

Meija J, Coplen TB, Berglund M, Brand WA, De Bièvre P, Gröning M, Holden NE, Irrgeher J, Loss RD, Walczyk T, Prohaska T (2016b) Isotopic compositions of the elements 2013. Pure Appl Chem 88:293–306. (IUPAC Technical Report)

Nozaki Y (2001) Rare earth elements and their isotopes in the ocean. In: Steele JH et al (eds) Encyclopedia of ocean sciences. Academic, London, pp 2354–2366

Taylor SR, McLennan SM (2009) Planetary crusts: their composition, origin and evolution. Cambridge University Press, Cambridge. 378pp

Wu FY, Li XH, Sheng YF, Gao S (2007) Lu-Hf isotope systematics and their applications in petrology. Acta Petrol Sin 23:185–220

Zaimes GG, Hubler BJ, Wang S, Khanna V (2015) Environmental life cycle perspective on rare earth oxide production. ACS Sustain Chem Eng 3:237–244